3-10-2021

Advanced Energy Modelling and Life Cycle Assessment of Indoor Agriculture

Sadaf Ekhtiari
University of Windsor

Advanced Energy Modelling and Life Cycle Assessment of Indoor Agriculture

By

Sadaf Ekhtiari

A Thesis

Submitted to the Faculty of Graduate Studies

through the Department of Civil and Environmental Engineering

in Partial Fulfillment of the Requirements for

the Degree of Master of Applied Science

at the University of Windsor

Windsor, Ontario, Canada

2021

Advanced Energy Modelling and Life Cycle Assessment of Indoor Agriculture

by

Sadaf Ekhtiari

APPROVED BY:

_____
V. Roussinova
Department of Mechanical, Automotive & Materials Engineering

_____
R. Ruparathna
Department of Civil and Environmental Engineering

_____
R. Carriveau, Co-Advisor
Department of Civil and Environmental Engineering

_____
D. Ting, Co-Advisor

Department of Mechanical, Automotive & Materials Engineering

January 26, 2021

DECLARATION OF CO-AUTHORSHIP / PREVOIUS PUBLICATIONS

I.   Co-Authorship

I hereby declare that this thesis incorporates material that is result of joint research, as follows:

Chapter 3 of the thesis was co-authored with Z. Naghibi and S.Ekhtiari under the supervision of professors R. Carriveau and D. Ting. Z. Naghibi contributed to the conceptualization, methodology, software model development, investigation, validation, and preparing the original draft. S. Ekhtiari contributed to the methodology, software model development, benchmarking, writing, reviewing and editing of the manuscript.

Within the Chapters 2 and 4, I carried out all background research, methodology, topic selection, simulation design and analysis, interpretation of results, and preparation of text, with guidance and review provided by Dr. Rupp Carriveau and Dr. David S-K. Ting.

I am aware of the University of Windsor Senate Policy on Authorship and I certify that I have properly acknowledged the contribution of other researchers to my thesis and have obtained written permission from each of the co-author(s) to include the above material(s) in my thesis.

I certify that, with the above qualification, this thesis, and the research to which it refers, is the product of my own work.

II.   Previous Publication

This thesis includes three original papers that have been previously published/ submitted for publication in peer reviewed journals, as follows:

Chapter 2	S. Ekhtiari, R Carriveau, D S-K. Ting. Life Cycle Assessment of a Greenhouse Bell Pepper Production in Southwestern Ontario: Evaluating Non-renewable vs Renewable Heating Energy Systems	To be Submitted
Chapter 3	Z. Naghibi, S. Ekhtiari, R. Carriveau, D. S-K. Ting (2020). Hybrid Solar Thermal/Photovoltaic-Battery Energy Storage System in a Commercial Greenhouse: Performance and Economic Analysis, *Energy Storage Journal*, DOI: 10.1002/est2.215	Published
Chapter 4	S. Ekhtiari, R. Carriveau, D. S-K. Ting. Parametric Optimization of Environment Variables to Minimize Energy Requirements and Improve Solar Thermal Energy System Performance in a Commercial Greenhouse	To be Submitted

I declare that I have obtained a written permission from the copyright owner(s) to include the above published material(s) in my thesis. I certify that the above material describes work completed during my registration as a graduate student at the University of Windsor.

III. General

I certify that, to the best of my knowledge, my thesis does not infringe upon anyone's copyright nor violate any proprietary rights and that any ideas, techniques, quotations, or any other material from the work of other people included in my thesis, published or otherwise, are fully acknowledged in accordance with the standard referencing practices. Furthermore, to the extent that I have included copyrighted material that surpasses the bounds of fair dealing within the meaning of the Canada Copyright Act, I certify that I have obtained a written permission from the copyright owner(s) to include such material(s) in my thesis.

I declare that this is a true copy of my thesis, including any final revisions, as approved by my thesis committee and the Graduate Studies office, and that this thesis has not been submitted for a higher degree to any other University or Institution.

ABSTRACT

This thesis investigates the agricultural greenhouse sector in a cold climate, which requires a large amount of natural gas for supplying the substantial heating demands. The heating demand of these structures is calculated, and potential sustainable design methods are implemented to reduce the reliance on carbon-based fuels. Assessment of the environmental impacts of a bell pepper greenhouse in Southwestern Ontario, Canada heated by natural gas was studied. A life cycle assessment (LCA) method is employed to scrutinize the bell pepper greenhouse, pinpointing areas that need improvement. It was concluded that Global Warming (GW) is the significant environmental hazard among other environmental categories (3.87e-2 kg CO_2-Eq). It should be noted, the main contributor to global warming is the natural gas being used as the heating resource (3.2e-2 kg CO_2-Eq). The analysis is extended to explore the deployment of solar energy as an alternative source for heating. Solar energy is found to be a superior alternative in terms of emissions. Furthermore, in order to integrate solar energy into the energy supplying systems of the greenhouses, a hybrid Solar Thermal/Photovoltaic-Battery Energy Storage (ST/PV-BES) system is modeled. Evaluation of the best configuration of photovoltaic (PV) and solar thermal (ST) modules, and battery energy storage (BES) size to have the minimum Levelized Cost of Energy (LCOE) was conducted. It is proved that the system is economically optimized. Moreover, to improve operational efficiency and reduce the energy demand of commercial greenhouses, parametric optimization of major growing environment variables including cladding material and window to wall ratio as well as the characteristics of the solar thermal model elements such as hot water tank capacity and heat exchanger effectiveness was carried out. It is demonstrated that the best greenhouse configuration which is a system with 80% window area and 20% brick wall area in both lower nodes and upper nodes results in heating and cooling demand energy reduction without significantly compromising the solar energy absorption. This scenario leads to increasing system performance from 36% to 39%. It is also concluded that doubling the tank capacity improves system performance from 36% to 43% and changing the heat exchanger effectiveness has minor impacts on the system performance.

DEDICATION

I dedicate this work to my parents, Vida and Shahbaz, and my sister, Sanaz, who have endlessly supported me throughout my life and given me the strength to reach for the stars and chase my dreams.

ACKNOWLEDGEMENTS

TABLE OF CONTENTS

LIST OF TABLES

LIST OF FIGURES

LIST OF ABBREVIATIONS/SYMBOLS

CHAPTER 2

2,4-D-Eq	Dichlorophenoxyacetic Acid Equivalent
AD	Acidification
CFC-11−Eq	Trichlorofluoromethane Equivalent
CO_2 −Eq	Carbon Dioxide Equivalent
CO_2	Carbon Dioxide
EU	Eutrophication
EC	Ecotoxicity
FU	Functional Unit
GHG	Greenhouse Gases
GW	Global Warming
H^+	Hydrogen Ion
LCA:	Life Cycle Assessment
LCC	Life Cycle Costing
LCI	Life Cycle Inventory
LCIA	Life Cycle Impact Assessment
N	Nitrogen
NOx	Nitrogen Oxides
OD	Ozone Depletion
ON	Ontario
PM2.5-Eq	Atmospheric Particulate Matter Equivalent
SM	Smog

CHAPTER 3

A. Parameters	
C_0	Total capital cost ($)
C_{PV}	Total capital cost of PV-BES system ($)
C_{ST}	Total capital cost of ST ($)
$C_{i,\,ST}^{CT}$	Annual carbon tax payment for fuel (natural gas) ($)
$C_{i,\,ST}^{CTS}$	Annual carbon tax savings ($)
$C_{i,\,PV}^{E}$	Annual Electricity cost to buy from the grid ($)
$C_{i,\,ST}^{f}$	Annual fuel cost for the axillary heating system
$C_{i,\,PV}^{O\&M}$	Annual operation and maintenance cost of PV-BES system ($)

$C_{i,\,ST}^{O\&M}$	Annual operation and maintenance cost of ST system ($)
C_i^{PV}	Total cost of PV-BES system for year i ($)
$C_{i,\,PV}^{S}$	Annual electricity income from selling electricity to the grid ($)
$C_{i,\,PV}^{Sa}$	Annual electricity saving ($)
$C_{i,\,ST}^{Sa}$	Annual fuel saving ($)
C_i^{ST}	Total cost of ST system for year i ($)
$C_{i,\,PV}^{R}$	Annual replacement cost of PV-BES system
CTi	Carbon Tax Inflation
d	Market discount rate
E_L^{PV}	Annual electricity generation of the PV-BES system (kWh)
E_L^{ST}	Annual heating generation of the solar thermal system (kWh)
Electricity i	Electricity price Inflation
i	Inflation rate
LRPi	LRP Inflation
NGi	Natural Gas Inflation

B.   Abbreviations

AH	Autonomy Hours
BES	Battery energy storage system
DHWS	Domestic Hot Water System
DOD	Depth of Discharge
FIT	Feed-in Tariff
LRP	Large Renewable Procurement
LCOE	Leveliezd Cost of Energy
LCS	Life Cycle Saving
MPPT	Maximum Power Point Tracker
NZEB	Net-Zero Energy Building
PBP	Payback Period
PV	Photovoltaic system
PVT	Photovoltaic-thermal
SOC	State of Charge
ST	Solar thermal system

CHAPTER 1

Introduction

1.1 Background

The governments' interest toward low-emission economy has been increased over the past years worldwide. Greenhouse gas emissions need to stabilize in 5~10 years to prevent climate change, and approach zero by the second half of the century [1]. Buildings' heating demand, and in particular those in cold climates, significantly rely on the energy production. The combustion of a carbon-based fuel such as natural gas, coal, gasoline, or propane typically provides heating energy demands. It leads to releasing greenhouse gases including carbon dioxide, methane and nitrous oxide into the atmosphere [2]. Converting the finite resources into usable forms and transporting them to the end-user around the world cause emissions. This fact highlights the urgent need to promote the development and implementation of advanced clean energy technologies to resolve the global challenges of energy stability, climate change and sustainability [3]. This work studies the agricultural greenhouse sector with a focus on greenhouses in cold climates. Greenhouse is an enclosed environment, covered with glass or a transparent plastic, providing a desirable microclimate for the growth of crops [4]. Since the covering materials are configured for optimum light transmission, a greenhouse environment's insulating characteristics are obviously inferior to those of a conventional building [5]. There is a part of the winter season where crops are present in the greenhouse regardless of farming schedules [6]. Greenhouses have substantial heating requirements in cold climates due to significant difference of up to 40°C between indoor and outdoor temperatures and the fact that operations can potentially reach 20 hectares in the site area. Usually, the heating systems, with consuming up to 90% of total energy demand, require the highest energy resources in greenhouses' operations [7]. Researchers have studied and proposed several energy management design and operating techniques for the greenhouses [8,9], for example, optimal positioning of the heating pipes, adjusting the set-point temperatures, and utilizing thermal curtains and a thermal mass on the interior of the greenhouse. The goal of this work is to go farther than management strategies and explore future greenhouse systems.

1.2 Methodology

This study mainly focuses on operating processes of greenhouses in southwestern Ontario. Ontario is the center of the development of greenhouses in North America. The required data have been collected from published studies and more comprehensive information from meetings with regional growers has been

supplemented. Two software programs have been used in this study, OpenLCA for Chapter 2 and TRNSYS for Chapters 3 and 4, respectively. OpenLCA is a footprint software and professional Life Cycle Assessment (LCA) with wide range of features and available databases which have been used in Chapter 2 to conduct the LCA study for greenhouses in Southwestern Ontario [10]. TRNSYS "Transient System Simulation Program", is a simulation environment for the transient simulation of energy systems [11]. TRNSYS has been used as a complete and extensible simulation environment to simulate the greenhouse microclimate and heating systems. The objective of Chapter 2 is to implement a Life Cycle Assessment (LCA) of bell pepper greenhouse production in Southwestern Ontario to investigate and evaluate the processes which cause the major environmental burdens. It represents solar energy as a low-emission alternative scenario to reduce the environmental harms caused by the conventional carbon-based fuels used for supplying the heating demand. Chapters 3 objectives include designing and modelling a solar hybrid (ST/PV-BES) system to meet the heating and electrical load of a commercial greenhouse Ontario, Canada. The system is technically and economically evaluated. Side-by-side PV and ST configurations are investigated in this chapter. The objective of Chapter 4 is minimizing the energy requirements for sample existing operations through parametric optimization of major growing environment variables including cladding material and window to wall ratio as well as the characteristics of the solar thermal model elements such as hot water tank capacity and heat exchanger effectiveness. This chapter utilizes the Transient Energy System Simulation Tool (TESST) and the Solar Thermal System model developed in Chapter 3 for parametric optimization and evaluating the system performance.

References

[1]   United Nations Environment Program (UNEP) (2014). The Emissions Gap Report 2014: A UNEP Synthesis Report http://www.unep.org/publications/ebooks/emissionsgapreport2014/

[2]   United States Environmental Protection Agency (USEPA) (2013). Inventory of U.S. Greenhouse Gas Emissions and Sinks: 1990-2011 http://www.epa.gov/energy/ghg-equivalencies-calculator-calculations-andreferences#vehicles

[3]   International Energy Agency (2012). Technology Roadmap – Solar Heating and Cooling, Paris, France

[4]   Semple, L. M. (2017). Heating Energy Demands and Sustainable Generation Concepts for Agricultural Greenhouses.

[5]   Fernandez, M.D., Rodrıguez, M.R., Maseda, F., Velo, R., Gonzalez, M.A. (2005). Modelling the Transient Thermal Behaviour of Sand Substrate heated by Electric Cables, Biosystems Engineering 90 (2), 203–215

[6]   Hemming, S., Kempkes, F.L.K., Janse, J. (2012). New Greenhouse Concept with High Insulating Double Glass and New Climate Control Strategies – Modelling and First Results from a Cucumber Experiment, Acta. Hort. 952, 231-239

[7]   Sturm, B., Maier, M., Royapoor, M., Joyce, S. (2014). Dependency of production planning on availability of thermal energy in commercial greenhouses-A case study in Germany, Applied Thermal Engineering 71, 239-247

[8]   Sethi, V.P., Sumathy, K., Lee, C., Pal, D.S. (2013). Thermal modeling aspects of solar greenhouse microclimate control: A review on heating technologies, Solar Energy 96, 56–82

[9]   Cuce, E., Harjunowibowo, D., Cuce, P.M. (2016). Renewable and sustainable energy saving strategies for greenhouse systems: A comprehensive review, Renewable and Sustainable Energy Reviews 64, 34-59

[10]   "OpenLCA Description". [Online]. Available: "https://www.openlca.org". [Accessed: 4-Jan-2021].

[11]   SEL, TRNSSOLAR, and Tess CSTB. Multizone Building Modelingwith Type56 and TRNBuild. TRNSYS;2004.

CHAPTER 2

Life Cycle Assessment of a Greenhouse Bell Pepper Production in Southwestern Ontario: Evaluating Non-renewable vs Renewable Heating Energy Systems

Sadaf Ekhtiari, Rupp Carriveau, David S-K. Ting
Turbulence and Energy Laboratory, University of Windsor
401 Sunset Ave, Windsor, ON, Canada

2.1 Introduction:

Predictions state that global population will reach nine billion by 2050, and that 80% of this population will live in urban areas [1]. This increase may cause a significant shift in the demand for food and vegetables [2,3]. Several solutions have been suggested to address this problem, among which urban agriculture – such as greenhouses – has proven promising for the future of food security [4]. Greenhouses can provide adaptive humidity, air temperature, and lighting for crop production [2]. In regions with cold climates and short growing seasons, such as Ontario, Canada, it is challenging to grow year-round vegetables; therefore, greenhouses are significantly utilized in this region to increase the agricultural yield per unit area [3]. In fact, Southwestern Ontario is home to the most greenhouses in North America, with 200 farms spread across 3,072 acres of harvested areas, producing 69% of the total agricultural production, including tomatoes, cucumbers, and peppers [5,6].

Although greenhouses can provide controlled environment for plant growth, they have a non-trivial environmental footprint. The great expansion of indoor agriculture systems can lead to increasing the energy demand. Energy is one of the largest concerns of the greenhouses in terms of cost and environmental harms [2]. Most of the greenhouses burn fossil fuels for heating the greenhouse space, which results in carbon dioxide (CO_2) emissions [2,7]. Moreover, the initial cost of fossil fuels is dramatically increasing [2]. These negative environmental impacts and limitation of fossil fuel resources [2] have increased interest to conduct studies on environmental effects of greenhouses, and the means to reduce their footprints and enhance their sustainability.

In the recent years, Life Cycle Assessment (LCA) has been used as a holistic technique for evaluating the environmental impact of agricultural products by identifying their lifetime energy and material usage, as well as their environmental releases. LCA techniques enable organizations to establish baseline environmental footprints and help them identify areas in which operations need improvements [9]. In general, the life cycle of products starts with raw material extraction and ends with end-of-life activities, which may include waste or recycling processes [8]. More specifically, each product has a special life cycle based on tits production process and region; therefore, LCA studies must be carried out for each region.

Numerous studies have investigated the LCA of varying kinds of fruits and vegetables in different regions. Each of these studies is unique in terms of its goal and system boundary. For instance, a cradle-to-gate LCA study was conducted on strawberries production in four states in the United States – California, Florida, North Carolina, and Oregon – to assess their environmental impacts [12]. The study mainly focused on global warming potential (GWP), concluding that the GWP of North Carolina's strawberry farms was the highest among the other states. Moreover, there have been several LCA studies on pineapple production in different countries, such as Costa Rica, Ghana, Uganda, and the Philippines [13-17]. Furthermore, [18] proposed a comparative LCA study on pineapples, avocados, and bananas in Costa Rica, Mexico, and Ecuador, respectively. The focus of the study was assessing the contribution of each of these fruits to GWP, and it was concluded that avocados have the largest effect on GWP when compared to the others. In addition, several LCA studies were done on tomato production in different regions in order to assess their harming of the environment – for example, in two Canadian provinces, Ontario [19] and Quebec [20], as well as other countries, such as Colombia [21] and Italy [22]. In another work, [23] conducted a gate-to-gate LCA study on crushing soybeans and rapeseeds, and refining crude soybean, rapeseed, and palm oil in Europe. This study revealed that the crushing step has the highest contribution to its environmental footprint. [24] presented a cradle-to-grave LCA study on the two central fruits of the Mediterranean fruit sector, peach and apple. The aim of the study was to determine the contributions of different stages of production to the environmental categories. It was concluded that the retail stage and agricultural stage are the main concerns. [25] conducted a comparative LCA study for three different crops – almond, pistachio, and apple – in Greece. It was revealed that the fertilizers, irrigation, and field management phases were the main hotspots in terms of contributing to environmental harm. Apples, however, showed the best environmental profile in relation to GHG emissions when compared to the almonds and pistachios. [26] presented an LCA study on bell pepper production in the Isfahan province of Iran. The focus of this study was to evaluate the environmental effects of bell pepper cultivation. It concluded that energy usage is the main contributor to the cultivation's environmental impact.

Another study that evaluated the life cycle of various products such as pepper, tomato, and watermelon in Italy proved that the highest contamination in all products, was due to two factors: packaging type and greenhouse structure [27]. Furthermore, in a different study [28], the energy consumption and environmental burdens of the pepper crop production in the Mediterranean region was evaluated using LCA methodology. The paper reported the amounts of global energy requirement, global warming potential, ozone depletion potential, acidification and eutrophication as 22.6 GJ, 1494.7 kg CO_2eq., 5.2E-04 kg CFC11eq., 9.5 kg SO_2eq. and 3.7 kg PO3- 4 eq., respectively, for the production of one tonne pepper crop. The environmental impacts of cucumber and tomato productions in both open field and greenhouse methods were investigated using LCA methodology [29]. It was proved that, for the production of one tonne of cucumber and tomato, cucumber production in greenhouses had a lower environmental impact than open-field production due to greenhouse production's higher yield and less total energy input. On the other hand, open-field tomato production had fewer environmental impacts than tomatoes produced in greenhouses, since greenhouses use natural gas as their heating source; in

addition, more diesel fuel is needed in greenhouses. The environmental impacts of the greenhouse tomato and cucumber were investigated in Isfahan, Iran. The results indicated that electricity, natural gas, and nylon inputs have the highest environmental impact among all the factors. It was also proved that greenhouse tomato production is less environmentally destructive than the greenhouse cucumber production [30]. In Brazil, the energy flow and environmental impacts of green coffee cultivation were evaluated. It was concluded that the use of chemical fertilizers had the most destructive environmental impact [31]. Another study focused on greenhouse gas emissions from strawberry production in a greenhouse in Japan. The process from farm to market was considered as system boundary. The study indicated that the highest shares of greenhouse gas emissions were related to fuel, electricity, and water [32]. In other studies, the environmental effects of the production of a number of foods – including chickpeas [33], peanuts [34], wheat [35], paddy [36] and milk [37] – were studied using LCA methods.

Despite the numerous studies conducted on greenhouse production and improvement scenarios in other regions, not many studies have focused on Canadian greenhouse production. Dry et al. [38] carried out a study based on energy modeling and data on the average vegetable production of Canadian greenhouses to assess the carbon emissions from greenhouses across Canada. Furthermore, integrated dairy farm/greenhouse systems were modeled in British Columbia, Canada in [39] by defining organic waste disposal as the main function of the product system.

Maintaining the proper balance of light and temperature is crucial for greenhouse production, and it requires a significant amount of heat in cold-temperature locations due to a wintry lack of light and cold-temperature conditions. Prior to 2008, the Ontario greenhouse industry had to deal with increasing energy costs to provide the required heating to meet demand [3]. Since then, following Europe's trend of sustainability, the energy efficiency of Ontario's greenhouses has been improved to reduce energy costs. Furthermore, minimizing environmental impacts has been attempted in response to concerns about climate change and water usage [40].

As highlighted above, there exists a number of LCA studies on bell pepper production in different regions of the world. Since factors like soil, mineral contents, water resources, and climate vary across each region, all these parameters impact the life cycle of the products, so separate LCA studies for a given product have to be carried out for each region. The Ontario bell pepper greenhouse industry is essential for the overall greenhouse vegetable production of both Ontario and Canada. In addition, the industry has been growing, and will continue to grow to meet competitive advantages. Furthermore, Ontario's ecosystems are quite different (i.e., in terms of climate and technology) from those elsewhere, so the effects of LCAs conducted elsewhere are not directly transferable to Southwestern Ontario's greenhouses. To the best of the authors' knowledge, there is no up-to-date study on the investigation of environmental impact categories for bell pepper production in Southwestern Ontario. Therefore, it is necessary to implement an LCA on bell pepper greenhouse production in Ontario. The main objectives of this study are to (1) evaluate and identify the direct and indirect environmental impacts of

greenhouse bell pepper production in Southwestern Ontario; (2) investigate the activities/processes in the life cycle that are responsible for its major environmental burdens (i.e., hotspots); and (3) represent different production scenarios which can reduce the environmental load caused by the hotspots. It is hypothesized that the most environmental harm stems from the source of energy required for heating the greenhouse.

2.2 Methodology

This study used LCA tools in order to assess the cradle-to-gate environmental impacts of the bell pepper greenhouses in Southwestern Ontario. According to the ISO 14044 framework, the LCA methodology includes four initial phases [10]. The first phase is goal and scope definition. In this phase, the functional unit and system boundaries of the study are defined. The second phase is related to the life cycle inventory (LCI). This phase can estimate the rate of consumption of resources and the amount of emissions that will be produced by the product during its manufacture. It also provides a list of the data needed for the study. The LCI can be illustrated with a flow diagram and a table of the data collected. The third phase is the life cycle impacts assessment (LCIA). In this phase, the important environmental impacts can be defined and categorized in terms of their significances. Finally, after the above three stages, the last phase of LCA is the interpretation of the results to meet the defined goal and scope of the study. The life cycle assessment framework is demonstrated in Figure 2.1.
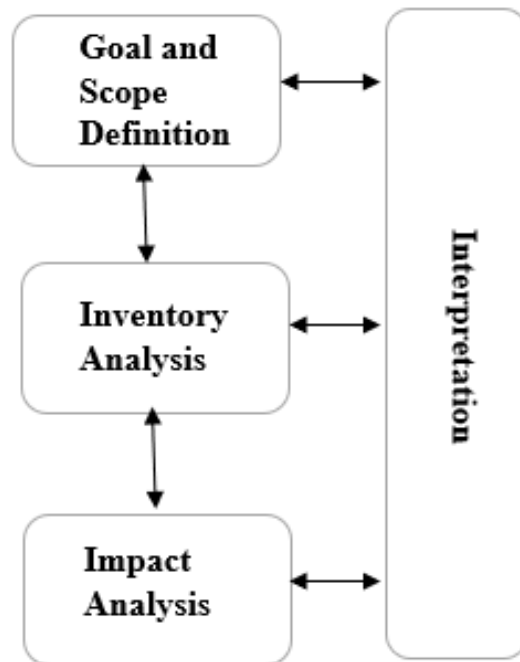
Figure 2.1 - Life cycle assessment framework

2.2.1 Goal and Scope Definition

The goal of this LCA study is to assess the environmental impacts of bell pepper production in the greenhouses in the region of Southwestern Ontario. The scope of the study clarifies the functional unit, which is 1 kg of bell pepper; this is an appropriate functional unit that can be used for other vegetables as well. In this proposed study, a cradle-to-gate approach is considered as a system boundary, which includes bell pepper seedlings and their cultivation, climate control (natural gas combustion for heating and electricity used for cooling, ventilation, and lighting), on-site packaging, and waste management. The greenhouse infrastructure, storage, distribution, and usage phases of the bell peppers were excluded from the study since the focus of the study is on the facilities' activities and operations.

2.2.2 Life Cycle Inventory (LCI)

This is the second phase of the LCA, which involves collecting and evaluating the inputs and outputs of producing 1 kg of bell peppers in the greenhouse. The required data for conducting this LCA study are divided into two groups: background and foreground data. The background data includes the production process of the inputs, such as manufacturing of chemical inputs, production and consumption of fuel and energy feedstocks, fuel consumption and released emissions of different transportation modes. The AGRIBALYSE v.1.3 database – a database for agricultural activities included in the OpenLCA (version 1.8) software – was used to provide the background data. Based on this database, the energy source for electricity consumption was considered to be the average Ontario mixture of electricity feedstocks (34% nuclear, 29% natural gas, 23% hydro, and 12% wind, with less than 1% biofuel and 1% solar) [41]. The foreground data (annual electricity and natural gas consumption, cultivation periods, water consumption, annual average yield, and total area of the greenhouse) were collected from the growers through interviews and questionnaires. The other required foreground data, such as chemical fertilizers, pesticides, growing mediums, and packaging materials, were collected through observation, sampling, and literature [1,7,10,21]. Table 2.1 demonstrates the LCI data for 1 kg of bell pepper production. Moreover, Figure 2.2 depicts an LCA system boundary flow diagram.

Table 2.1 - The inflows and outflows of the process of 1 kg of bell pepper production in the region of Southwestern Ontario

Nursery	
Bell pepper seeds (gr)	0.1
Seedlings (items)	1
Pesticides	
Fungicides (kg)	0.00005
Insecticides (kg)	0.00004
Fertilizers	
Calcium Nitrate(kg)	0.0117
Potassium Nitrate (kg)	0.0119
Potassium Sulphate (kg)	0.0015
Potassium Chloride (kg)	0.00113
Magnesium Sulphate (kg)	0.00318
Ammonium Nitrate (kg)	0.00412
Energy	
Heating – Natural gas (GJ)	0.256
Electricity (kWh)	0.056
Packaging Material	
Cardboard boxes (kg)	0.084
Water	
Water Consumption (L)	18.4
Waste	
Packaging waste (t)	0.0000237
Waste (inorganic, landfill) (t)	0.0000647
Growing Media	
Rockwool Substrate (kg)	0.00969
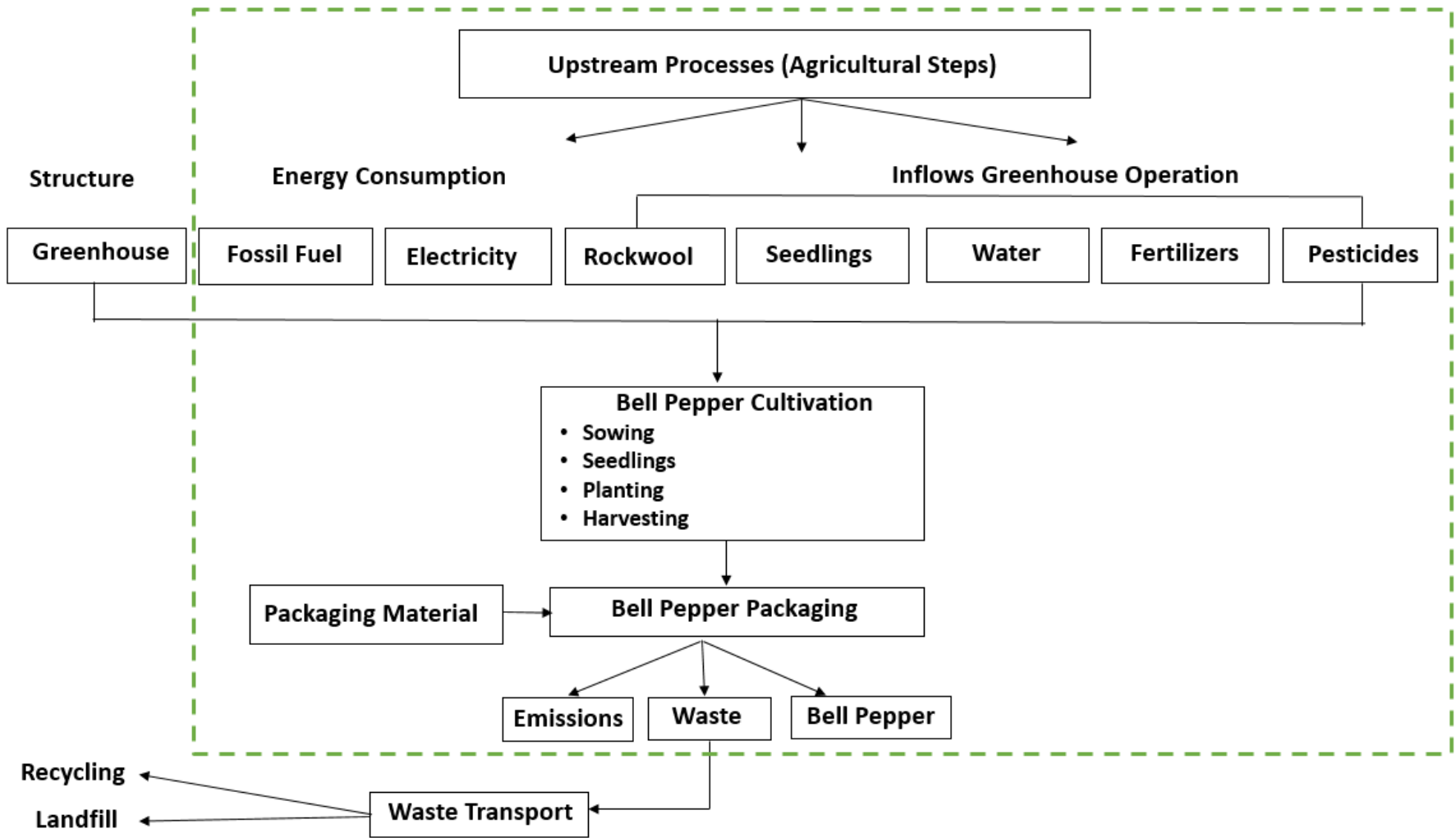
Figure 2.2 - System boundaries for the life cycle assessment of bell pepper production

2.2.2.1 Modelling Average Greenhouse Production System

The study area for this study is Leamington in Essex County, Ontario, Canada. Canada emerged as the largest producer of greenhouse products in North America, with Ontario leading the greenhouse vegetable sector by representing 69% of the total production and harvested area in Canada. Among this figure, 33% accounts for the harvested area of bell pepper production producing 438,674 tons per square meter annually [5]. The typical greenhouse structure in this study area is made from steel, aluminum, and plastic (polyethylene) as the covering material. These components need maintenance based on their lifespans. In this study, the lifespans of both steel and aluminum are considered to be 25 years, and with plastic lasting four years. It was assumed that the modeled greenhouse was a 24-acre, gutter-connected, venlo-type structure located in Essex County, Ontario, Canada. The building has a gutter height of 5.5 m and a roof slope of 25°. In order to normalize the model, one acre of the greenhouse was considered to produce 20,000 kg.

2.2.2.2 Bell Pepper Seedlings and Cultivation

When bell pepper seedlings are produced in the greenhouses, the seeds are planted in soil in plastic trays, then they are fertilized and watered. Seedlings are started in the spring, when the soil temperature is around 60 F° and are then transplanted in the first month of the winter [42,43]. Based on the average of the nurseries' approximate estimations (confidential data), the energy inputs of seedling production for a typical greenhouse is assumed to be 3% of the annual energy demand for the greenhouse production of bell peppers. In addition to this, it is assumed that all other inputs – for example, fertilizer and water – are also 3% of the annual consumption. The necessary operations for bell pepper cultivation are sowing and seedlings, the fertigation system, closed loop water consumption, pest and disease control, rockwool consumption, and then harvesting activities. The required energy inputs for the manufacturing of all the material inputs (i.e., rockwool, fertilizer, pesticides, etc.) are also included.

2.2.2.3 Climate Control

Energy sources for bell pepper greenhouses mainly include (1) electricity for ventilation, cooling, and lighting systems, and (2) natural gas for heating. Most greenhouses, including the Southwestern Ontario greenhouses, have fossil fuel-based central heating systems. Natural gas combustion is the most common type of the fossil fuel used in greenhouses. It merits mentioning that some of the growers use other types of heating systems, such as bunker oil, hot water, or others [7].

2.2.2.4 Packaging and Waste Management

In order to distribute the bell peppers, they will be packed with plastics and cardboard boxes. These packaging materials are considered part of the waste produced during the bell pepper production process. Some of the wastes are related to the greenhouse infrastructure, such as the plastic covering, which was assumed to be recycled [44]. Another type of waste from greenhouse operations is organic

waste, which will be generated during the harvesting activities. The packaging materials and the residue of the damaged rockwool are considered to be the landfill wastes.

2.2.2.5 Alternative Scenario Description

It has been observed that some of the greenhouses in the Leamington area use only natural gas for heating, while others have considered using solar energy as a heating source; therefore, two alternative heating scenarios were modeled based on (1) 100% natural gas and (2) 100% solar energy. In this proposed LCA study, the reference greenhouse uses 100% natural gas as a heating resource, and the environmental impacts were assessed based on this assumption. Then, one alternative heating scenario was modeled based on using 100% solar energy for heating, instead of using natural gas; this was done to compare the environmental impacts caused by these two energy resources [21].

2.2.3   Life Cycle Impact Assessment (LCIA) Method

The OpenLCA (version 1.8) software was used for the LCA modeling. The TRACI 2.1 life cycle impact assessment (LCIA) method was used for analysis of the mid-level impacts. TRACI 2.1 is the only available LCIA method based on North American characterization factors, and it applies Canada's 2005 normalization factors [45]. According to this impact assessment method, a subset of the impact categories was chosen to evaluate the effects of the different inputs and outputs of the aforementioned process on the non-renewable energy sources, health, and ecosystem. The TRACI impact assessment method will focus on the global warming potential (GWP), acidification potential (AP), ozone depletion (OD), eutrophication potential (EP), ecotoxicity, and respiratory effects (RE). Table 2.2 shows a description of the TRACI impact categories which were used in this LCA study.

Table 2.2 - Description of the environmental impact categories of this LCA study

Impact Category	Unit	Description
Acidification	moles of H+-Eq	Acidification leads to increasing the level of hydrogen ion $[H^+]$ in water and soil because of some processes [1].
Ecotoxicity	kg 2,4-D-Eq	Ecotoxicity will be caused because of toxic chemicals which will be produced to the environment due to man-made activities and has adverse effect on the sustainability indicators [46].
Global Warming	kg CO2-Eq	Global warming will be caused due to some emissions such as GHG (greenhouse gas emissions) which will be produced because of some activities. The GHG trap heat from the sunlight and then reflect it to the atmosphere [1, 16, 47].
Eutrophication	kg N	The Eutrophication is the process which leads to enrichment of dissolved nutrients in the water resulting in growth of algae life, so the oxygen depletion of the water will be caused [46].
Ozone Depletion	kg CFC-11-Eq	Chlorofluorocarbons (CFCs) and hydrochlorofluorocarbons (HCFCs) release due to industries and human activities and will destroy the earth's protective ozone layer which lead to Ozone depletion. The higher rate of UVB rays will be caused by the ozone depletion [48].
SMOG (Photochemical Oxidation)	kg NOx-Eq	SMOG will be produced because of the reaction between ultraviolet ray of the sun and nitrogen oxides in the atmosphere. This is harmful for eye and causes respiratory irrigation.
Human Health (Respiratory Effects, Average)	kg PM2.5-Eq	The respiratory effect is a kind of disease which damages the cells of the lung tissue because of the pollutants such as radicals, metals, emissions in the air, etc. [49].

2.3 Results and Discussion

This section presents the overall LCA results, contribution analysis, and alternative heating scenario.

2.3.1 Overall LCA Results

Table 2.3 illustrates the results of the LCIA based on the LCI inputs and outputs. Thus, it outlines the different factors that impact the environment. The most significant environmental impact is caused by global warming, which is due to greenhouse operation. Acidification is the next most significant environmental concern, followed, in order, by smog (photochemical oxidation), human health (respiratory effects), eutrophication, ecotoxicity, and ozone depletion.

Table 2.3 - The LCIA results for each single indicator

Impact Category	Unit	Amount
Global Warming	kg CO2-Eq	3.87e-2
Acidification	moles of H+-Eq	6.4e-4
SMOG (Photochemical Oxidation)	kg NOx-Eq	1.6e-5
Human Health (Respiratory Effects)	kg PM2.5-Eq	8.5e-7
Eutrophication	kg N	6.724e-7
Ecotoxicity	kg 2,4-D-Eq	5.033e-7
Ozone Depletion	kg CFC-11-Eq	8.73e-10

2.3.2   Environmental Contribution of Greenhouse Stages

One of the main objectives of this proposed study is analyzing the contribution of each stage of bell pepper production in the greenhouse. According to Figure 2.3 and Table 2.4, the natural gas for heating creates the main environmental hazards. With respect to each environmental factor, heat makes a significant contribution. It contributes to 15% of ecotoxicity and 85% of global warming. The next significant contributor is fertilizers, which, at its lowest rate, contributes to 8% of global warming, but 61.5% of ecotoxicity. Electricity and pesticides rank as the third highest, contributing to between 3% and 15% of six environmental factors, including GW and EC, SM, OD, AD, and EU. The other contributors, in order, were rockwool, water, waste, and packaging. Based on the database used, packaging materials are wood-free and have significantly less impact, which is not visible in Figure 2.3. As depicted in the figure, the main contributor to the environmental hazards is heating; thus, an alternative heating scenario was defined to address this problem and to conduct a comparative case study on the environmental impacts of these two types of energy resources.
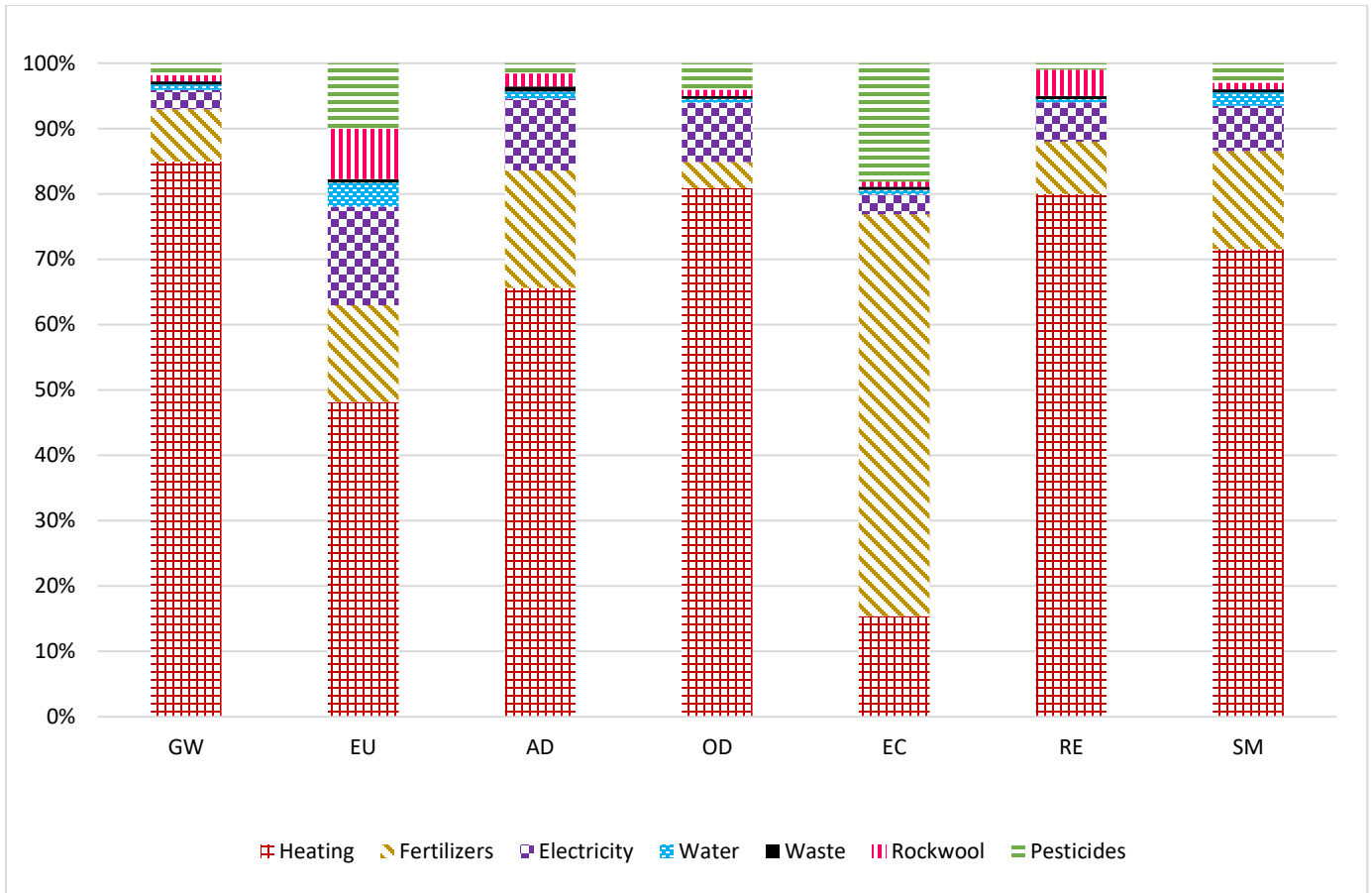
Figure 2.3 - Contribution of life cycle impacts of producing 1 kg of packaged bell pepper in the region of Leamington, Ontario. GW = Global Warming, EU = Eutrophication, AD = Acidification, OD = Ozone Depletion, EC = Ecotoxicity, RE = Respiratory Effects

Table 2.4 - Contribution analysis of the cradle-to-gate life cycle impacts of producing 1 kg of packaged bell peppers in Ontario greenhouse.

Category \ Contributor	GW	AD	Smog	EU	EC	RE	OD
Heating	3.29e-2	4.20e-4	1.19e-5	3.23e-7	7.75e-8	6.8e-7	7.01e-10
Fertilizers	3.10e-3	1.15e-4	2.49e-6	9.92e-8	3.10e-7	6.8e-8	3.49e-11
Electricity	1.16e-3	7.04e-5	1.16e-6	1.01e-7	1.51e-8	5.10e-8	7.86e-11
Water	3.10e-4	6.80e-6	3.33e-7	2.48e-8	3.52e-9	4.30e-9	5.24e-12
Waste	1.90e-4	5.00e-6	8.32e-8	3.36e-9	2.52e-2	4.3e-9	3.49e-12
Rockwool	3.80e-4	1.28e-5	1.66e-7	5.17e-8	4.03e-9	3.4e-8	8.73e-12
Pesticides	7.00e-4	1.00e-5	4.99e-7	6.72e-8	9.11e-8	8.5e-9	3.49e-11
Total	3.87e-2	6.4e-4	1.6e-5	6.7e-7	5.03e-7	8.5e-7	8.67e-10

15

2.3.3 Alternative Heating Energy Improvement Scenario

As demonstrated in Figure 2.3, the main hotspot for creating environmental hazards is the energy involved in heating the greenhouse. Although the other contributors affect the environment, when compared to natural gas being used as a heating resource, their impacts are negligible. One of the aims of this study is to provide an alternative heating scenario, as well as comparing its results to when natural gas is used as a heating resource. The offered alternative uses 100% solar energy for heating the greenhouse. In order to analyze the environmental impacts of this alternative, another assessment was done using the same software and databases (OpenLCA v.1.8 and AGRIBALYSE v.1.3) based on ISO 14044 framework.

As shown in Figure 2.4, solar energy was substituted for natural gas as a heating source for the greenhouse, and, based on this change, the environmental impacts caused by the natural gas were eliminated. This left fertilizers as the largest contributor to environmental hazards, ranging from 55% to 64% in each of the environmental categories. Thus, after addressing the use of natural gas, fertilizers became the central environmental concern. The next main contribution to environmental hazards was electricity, which contributed between 16% and 24% in each of the categories. The contribution of pesticides was next after electricity, contributing between 12% and 18% of the environmental categories. The other contributors, in order, were rockwool, water, waste, and packaging.
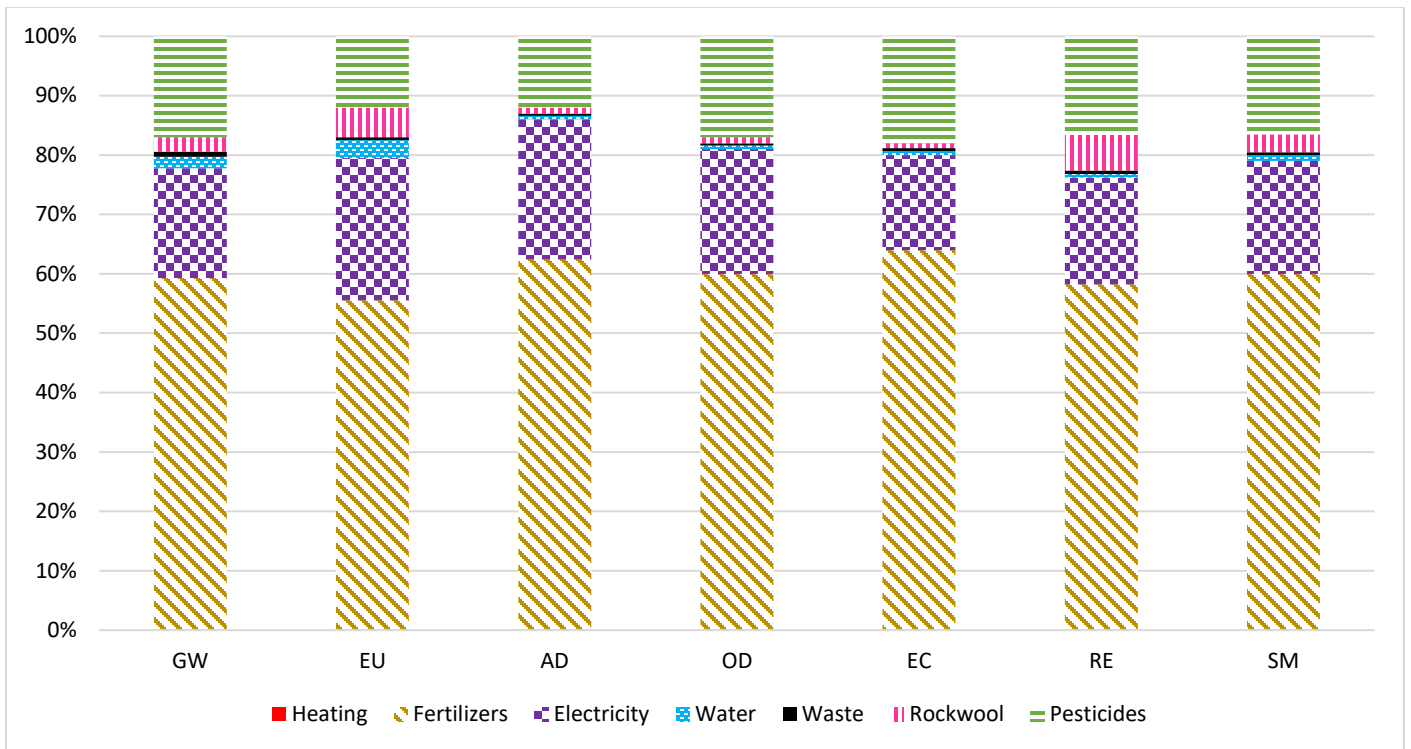
Figure 2.4 - Contribution analysis of life cycle impacts of substituting natural gas with solar energy for the heat supply. GW = Global Warming, EU = Eutrophication, AD = Acidification, OD = Ozone Depletion, EC = Ecotoxicity, RE = Respiratory Effects

Table 2.5 shows the improvement rate for each environmental category when solar energy was utilized as the main heating resource for the greenhouse operations instead of natural gas. As depicted in the table below, substituting solar energy for fossil fuel will result in reducing global warming – the main environmental harm – by 78.4%. Also, this alteration can reduce the other environmental categories, such as respiratory effect, ozone depletion, and smog, by around 70%. The improvement rates of the other environmental categories, acidification, eutrophication, and ecotoxicity, are 49%, 39%, and 22%, respectively.

Table 2.5 - Comparison of results between using solar energy and fossil fuel as heating resources

Impact Category	Unit	Solar Energy	Fossil Fuel	Improvement Rate (%)
Global Warming	kg CO2-Eq	8.00e-3	3.7e-2	78.4
Acidification	Moles of H+-Eq	3.20e-4	6.3e-4	49.2
SMOG (Photochemical Oxidation)	kg NOx-Eq	4.68e-6	1.603e-5	70.8
Eutrophication	kg N	4.10e-7	6.724e-7	39.0
Ecotoxicity	kg 2,4-D-Eq	3.93e-7	5.033e-7	21.9
Human Health (respiratory effects)	kg PM2.5-Eq	2.20e-7	8.5e-7	74.1
Ozone Depletion	kg CFC-11-Eq	2.50e-10	8.73e-10	71.4

2.4 Conclusion

As the population grows, the demand for foods like vegetables increases as well. Modern agriculture plays a significant role in supplying these requirements and providing food security. The aim of this study was to (1) determine and identify the direct and indirect environmental impacts of greenhouse bell pepper production in Southwestern Ontario; (2) investigate the activities/processes in the life cycle that are responsible for the major environmental burdens (i.e., hotspots); and (3) represent different production scenarios which can reduce the environmental impact caused by the hotspots. The results demonstrate that global warming is the main environmental hazard among the other environmental categories. Furthermore, natural gas, a type of fossil fuel that is used as the energy source for heating the greenhouses, was the main contributor to the global warming by contributing around 85%. Also, it is a significant contributor to other forms of environmental harm, with amounts ranging from 15% to 85%. This conclusion underscores the importance of studying the effects of energy alternatives on the environment. Thus, the proposed study suggests utilizing renewable energy (such as solar energy) as the heating resource instead of natural gas in order to reduce the environmental impacts. It was demonstrated that adopting this alternative can lead to eliminating the environmental hazards of using natural gas in the greenhouses. Moreover, the amount of environmental harm can reduce significantly, including 22% for ecotoxicity and 74% for global warming. Therefore, by using renewable energy instead of fossil fuels, greenhouses can develop a more sustainable model for modern agriculture. Further study is required, however, to investigate the feasibility of utilizing solar energy in the greenhouses' systems. As a future study, one can conduct a life cycle costing (LCC) analysis on using solar energy as the main heating source for greenhouses. The LCC can help determine if this alternative can be economically sustainable or if other actions are needed to be applied by the industry to make it more sustainable.

References

[1]   The United Nations. World Population Prospects: The 2017 Revision; United Nations: New York, NY, USA, 2017.

[2]   Hassanien, R. H. E., Li, M., & Lin, W. D. (2016). Advanced applications of solar energy in agricultural greenhouses. Renewable and Sustainable Energy Reviews, 54, 989-1001.

[3]   Dias, G. M., Ayer, N. W., Khosla, S., Van Acker, R., Young, S. B., Whitney, S., & Hendricks, P. (2017). Life cycle perspectives on the sustainability of Ontario greenhouse tomato production: Benchmarking and improvement opportunities. Journal of Cleaner Production, 140, 831-839.

[4]   Al-Kodmany, K. (2020). The Vertical Farm: Are We There Yet?. In Environmental Management of Air, Water, Agriculture, and Energy (pp. 53-96). CRC Press.

[5]   Agriculture and Agri-Food Canada (AAFC), "Statistical Overview of the Canadian Greenhouse Vegetable Industry, 2017." [Online]. Available: http://www.agr.gc.ca/eng/industry-markets-and-trade/canadian-agri-food-sector-intelligence/horticulture/horticulture-sector-reports/statistical-overview-of-the-canadian-greenhouse-vegetable-industry-2017/?id=1549048060760. [Accessed: 5-Aug-2020].

[6]   Ontario Greenhouse Vegetable Growers, "Fact Sheet," 2019.

[7]   Energy and environmental evaluation of greenhouse bell pepper production with life cycle assessment approach

[8]   Hendricks, P. (2012). "Life cycle assessment of greenhouse tomato (Solanum lycopersicum L.) production in Southwestern Ontario" M.S. thesis, Univ. Guelph, Guelph, ON, Canada, 2012.

[9]   Dr. Rajeev Ruparathna. " Life Cycle Thinking and Management. " University of Windsor, May 2019. Class Lecture

[10]   ISO, I. for S.(2006b) ISO 14044: 2006-Environmental management-Life cycle assessment-Requirements and guidelines. International Organization for Standardization.

[11]   Roy, P., Nei, D., Orikasa, T., Xu, Q., Okadome, H., Nakamura, N., & Shiina, T. (2009). A review of life cycle assessment (LCA) on some food products. Journal of food engineering, 90(1), 1-10.

[12]   Tabatabaie, S. M. H., & Murthy, G. S. (2016). Cradle to farm gate life cycle assessment of strawberry production in the United States. Journal of Cleaner Production, 127, 548-554.

[13]   Ingwersen, W. W. (2012). Life cycle assessment of fresh pineapple from Costa Rica. Journal of Cleaner Production, 35, 152-163.

[14]   Adebah, E. C., Langeveld, C. A., & Kermah, M. (2010). Environmental impact of organic pineapple production in Ghana: a comparison of two farms using Life Cycle Assessment

(LCA) approach. In VII International Conference on Life Cycle Assessment in the Agri-food Sector, Bari, Italy (pp. 325-330). Universita degli Studi di Bari Aldo Moro.

[15] Antwi, V. (2014). Use of monte carlo analysis in life cycle assessment: case study–fruits processing plant in Ghana (Doctoral dissertation).

[16] Mfitumukiza, D., Nambasa, H., & Walakira, P. (2019). Life cycle assessment of products from agro-based companies in Uganda. The International Journal of Life Cycle Assessment, 24(11), 1925-1936.

[17] de Ramos, R. M. Q., & Taboada, E. B. (2018). Cradle-to-Gate Life Cycle Assessment of Fresh and Processed Pineapple in the Philippines. Nature Environment and Pollution Technology, 17(3), 783-790.

[18] Hadjian, P., Egle, J., & Griesshammer, R. Life Cycle Assessment of Three Tropical Fruits (Avocado, Banana, Pineapple).

[19] Dias, G. M., Ayer, N. W., Khosla, S., Van Acker, R., Young, S. B., Whitney, S., & Hendricks, P. (2017). Life cycle perspectives on the sustainability of Ontario greenhouse tomato production: Benchmarking and improvement opportunities. Journal of Cleaner Production, 140, 831-839.

[20] Andrews, E., Lesage, P., Benoît, C., Parent, J., Norris, G., & Revéret, J. P. (2009). Life cycle attribute assessment: case study of Quebec greenhouse tomatoes. Journal of industrial ecology, 13(4), 565-578.

[21] Bojacá, C. R., Wyckhuys, K. A., & Schrevens, E. (2014). Life cycle assessment of Colombian greenhouse tomato production based on farmer-level survey data. Journal of Cleaner Production, 69, 26-33.

[22] Manfredi, M., & Vignali, G. (2014). Life cycle assessment of a packaged tomato puree: a comparison of environmental impacts produced by different life cycle phases. Journal of Cleaner Production, 73, 275-284.

[23] Schneider, L., & Finkbeiner, M. (2013). Life cycle assessment of EU oilseed crushing and vegetable oil refining. FEDIOIL Report, May.

[24] Vinyes, E., Asin, L., Alegre, S., Muñoz, P., Boschmonart, J., & Gasol, C. M. (2017). Life Cycle Assessment of apple and peach production, distribution and consumption in Mediterranean fruit sector. Journal of Cleaner Production, 149, 313-320.

[25] Bartzas, G., Vamvuka, D., & Komnitsas, K. (2017). Comparative life cycle assessment of pistachio, almond and apple production. Information processing in agriculture, 4(3), 188-198.

[26] Naderi, S. A., Dehkordi, A. L., & Taki, M. (2019). Energy and environmental evaluation of greenhouse bell pepper production with life cycle assessment approach. Environmental and Sustainability Indicators, 3, 100011.

[27]   Cellura, M., Longo, S., Mistretta, M., 2012a. Life Cycle Assessment (LCA) of protected crops: an Italian case study. J. Clean. Prod. 28, 56–62.

[28]   Cellura, M., Ardente, F., Longo, S., 2012b. From the LCA of food products to the environmental assessment of protected crops districts: a case-study in the south of Italy. J. Environ. Manag. 93, 194–208.

[29]   Zarei, M.J., Kazemi, N., Marzban, A., 2019. Life cycle environmental impacts of cucumber and tomato production in openfield and greenhouse. J. Saudi Soc. Agric. 18 (3), 249–255.

[30]   Khoshnevisan, B., Rafiee, S., Omid, M., Mousazadeh, H., Clark, S., 2014a. Environmental impact assessment of tomato and cucumber cultivation in greenhouses using life cycle assessment and adaptive neuro-fuzzy inference system. J. Clean. Prod. 73, 183–192.

[31]   Coltro, L., Mourad, A., Oliveira, P., Baddini, J., Kletecke, R., 2006. Environmental profile of Brazilian green coffee (6 pp). Int. J. Life Cycle Assess. 11 (1), 16–21.

[32]   Yoshikawa, N., Amano, K., Shimada, K., 2008. Evaluation of environmental loads related to fruit and vegetable consumption using the hybrid LCA method: Japanese case study. In: Life Cycle Assessment VIII, September 30- October 2, Seattle.

[33]   Elhami, B., Akram, A., Khanali, M., 2016. Optimization of energy consumption and environmental impacts of chickpea production using data envelopment analysis (DEA) and multi objective genetic algorithm (MOGA) approaches. Inf. Process. Agric.3 (3), 190–205.

[34]   Nikkhah, A., Taheri-Rad, A.R., Khojastehpour, M., Emadi, B., Khorramdel, S., 2015. Environmental impacts of peanut production system using life cycle assessment methodology. J. Clean. Prod. 92, 84–90.

[35]   Fathollahi, H., Mousavi-Avval, S.H., Akram, A., Rafiee, S., 2018. Comparative energy, economic and environmental analyses of forage production systems for dairy farming. J. Clean. Prod. 182, 852–862.

[36]   Nabavi-Pelesaraei, Ashkan, Rafiee, Shahin, Mohtasebi, Seyed Saeid, Hosseinzadeh-Bandbafha, Homa, Chau, Kwok-wing, 2018. Integration of artificial intelligence methods and life cycle assessment to predict energy output and environmental impacts of paddy production. Sci. Total Environ. 631–632, 1279–1294.

[37]   Rafiee, S., Khoshnevisan, B., Mohammadi, I., Aghbashlo, M., mousazadeh, H., Clark, S., 2016. Sustainability evaluation of pasteurized milk production with a life cycle assessment approach: an Iranian case study. Sci. Total Environ. 562, 614–627.

[38]   Dyer, J.A., Desjardins, R.L., Karimi-Zindashty, Y., McConkey, B.G., 2011. Comparing fossil CO_2 emissions from vegetable greenhouses in Canada with CO_2 emissions from importing vegetables from the southern USA. Energy Sustain. Dev. 15, 451e459.

[39]   Zhang, S., Bi, X.T., Clift, R., 2013. A life cycle assessment of integrated dairy farm greenhouse systems in British Columbia. Bioresour. Technol. 150, 496e505.

[40] Mann, H., 2012. Greenhouse wastewater discharges provoke legislation debate. Better Farming. At: www.betterfarming.com/online-news/greenhousewastewater-discharges-provoke-legislation-debate-5435 (Published:18.5.2012, accessed 10.94.16).

[41] IESO. Ontario's Energy Capacity. https://ieso.ca/en/Learn/Ontario-Supply-Mix/Ontario-Energy-Capacity. Accessed Nov. 16th,2020

[42] Tomato & Pepper Fertilizer, available online: https://homeguides.sfgate.com/tomato-pepper-fertilizer-43447.html [Aug 12, 2019].

[43] Jolliffe, P. A., & Gaye, M. M. (1995). Dynamics of growth and yield component responses of bell peppers (Capsicum annuum L.) to row covers and population density. Scientia Horticulturae, 62(3), 153-164.

[44] What are the Most Recyclable Materials? available online: https://www.azocleantech.com/article.aspx?ArticleID=585 [Aug 12, 2019].

[45] Bare, J.C., Norris, G.A., Pennington, D.W., McKone, T., 2003. TRACI: the tool for the reduction and assessment of chemical and other environmental impacts. J. Ind. Ecol. 6, 49e78

[46] Page, G., Ridoutt, B., & Bellotti, B. (2014). Location and technology options to reduce environmental impacts from agriculture. Journal of cleaner production, 81, 130-136.

[47] Sanscartier, D., Deen, B., Dias, G., MacLean, H. L., Dadfar, H., McDonald, I., & Kludze, H. (2014). Implications of land class and environmental factors on life cycle GHG emissions of Miscanthus as a bioenergy feedstock. Gcb Bioenergy, 6(4), 401-413.

[48] Chlorofluorocarbons (CFCs) and hydrofluorocarbons (HFCs). https://www.pca.state.mn.us/air/chlorofluorocarbons-cfcs-and-hydrofluorocarbons-hfcs. Accessed Nov 17th, 2020

[49] Air Pollutants Affect the Respiratory and Cardiovascular System, available online: https://www.disabled-world.com/health/respiratory/air-pollutants.php [Aug 12, 2019]

CHAPTER 3

Hybrid Solar Thermal/Photovoltaic-Battery Energy Storage System in a Commercial Greenhouse: Performance and Economic Analysis

Zahra Naghibi, Sadaf Ekhtiari, Rupp Carriveau, David S-K. Ting
Turbulence and Energy Laboratory, University of Windsor
401 Sunset Ave, Windsor, ON, Canada

3.1 Introduction

In cold climate regions, like Canada, a short growing season makes it challenging to meet vegetable demand year-round unless they are produced in greenhouses [1]. Southwestern Ontario has the highest density of the vegetable greenhouses in North America which has been expanded by 49% since 2012 [3],. Moreover, a multi-decade trend of growth is anticipated for the acreages of the greenhouses in this region [2].

This rapidly expanding sector will demand significant energy for heating and electricity. Specifically, in the Kingsville-Leamington region, it was predicted that the electricity demand will be increased by more than 200 percent from 2018 to 2024. According to IESO, it was expected the Ontario's greenhouses electricity consumption increase 180 percent from 1.4 TWh in 2018 to 3.9 TWh by 2024 [4]. Most of the energy needed for the heating is supplied by the province's fuel sector, and the required electricity is met mostly by the grid [5]. The combined economic and environmental costs associated with fossil fuels have increased interest in the concept of renewable energy technologies to meet both heat and electricity demands. Although the grid electricity system in Ontario is 95% carbon-free, transmission constraints have limited the ability of the grid to meet the planned massive sector expansion [6]. Among all the renewable resources, solar energy has gained particular attention owing to its abundance, environmental profile, and falling costs [7]–[11]. Solar systems can provide both electricity and heating depending on the technology used. Solar thermal (ST) collectors can provide heat to cover the heating load, and photovoltaic (PV) modules can provide electricity to meet the electrical loads.

Many researchers have evaluated PV and ST systems as stand-alone systems [13]–[20] and have largely only analyzed simultaneous PV and ST systems on smaller scale applications (i.e. residential, smaller commercial). Liao et al. [21] studied the economic benefits of a distributed system with PV and BES on the overall life cycle in the context of an industrial zone in Shanghai. It was concluded that the net present value (NPV) of a PV-BES system with an optimised configuration is higher than the NPV of a PV system alone. Sharadga et al. [22] presented a study on PV/T system which is a combination of solar photovoltaic cells and solar thermal collector. The hybrid system uses the cooling water of a concentrated PV/T as a preheated water for lithium bromide-water-based Kalina cycle. It was concluded that a) the overall efficiency range increases from 18%-23% to 22%-27% by combining PV/T with the proposed solar Kalina cycle and b) the

electrical conversion efficiency of the proposed system is 40% to 68% more compared to PV/T alone system. Here we consider the side-by-side configurations of PV and ST systems for an industrial scale greenhouse. We do not consider PVT technology in this study. For reference, side-by-side configurations of PV and ST systems have had many applications in net-zero energy houses (NZEH). For instance, Croxford and Scott [23] compared two solar systems for a residential block in London, UK. They examined two solar systems, called the nominal solar thermal system, and building integrated photovoltaic roof. The nominal solar thermal system consisted of solar panels, electric pumps, and a PV system to meet the electricity demand of the pumps. The building integrated PV roof consisted of 13.3 kWp PV panels and inverters. Both PV and ST systems demonstrated the potential to contribute significantly to supply residential energy demand and reduce CO_2 emissions. According to the results, the carbon payback for ST and PV systems was 2 years and 6 years, respectively. The carbon payback is the number of service years required to offset the carbon emissions generated to manufacture the PV and ST systems [24]. Leckner and Zmeureanu [25] presented the life cycle cost and life cycle energy analysis of a NZEH that had several combinations of PV and ST. They showed that a combination of 4 flat-plate solar collectors and 35.8 PV modules could supply14,000 kWh, (requirement of their subject NZEH). Based on their results, it is technically feasible to reach the goal of NZEH even in the cold climate of Montreal. Rodríguez et al. [26] assessed the energy performance, CO_2 emissions, and economics of several designs of PV, ST, and natural gas internal combustion engines for residential buildings in five different locations in Spain. Likewise, Testie et al. [27], [28], proposed an optimal design method for the configuration of PV, ST, and solar thermal energy storage for a nearly zero-energy building (NZEB) in Italy. They examined the energy and economic aspects of the solar system. Building on this research, Ascione et al. [29] used a genetic algorithm to optimize the configuration of PV, ST, and heat pump systems for an NZEB in Italy. Their optimal mix minimized the primary energy demand and investment cost.

PV and ST systems can be used in other applications, such as domestic hot water systems (DHWS) [30], evaporators [31], and cold storages [32]. For example, Mustaka [30] used PV and ST systems in DHWS applications. This study included performance and economic comparison between a conventional installation of PV and ST with both glazed and unglazed PVT liquid collectors [30]. Building roof areas of 100 m^2 were considered for all systems in the analysis. The study found that the solar system with the unglazed PVT collectors did not compete with the conventional combined installation of PV and PT for this SDHW application. They concluded that unglazed PVT collectors were not economically applicable in the SDHW systems they studied. Mustaka demonstrated that market prices for glazed PVT collectors need to come down by about 50% to meet the payback requirements of their study [30]. In another small scale study, Gunasekar et al. [31] used an artificial neural network (ANN) model to predict the energy performance of a PVT evaporator used in solar assisted heat pumps.. The study considered the effects of four ambient parameters—solar intensity, temperature, wind velocity, and relative humidity—on the energy performance of parameters, including evaporator heat gain, solar energy input ratio, PV panel efficiency, and panel surface temperature. Results show that the influence of wind velocity and relative humidity were less than

solar intensity and ambient temperature. Basu and Ganguly [32] proposed a solar system consistingof PV and ST for the design of a potato cold storage facility. The energy performance of the system was evaluated over a year, and an economic analysis was performed to verify the financial benefits of the proposed system. They found that the proposed system provided a net annual energy surplus of about 36 MWh, and payback periods were less than four years.

ST and PV systems also see use in medium to large scale applications. Kim et al. [32] developed a multi-criteria decision support system for PV and ST systems using a multi-objective optimization algorithm. A database of the variables affecting the solar system performance, such as geographical information, meteorological information, solar angles, etc., was established based on available regional data in South Korea. The algorithm was able to find the optimal PV and ST system configurations based on energy performance, economics, and environmental assessment of the system. Mousa et al. [33] provided a life-cycle assessment (LCA) methodology to assess the environmental impacts of ST and PV technologies. The life-cycle energy and environmental impacts of PV versus ST systems were analyzed to find the best techno-environmental solution to meet the heating load of medium-scale industrial units (i.e. on the order of 100 kW). The results indicated that ST systems have a lower embodied energy payback time (EPBT) in locations with high direct normal irradiance than a PV system. However, in terms of the greenhouse gas emission payback times, the results did not reveal an advantage for either ST or PV technologies. In other studies [35][36], options ranging from 100% PV to 100% ST were conducted to identify the best mix for industrial process heat applications were studied. It was revealed that a mix of ST and PV in the side-by-side configuration improved performance, the levelized cost of energy (LCOE), and the environmental payback time.

In the previous studies highlighted here, there were no considerations of the trade-off problem that occurs when the PV and ST systems are integrated with a BES system. Moreover, previous studies have not focused on modern commercial greenhouses. In this study, a solar hybrid (ST/PV-BES) system designed to meet the heating and electrical load of a commercial greenhouse Ontario, Canada will be technically and economically evaluated. Side-by-side PV and ST configurations are investigated in this study. The total annual energy performance of the system is estimated using TRNSYS simulation software, version 17. The relative influence of different economic parameters on the cost competitiveness of the proposed ST/PV-BES system is also considered. Finally, the effect of financial incentives such as carbon tax and Large Renewable Procurement (LRP) rates on the economics of system design are also evaluated.

3.2 Methodology

In this study, a dynamic simulation of the ST/PV-BES system was implemented in TRNSYS. The performance of the system during a one-year operation was evaluated. TRNSYS "Transient System Simulation Program", is a simulation environment for the transient simulation of energy systems [37]. In recent years, there has been an increasing interest in the development of transient energy

models in the agricultural sector [38]. TRNSYS as a complete and extensible simulation environment has been a popular choice for many researchers [39]–[44]. In this section the reference greenhouse specifications are described. Then inputs of the transient model of the solar system will be introduced. These inputs are the hourly meteorological load and hourly energy consumption of the greenhouse including heating and electrical loads. Finally, the details and working flow of ST/PV-BES subsystems will be discussed.

3.2.1 Reference greenhouse

The reference 24 acre greenhouse is located in Essex County, Ontario, Canada, a region with a cold climate. The Venlo-type structure has a gutter height of 5.5 m and a roof slope of 25°. The greenhouse produces bell peppers.

3.2.2 Meteorological information

The Weather Data Processor is used to supply climate data to the model. Data is pulled from the Canadian Weather for Energy Calculation (CWEC) dataset for Windsor (latitude of 42.32°N and longitude of 83.03°W). The CWEC dataset contains hourly weather information for an artificial one-year period composed of twelve typical months selected from the Canadian Weather Energy and Engineering Datasets (CWEEDS) – a 30 year compilation [45], [46]. The input weather data consists of hourly dry bulb temperature, total horizontal radiation, beam radiation, diffuse radiation, total tilted radiation, angle of incidence for the collectors, and ground reflections. CWEC dataset contains both bright and overcast days and combinations of the two [47]. This dataset has seen wide application in heating load calculation and solar system design [48].

3.2.3 Annual energy consumption

The greenhouse requirements of thermal and electrical energy are evaluated according to internal loads and external climate conditions. The hourly load profile is useful for properly designing and sizing of the greenhouse solar energy system and providing accurate data for effective computer simulation.

3.2.3.1 Heating load

For calculation of the heating load, in order to normalize the model, 1 acre of the greenhouse is simulated. This acre consists of 10 bays, each with a width of 5m. To evaluate the thermal conditions near and far from the crop, two lower and upper thermal zones were considered [49]. The height of the lower zone is 3.5 m. A plug-in called TRNSYS3d for Google SketchUp™ is used to input the geometric information into the building model. The SketchUp schematic is shown in Fig. 3.1.
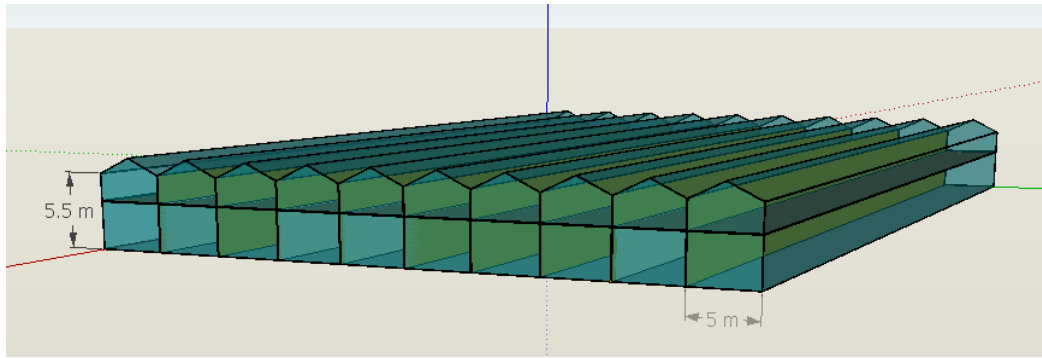
Figure 3.1- 3-Dimensional Greenhouse Model in Google SketchUp

Type 56 was used to model the thermal properties of the greenhouse. It is a multi-zone building in the sub-program TRNBuild. The infiltration ratio was assumed to be in the range of 0.5-1.5 ACH [50]. The day and night set-point temperatures for the bell peppers were 22°C and 18°C, respectively. This night set-point temperature is increased 1 °C / hour in the early morning hours to reach the day set-point temperature prior to the sunrise. Morning pre-heating is supplied between 3 am and 6 am year-round, regardless of the indoor temperature. From Mid-November to January, the indoor temperature is maintained above freezing at about 5 °C as there are no crops in the greenhouse [49]. The heating system of the reference greenhouse has an assumed overall efficiency of 75% [49]. It consists mainly of hot water piping located near the floor and the top of the fully grown crops. When the inside temperature or relative humidity exceeds 25 °C and 85% respectively, the ventilation system activates, providing 60 ACH. Air-inflated, double-polyethylene is used to cover the roof and walls of the greenhouse. The heat transfer coefficient of the greenhouse cover was set at 5 $W/m^2.°C$ which is in the range of values reported by others [51]. Typically double-polyethylene film has a light transmittance of 75% [52].

The sensible heating demand of the 1-acre greenhouse was calculated in TRNSYS over a full year with a timestep of 1 hour. The profile was multiplied by 24 to develop the profile for the 24-acre greenhouse. The sensible heating demand in the greenhouse must be provided by the heating system. The hourly sensible heating load profile for the modeled greenhouse is shown in Fig. 3.2. The system requires the hourly heating demand as an input. According to Fig. 3.2, the mid-January peak hourly demand is around 16.5 MWh. Morning pre-heating loads were set at 8.3 kWh. Crop termination is the reason for the low energy demand in November and December.

The monthly sensible heating demand is illustrated in Fig. 3.3 and it is compared with the actual data from the reference greenhouse. A good correlation is observed between actual and modeled data. The total annual heating energy demand for the modeled greenhouse was determined to be 36110 MWh which is within about 5% of the actual data. This value is equivalent to 370 kWh/m^2 annual energy consumption for the heating load. The good correlation between the monthly values of the heating demand supports its use for the thermal energy storage system design.
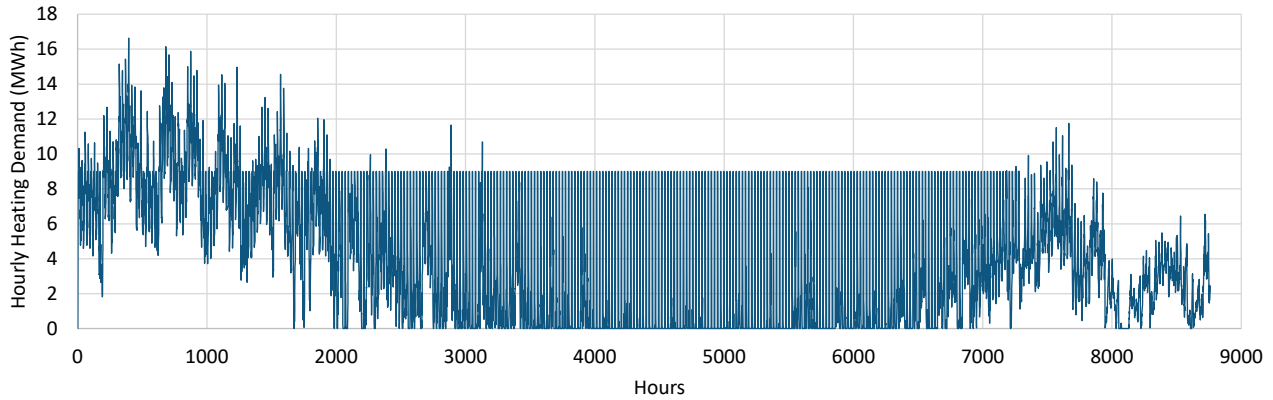
Figure 3.2- Hourly heating demand of the greenhouse from TRNSYS Model
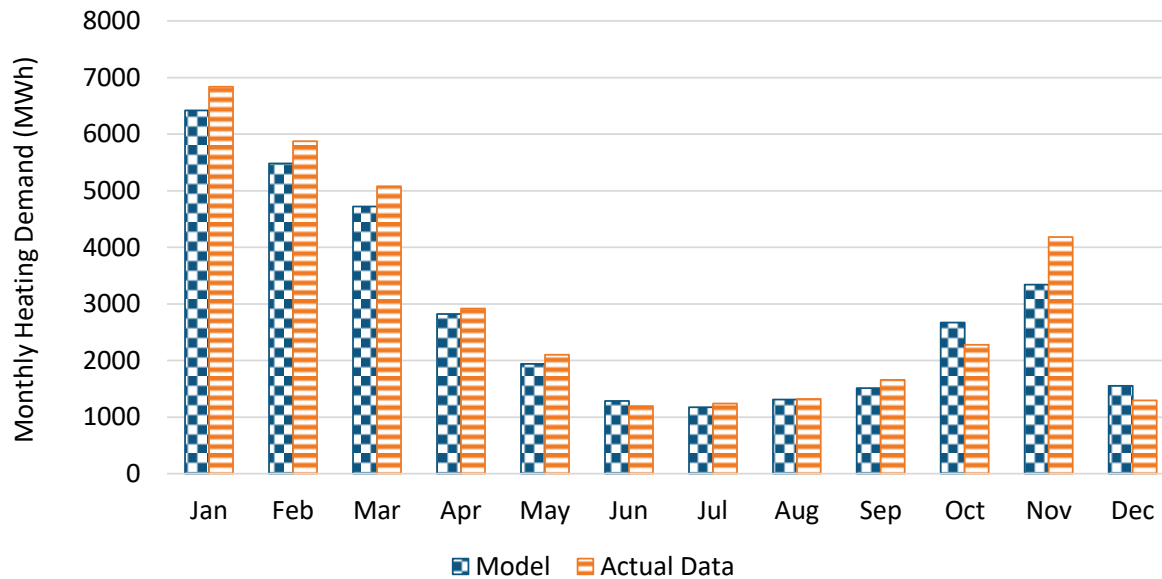
Figure 3.3- Actual and modeled monthly heating demand of the greenhouse

3.2.3.2 Electricity load

Based on the data from the grower, the electricity is used for the following purposes in the reference greenhouse:

- Irrigation: the irrigation system in the greenhouse is a drip irrigation system. Watering events are scheduled based on the crop size and season. The water demand of crops changes as the crop grows from seedling to mature crop and in between seasons. Actual data for irrigation flows of 5 minutes time spans over 1 year were used to estimate the hourly electricity consumption of the pumps in the irrigation system. The pumpset has a maximum capacity of 210 m^3/hr. Two pumps are rated at 22 kW, there are two 11 kW pumps, and one 2.2 kW pump are required to maintain the system pressure equal to 50 psi. During the summer days, watering starts from 30 minutes after sunrise to approximately one hour before sunset. Every watering event takes 8-20 minutes. The frequency of

28

the watering events in the summertime is varies from 2 (start and end of the day) to 4 (close to the noon) times in one hour. During the wintertime, this value changes to approximately 4 times a day.

- Heating: As mentioned before, the heating system of the reference greenhouse is a hydronic system based on boilers. The heating system distributes the heat via hot water, which gives up heat as it passes through pipes throughout the greenhouse. The cooled water then returns to the boiler to be reheated. The fuel for the boilers is natural gas. Three 7.5 kW boiler circulation pumps circulate water within the boiler to enhance boiler operation. One 22 kW transport pump and two 18.5 kW transport pumps push water out of the zones. Eight 2.2 kW tube rail pumps and eight 1.1 kW grow pipe pumps circulate hot water in the greenhouse. The transport pumps are on frequency drives. Thus, they can run anywhere between 30-100% capacity depends on the greenhouse heating demand. All other pumps are either on or off.

- Light: The reference case is a traditional greenhouse without artificial growing lights. Thus, the only light which is needed is that of warehouse lighting. A light with a 0.3 W/m^2 intensity of was assumed during dark hours.

- Other items: leach return pumps, ventilation fans, shade and thermal curtain motors, and some electrical appliances used in the greenhouse are grouped under other items. The reference greenhouse has a complete recirculating system. Thirty percent of over drain was considered in the summer months in this study. The electricity needed to run leach return pumps was calculated based on the power that needs to be supplied to remove the volume of the water leaches. The first half (15%) happens at 10 am and the second half (15%) happens at 2 pm. To find the ventilation requirement, a moisture and energy balance of the greenhouse was required. Elements of the heating load calculation were also used to find the ventilation fans schedule. The calculation of fan electricity load was based on the requirements to maintain 60 ACH. Two types of curtain operate in the greenhouse: thermal curtains and shading curtains. Thermal curtains add additional thermal boundaries and reduce the volume of the greenhouse that needs to be heated. When solar radiation is less than 5 W/m^2 (0.018 MJ/m^2hr), the thermal curtain is closed [49], and when it is more than this threshold it opens. For the shade curtain, when the solar radiation is more than 2 MJ/m^2hr, it is closed, and when it exceeds this value, it opens. The list of electrical appliances, their wattage, and their usage schedule was provided from the grower. These electrical appliances are the air compressors, packing line motors, high-pressure spray motors, bag machines, box machines, garage doors, and UV machines. The electricity used to charge two forklifts, two power bees, two golf carts, and 31 scissor karts was also calculated.

Based on the above information, the hourly electricity demand of the greenhouse was developed to be used as an input to the system. The profile is shown in Fig. 3.4. The profile has a maximum value of 240 kW. The hourly electricity consumptions of a typical summer and winter day are compared in Fig. 3.5. During the night, the electricity consumption in the wintertime is more than that in the summertime. The reason is that pumps are running full for a longer period during the cold nights. On the other hand, during the day, higher electricity consumption is observed in the summertime. Higher harvesting activities contribute to this.
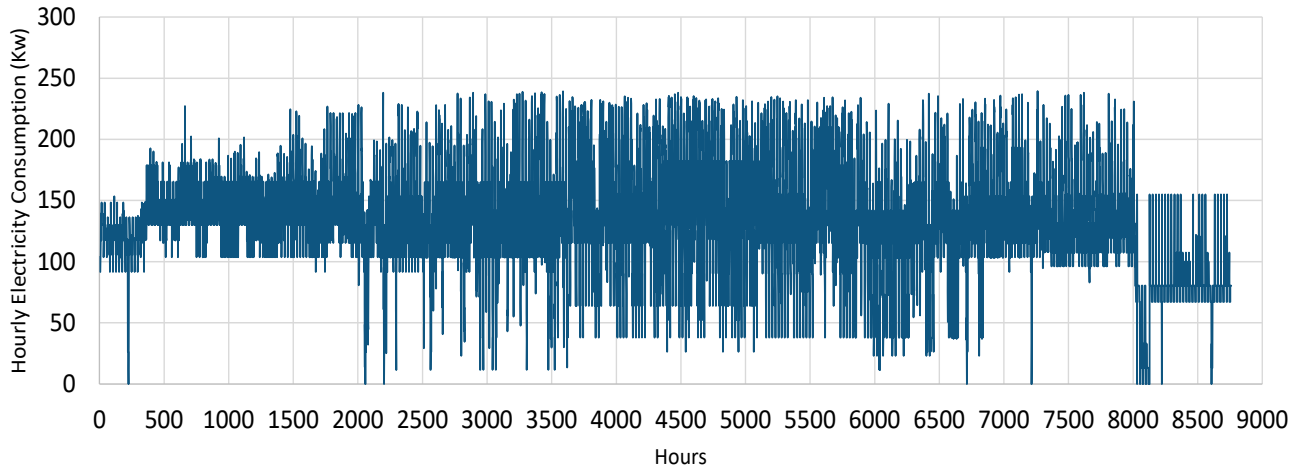
Figure 3.4- Hourly electricity demand of the greenhouses
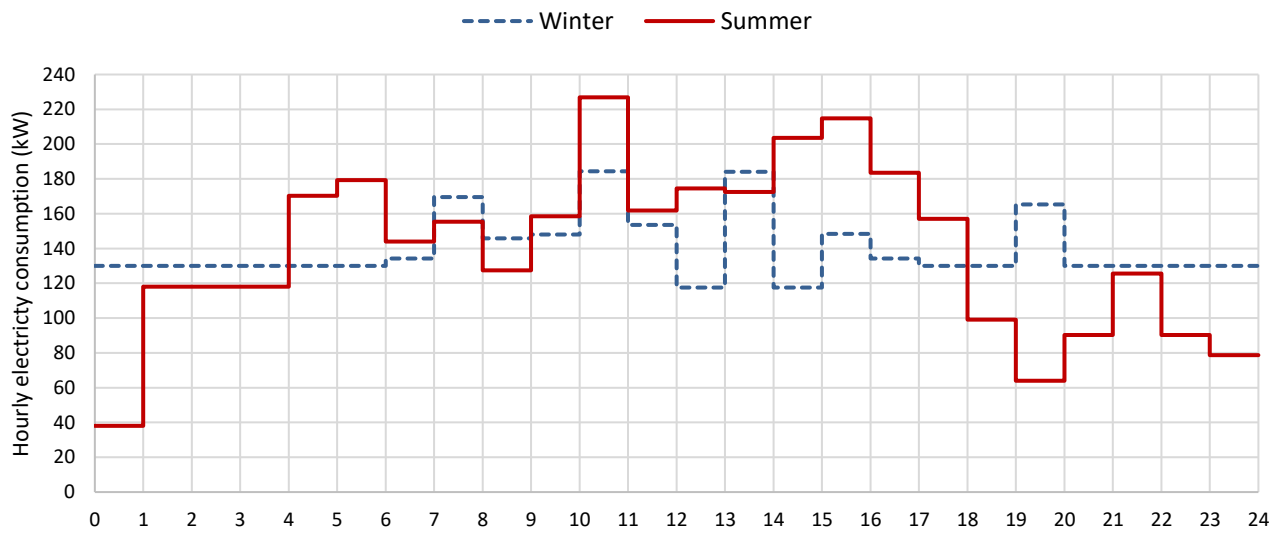
Figure 3.5- Hourly electricity demand in a typical summer and winter day
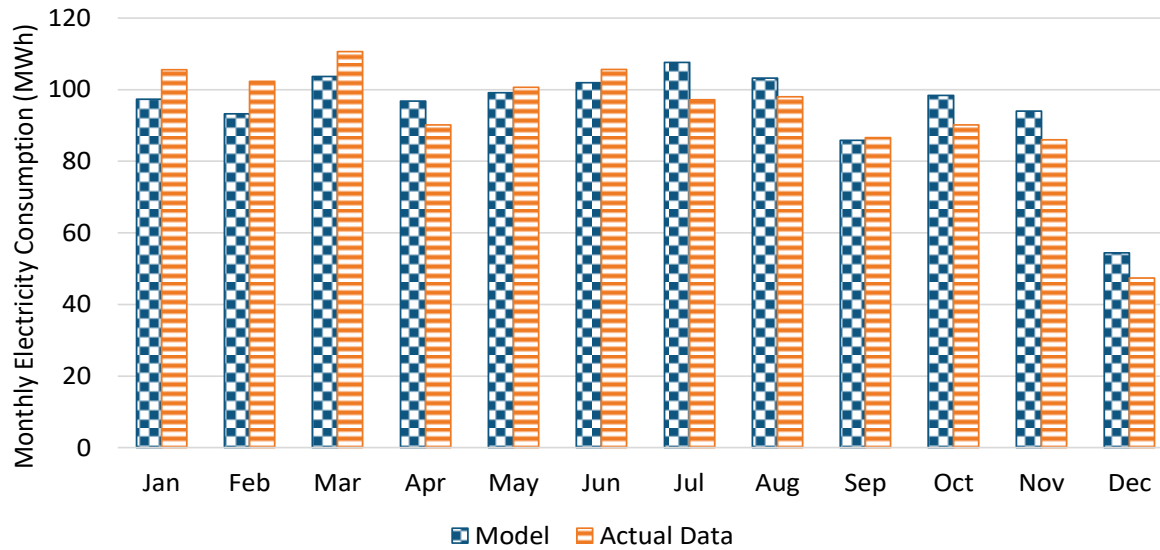
Figure 3.6- Actual and estimated monthly electricity demand of the greenhouse

Figure 3.6 compares the monthly electricity consumption from the developed hourly profile and electricity demand based on the greenhouse monthly usage data. These profiles reveal a good correlation. Based on the real data, the total electricity demand in the reference greenhouse was 1120 MWh. The developed profile gives a value of 1135 MWh for an annual electricity consumption. The difference is negligibly small at 1.4%. Therefore, based on the developed profile, the average annual electricity demand of the greenhouse is 11 kWh/m^2. Fig. 3.7 illustrates the annual breakdown of electricity consumption for the greenhouse. As shown in the figure, electricity for running the heating system represents the largest portion, that is more than half. The second largest portion is other items, with 20% of total electricity consumption. Electricity for irrigation is also a major draw. As it is a conventional greenhouse without growing light, the electricity for lighting accounts for only 9% of the total electricity consumption.
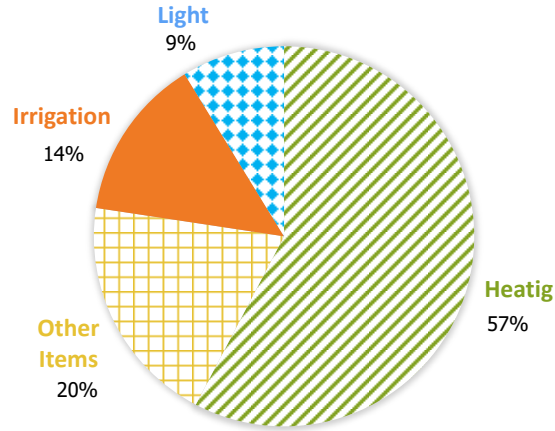
Figure 3.7- Annual breakdown of electricity consumption
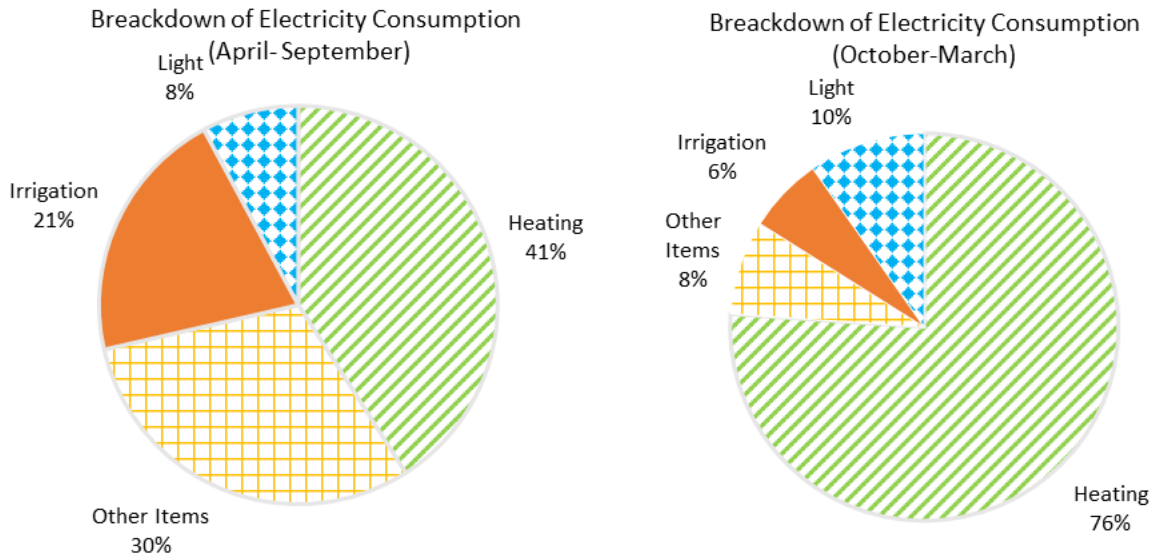
Figure 3.8- Breakdown of electricity demand in a) April to September and b) From October to March

Fig. 3.8 compares the breakdown of electricity consumption in warm months and cold months. More than three quarters of electricity goes for heating in the wintertime in contrast to only 41% in the summertime. In the wintertime, the sum of light, irrigation, and other items only makes up one quarter of the total electricity usage. In the warm months, the portions of heating and other items are almost the same due to harvesting and other items. Clearly, irrigation and leachate draws are higher in the warm months. The electricity for warehouse light in warm months is less than cold months because of the shorter night.

3.2.4 Solar System Description

An analysis of the ST/PV-BES system model was developed to calculate the solar energy harvesting rates. Dynamic simulation of the system is carried out using TRNSYS software version 17. System simulation was made for 1 year using a simulation time step of 1 hour.

The solar system consists essentially of 2 main subsystems:

(1) ST subsystem
(2) PV-BES subsystem

The main subsystems and their components included in the hybrid scheme are shown in Fig. 3.9. The ST subsystem operates to meet the heating load. Solar collectors, which convert the incident solar radiation into heat, are the key components of the ST solar systems. The harvested heat is carried by the working fluid for greenhouse space heating; and is stored in a tank to be restored at nights or cloudy days. The auxiliary system burns natural gas. The PV-BES subsystem operates to cover electricity demand. The PV panels first meet the load, while the electricity surplus is directed to the BES system, until it is fully charged. Then, the extra electricity is sold back to the grid. In contrast, during the night or low irradiance conditions, the BES supplies the electricity deficit until its state of charge (SOC) falls to its minimum level. Then the grid supplies the shortfall. In the following section, the components of the solar system are explained.
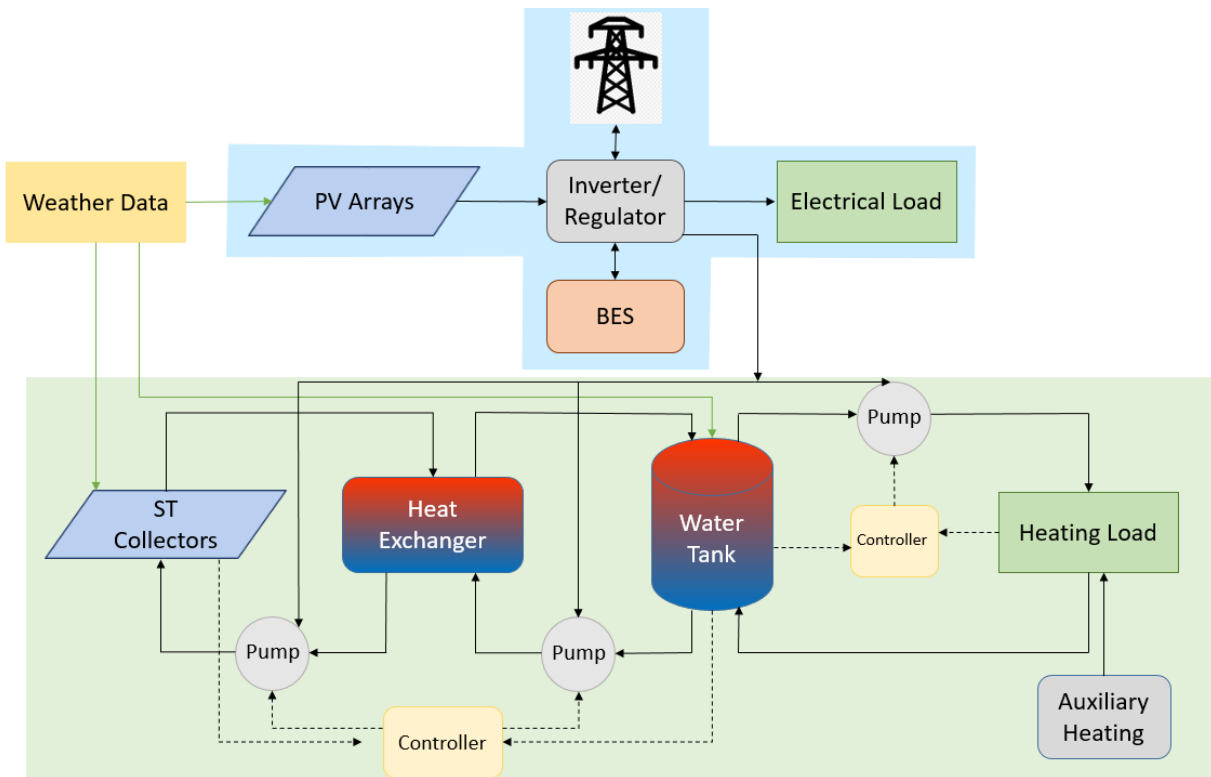
Figure 3.9- Schematic diagram of the main components of the solar system

3.2.4.1 ST subsystem

The thermal part of the solar system is responsible for satisfying the heating load. The STE system consists the following elements:

Flat-plate solar collectors: For low to medium temperature applications, flat-plate solar collectors are used [53]. The solar collector array consists of units connected in both series and parallel. The tilt angle of the ST collector was optimized for the latitude of the location [26]. A solution of 50% propylene glycol and water was assumed to be circulated through the collector loop to prevent wintertime freezing [54]. The specific heat of working fluid has been assumed equal to 3.6 kJ/kg°C [44]. Type 1c was used to model the performance of the flat-plate solar collector. The flat plate solar collector model in TRNSYS is based on a quadratic efficiency equation [55]. This equation is the generalization of the Hottel-Whillier equation.

$$\eta = a_0 - a_1 \frac{(\Delta T)}{I_T} - a_2 \frac{(\Delta T)^2}{I_T} \tag{1}$$

ΔT is the difference of the Inlet temperature of the fluid to the collector and ambient air temperature; I_T is the global radiation incident on the solar collector; and a_0, a_1, and a_2 are the intercept efficiency, efficiency slope, and efficiency curvature, respectively. The values of a_0, a_1, and a_2 are obtained from product certification data [56]. The area of each selected module is 1.865 m^2. The data used for the flat-plate solar collector is summarized in Table 3.1. The Incidence Angle Modifier (IAM) was supplied in an external file to account for the effect of the inclination of solar irradiance with respect to the surface of the solar collector.

Table 3.1- Flat-plate solar collector parameters

Main Parameters	Value	Unit
Working Fluid Specific Heat	3.32	kJ/kg K
Intercept Efficiency	0.604	-
Efficiency Slope	3.73	kJ/h m^{2}K
Efficiency Curvature	0.0086	kJ/h m^{2}K^2
Tested Flow Rate	32	kg/h m^2

Heat exchanger: Because the working fluid in the solar collector loop is an anti-freeze, a heat exchanger was necessary to transfer heat absorbed in the collector by the fluid to the water in the water tank. An external heat exchanger was used in this simulation. The counter-flow heat exchanger of TRNSYS Type 91, which relies on an effectiveness minimum capacitance approach, was used. The heat exchanger effectiveness is assumed to be 0.8 [57]. In the constant effectiveness mode, the maximum possible heat transfer is calculated based on the minimum capacity rate fluid and the cold side and hot side fluid inlet temperature.

Hot water storage tank: TRNSYS Type 534 was used to model a cylindrical tank [58]. The modeled tank was divided into five isothermal temperature nodes to model the stratification. The total volume of the water tank was set to 100 l/m^2 of the solar thermal collector area in all cases. The tank height to diameter ratio is 2:1. The connections were placed at the top and bottom of the tank.

Circulating pumps: TRNSYS Type 3 was used to model variable speed pumps. This type computes the maximum flow capacity and the mass flow rate. The maximum flow capacities in all cases were specified based on the ST system size. The mass flow rate is determined based on a variable control function from controllers.

Controllers: On/Off differential controllers were used for each circuit, receiving inputs of the fluid temperature that exits the collector, the temperature of the bottom node of the water tank, the cut-off temperature of the system, and the availability of the heating demand. Based on the receiving inputs, controllers generate an output control function which may be On (1) or Off (0) to switch pumps on or off.

Heating load: TRNSYS Type 682 was used to impose the calculated heating load on the flow stream exiting the solar thermal system. This type acts as an interaction point between the greenhouse and the solar thermal system.

3.2.4.2 PV-BES subsystem

The objective of the hybrid grid-connected PV-BES system is to serve the electrical load. This subsystem consists of the following elements:

PV arrays: PV arrays convert sunlight into DC electricity. An equivalent circuit model was used to model a poly-crystalline PV panel using TRYNSYS Type 94. A maximum power point tracker (MPPT) algorithm that finds the maximum power point automatically is also included. MPPT forces the PV array to operate at the point of maximum power along its IV (current vs voltage) curve [59]. The PV panels slope is set to 42 degrees in accordance with the local latitude [60]. The electrical data and temperature characteristics of the PV panel are shown in Tables 3.2 and 3.3 based on the selected product datasheet [61]. Selected modules are 330 Wp with an area of 1.94 m^2. All data are for standard test conditions of an irradiation of 1000 W/m^2 and cell temperature of 25°C. For the Tau-alpha product, a value of 0.9 was used [62]. The poly-crystalline bandgap is equal to 1.12 eV.

Table 3.2- PV panel electrical data

Main Parameters	Value	Unit
Nominal Max Power (Pmax)	330	W
Opt. Operating Voltage (Vmp)	37.2	V
Opt. Operating Current (Imp)	8.88	A
Open Circuit Voltage (Voc)	45.6	V
Short Circuit Current (Isc)	9.45	A

Table 3.3- PV panel temperature characteristics

Main Parameters	Value	Unit
Temperature Coefficient (Pmax)	-0.40	%/°C
Temperature Coefficient (Voc)	-0.31	%/°C
Temperature Coefficient (Isc)	0.05	%/°C

Battery energy storage (BES): BES systems smoothen the mismatch between the occurrence of peak load and the maximum power generated by the PV arrays [15], [63]. There are many types of BES systems available, including lead-acid, nickel-cadmium, nickel hydride, and lithium. Several studies have been conducted to evaluate different battery types based on their features. They each have their own advantages and disadvantages which makes them the optimized choice for a specific application [62]. In particular, deep-cycle lead-acid batteries are the most common choice for energy storage in most PV applications [63] owing to their low cost, the maturity of technology, and availability in the market [18]. Therefore, they were also selected to be utilized in this study. It should be mentioned that the lead-acid batteries are modeled with TRYNSYS Type 47 using the Hyman and Shepherd equations. The capacity of each cell was 2.568 kWh based on the selected product [64]. The charging efficiency is the ratio of the discharge over the charge [65]. This value was assumed to be 90% [66].

Inverter and regulator: The solar arrays deliver power to two power conditioning devices. The first device is a regulator, distributing power to the battery bank, grid, and the load with a 92% efficiency [65]. The second one is an inverter, converting the direct current (DC) electricity output of PV arrays into alternating current (AC) electricity needed by electrical appliances with a 96% efficiency [67]. These two components are represented by TRYNSYS Type 48b. Type 48 simulates a power regulator and inverter that can be used in connection with PV array, battery, load, and grid. Type48b (mode 1) is a maximum power point tracking regulator/inverter. This type can monitor the battery SOC.

The mode of operation in the proposed system was partial charging. In this mode, the first priority is meet the load with the electrical output of the PV arrays, and the surplus is directed to charge the batteries. Electricity exchanges with the grid were permitted, yet the battery charging directly from the grid was not allowed. SOC is an important parameter to evaluate the charge control of the battery. This parameter is used to protect the battery from over-discharging and over-charging conditions [68]. The low limit on SOC was 20% and high limit on SOC was 100%. Thus, the Depth of Discharge (DOD) in this case was equal to 80%. Table 3.4 summarizes the battery and regulator/inverter parameters used in the simulation.

Table 3.4- Battery and inverter/regulator parameters in the PV subsystem

Main Parameters	Value
Inverter Efficiency	0.96
Regulator Efficiency	0.92
Battery type	Lead-Acid Battery
High limit on FSOC	1
Low limit on FSOC	0.2
Cell Capacity	2.568 kWh
Battery charging efficiency	0.9

3.3 Economic model

The economic analysis examined: the time value of money, replacement costs, and inflations. The levelized cost of energy (LCOE), life cycle savings (LCS), and Payback Period (PBP) for varying capacities of ST collectors, PV modules, and BES were calculated.

3.3.1 Economic Assessment Method

LCOE is a widely adopted method to assess the economical feasibility of renewable energy systems. This method has been used in many studies [15], [35], [69]–[71]. Levelized cost of energy (LCOE) is an economic assessment of the total cost to build, maintain, and operate a power generation system over its lifetime divided by the total energy output of the system over its lifetime [15]. It represents the equivalent energy cost for heating and electricity that makes the revenues equal to the costs during the lifetime of the solar system (ST/PV-BES). Revenues and costs are discounted and affected by inflation [71]. This parameter provides the unitary cost of the produced energy and enables a comparison between different size of PV and ST modules and BES system. The PV and ST system life span was assumed 25 years [33].

The following, Eq. (2), introduces the LCOE.

$$\text{LCOE} = \left(C_0 + \sum_{n=1}^{25} \frac{(C_i^{PV} + C_i^{ST})(1+i)^{n-1}}{(1+d)^n} \right) \Big/ \sum_{n=1}^{25} \frac{(E_L^{PV} + E_L^{ST})(1+i)^{n-1}}{(1+d)^n} \qquad (2)$$

Capital cost of the project consists of the costs of ST system and PV-BES system. Thus, C_0 is the sum of C_{ST} and C_{PV}. The total annual cost of the solar system (C_i^{PV} and C_i^{ST}) can be calculated based on Eqs. 3 and 4.

$$C_i^{PV}=C_{i, PV}^E+C_{i, PV}^{O\&M}+C_{i, PV}^R-C_{i, PV}^S \qquad (3)$$

$$C_i^{ST}=C_{i, ST}^f+C_{i, ST}^{O\&M}+C_{i, ST}^{CT} \qquad (4)$$

In these equations the annual electricity costs to buy from the grid, annual operation and maintenance costs, replacement costs, and annual carbon tax payment for natural gas consumption were considered when calculating the total annual cost of the solar system. In Eq. 2, the possibility of the selling electricity to the grid was considered. E_L^{PV} and E_L^{ST} are the annual electricity generation of the PV-BES system and annual energy production of the ST system, respectively.

The LCS is defined as the difference between the life cycle cost of a conventional fuel-only system and the life cycle cost of the solar plus auxiliary system [72]. In this study, LCS represents the total value that will be saved during the entire solar system lifetime by using ST/PV-BES system plus auxiliary system and grid as back-ups, instead of using natural gas for heating and grid for supplying electricity. To assess life cycle savings, the PW of solar savings at the end of every year (n) in a 25-year duration with the discount rate (d) is obtained based on Eq. (5) [73]:

$$LCS=-C_0+\sum_{n=1}^{25}\frac{\text{Solar Savings}}{(1+d)^n} \qquad (5)$$

In this equation, C_0 is the total capital cost, which is the sum of C_{ST} and C_{PV}. Solar savings for the ST and PV-BES subsystems are defined by Eq.6.

$$\text{Solar Savings}=\left(C_{i,PV}^{Sa}+C_{i,PV}^S-C_{i, PV}^{O\&M}-C_{i, PV}^R\right)+(C_{i, ST}^{Sa}+C_{i, ST}^{CTS}-C_{i, ST}^{O\&M}) \qquad (6)$$

There are many definitions for the Payback Period (PBP). Here, PBP is defined as the time needed for the cumulative solar system savings to become equal to the initial investment [72]. This time is obtained with discounting the solar savings.

3.3.2 Financial Incentives

According to the report of IEA [74], governments have a major role to increase penetration of solar energy, through their support in innovative research and development, but more importantly through the development of appropriate market conditions and development of incentive policies to support market creation. Two incentive policies in Ontario were applied in this study: Carbon tax and feed-in tariff (FIT)/ large renewable procurement (LRP). Carbon tax was assumed at a rate of 20 $/ton of equivalent ($CO_{2e}$) emissions [75]. The annual growth of the carbon tax was assumed to be 3%. The natural gas emission factor is 0.055 ton CO_2/GJ [26], [76]. Based on Ontario's grid statistics [77],

only a small portion of the electricity from the grid is sourced from fossil fuels. Thus, carbon tax was not applied to the electricity purchased from the grid. Ontario's Feed-in Tariff (FIT) was established to encourage the penetration of renewable energy in Ontario [78]. The FIT program is available to renewable energy systems generally smaller than 500 kWp [79]. For the larger projects, the Large Renewable Procurement (LRP) program, which has a competitive bidding process, was created [80]. It was assumed that the electricity could be sold back to the grid (LRP rate) with the same price of buying electricity from the grid.

3.3.3 Economic Assumptions

For the ST system, flat-plate solar collector price was assumed to be 250 $/m^2 [81][82]. It was assumed that the water tanks, pumps, and piping system of the current heating system could be used for the solar system and no extra costs were considered for these components. The PV-BES system capital cost includes several considerations. Photovoltaic costs were assumed to be 1.9 $/kWp for PV model, inverter, and installation. The PV price was assumed at 325 $/m^2. Based on the price analysis of the lead-acid battery, the price was assumed to be 150 $/W. For the battery charge controller and MPPT, the price was equal to 0.06 $/W. The costs of battery, charge controller and MPPT are estimated based on the local product datasheets. Replacement of battery bank, inverter, MPPT, and regulator were included in the PV-BES operation and maintenance costs every 10 years [69]. The energy output from the PV system depends on the degradation rate of the modules. The annual degradation rate of poly-crystalline was estimated at 0.5% [69]. The yearly operation and maintenance cost for ST and PV-BES subsystems was assumed to be 1% capital cost [83].

The natural gas price was assumed at 7 $/GJ based on the average value in Ontario [84]. Based on the greenhouse electricity bill, electricity cost was assumed at16 cents/kWh. Market discount rate was assumed to be 2.5%. Average inflation rate for all economic factors including fuel price, electricity price, and annual operation and maintenance costs was assumed 3%. Table 3.5 summarizes the assumed values for economic parameters.

Table 3.5- Base economic conditions considered for optimization study

Main Parameters	Value	Unit
Solar system lifetime	25	Years
Flat-plate solar collector price	250	$/m2
PV system price (Module, Inverter, Installation)	1.9	$/kWp
Battery price	150	$/Wh
Battery charge controller and MPPT	0.06	$/Wh
Replacement Period (Battery, Inverter, Battery charge controller)	Every 10 years	-
Operation and maintenance costs	1% Capital Cost	-
Annual PV system degradation ratio	0.5	%
Natural gas price	7	$/GJ
Electricity price to buy from the grid	0.16	cent/kWh
LRP rate	0.16	cent/kWh
Market discount rate	2.5	%
Average inflation rate	3	%
Carbon tax	20	$/ton
Cost functions	LCS, LCOE, PBP	$/ton

3.4 Study Plan

The study is carried out considering different system configurations to assess their impact on the system economics. Greenhouse area footprint is 24 acres. It was assumed that 100% of the greenhouse's footprint could be devoted to the solar energy harvesting system. In order to have a shadow-free solar harvesting field, the spacing between solar modules was carefully considered. The ratio between the required surface on the ground and the solar collector area was assumed to be 3 [71]. The ground area is shared between PV arrays and ST modules with varying proportions. Different system configurations were studied to seek the most economic option. PV system size, ST system size, and BES size are varied in each configuration. PV and ST modules are considered in 3 variants differing in the ratio of PV and ST collector area. The variants are:

- 0.9ST-0.1PV (90% of the area is allocated to the ST modules and 10% of the area is allocated to the PV modules)
- 0.8ST-0.2PV (80% of the area is allocated to the ST modules and 20% of the area is allocated to the PV modules)
- 0.7ST-0.3PV (70% of the area is allocated to the ST modules and 30% of the area is allocated to the PV modules)

The BES system capacity is expressed by the number of autonomy hours, AH. AH represents the number of hours that a fully charged battery is able to supply the energy demand considering the average hourly electricity load [71]. In all three mentioned cases, the BES size was changed from 2 AH to 14 AH with the step of 2 AH. Thus, 21 configurations were studied. In the mentioned configurations, the ST system size is changing from 70%-90% of the required area and the PV systems size is changing from 10%-30% of the required area. The reason for the smaller PV system in comparison with the ST system is the smaller amount of the electrical load in comparison with the heating load. LCOE was employed as an objective function in this analysis. The aim is to find the optimum value of PV size, ST size, and BES size in order to minimize LCOE. The optimized configuration was used as a starting point for the sensitivity analysis. The influence of the following parameters in the PBP and LCOE is assessed through sensitivity analysis. In this analysis, one parameter was varied at a time while the rest of them were maintained constant with the aforementioned values.

- PV system cost
- ST system cost
- BES system cost
- Natural gas cost
- Electricity price to buy from the grid
- LRP rate

Finally, a set of potential future scenarios were assessed, simultaneously varying government financial incentives, electricity, and natural gas costs.

3.5 Results and Discussion

3.5.1 Economic results

In Fig. 3.10, the results for LCOE are presented for all ST/PV-BES configurations. It is clear from this graph that the configurations with the larger ST systems are more economic in all BES sizes. The primary reason for this is the larger amount of heating demand. Increasing the proportion of the PV system, also increases the optimized size of the BES. For example, when the PV portion is 10%, a 6 AH BES produces the lowest value for LCOE, and when this portion increases to 30%, the BES size with the lowest LCOE increases to 10 AH. The best scenario, is an LCOE value of 22.77 $/GJ, is for a system with 90% ST, 10% PV, and 6 AH BES (equivalent to 1079 kWh). In this case, the total ST collector area is 7.2 acres, and the total PV area is 0.8 acres (equivalent to 550 kWp). The total initial cost of this configuration will be paid off after 22 years and the total LCS is $820,000 at the end of the system lifetime. Details of this scenario's performance are discussed in the next section. It should be noted that the minimum LCOE achieved is far more than 8.19 $/GJ, which is the LCOE for the case without the solar system that uses natural gas for the heating system and the grid for the electricity. Therefore, solar systems cannot compete with conventional systems, mainly because of the low price of natural gas.
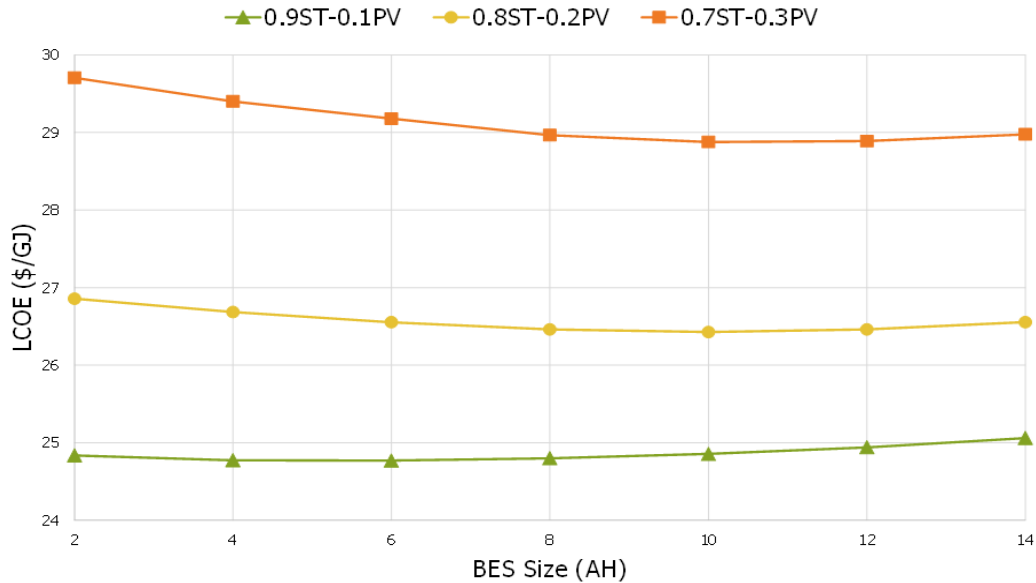
Figure 3.10- LCOE values for different ST/PV-BES system configurations

3.5.2 System performance

Monthly solar fractions were evaluated to assess the overall performance of the optimized size of the ST/PV-BES system. The solar fraction is defined as the ratio of the energy supplied by the solar system and the total energy demand of the greenhouse. This value was evaluated for the ST subsystem and PV/BES subsystem separately. Heat supplied to the greenhouse by the solar system and the required auxiliary heating source are plotted by different coloured patterns in the overall monthly heating demand bars to be distinguishable in Fig. 3.11. Also, the ST solar fraction is calculated and plotted in Fig. 3.11. It can be seen in the summer months when the solar irradiation is highest, the ST subsystem is able to cover almost the entire heating load. The ST system solar fraction is changing from an average value of 20% in the winter months to an average value of 94% in the summer months. This subsystem is able to cover 36% of annual greenhouse heating load. Electricity supplied to the greenhouse by the solar system and the electricity from the grid are plotted by different coloured patterns in the overall monthly electricity demand bars to be distinguishable in Fig. 3.12. Also, the PV-BES solar fraction is calculated and illustrated in Fig. 3.12. The monthly PV-BES solar fraction is changing from an average value of 37% in winter months to an average value of the 70% in the summer months. The annual PV-BES system solar fraction is 51%.
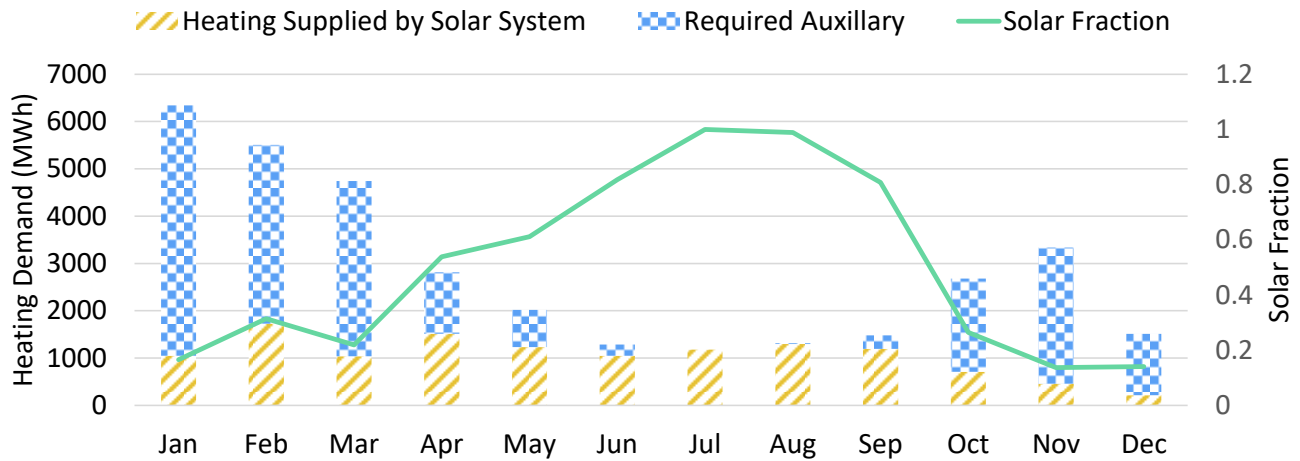
Figure 3.11- Heating supplied, required auxiliary heat, and monthly solar fraction
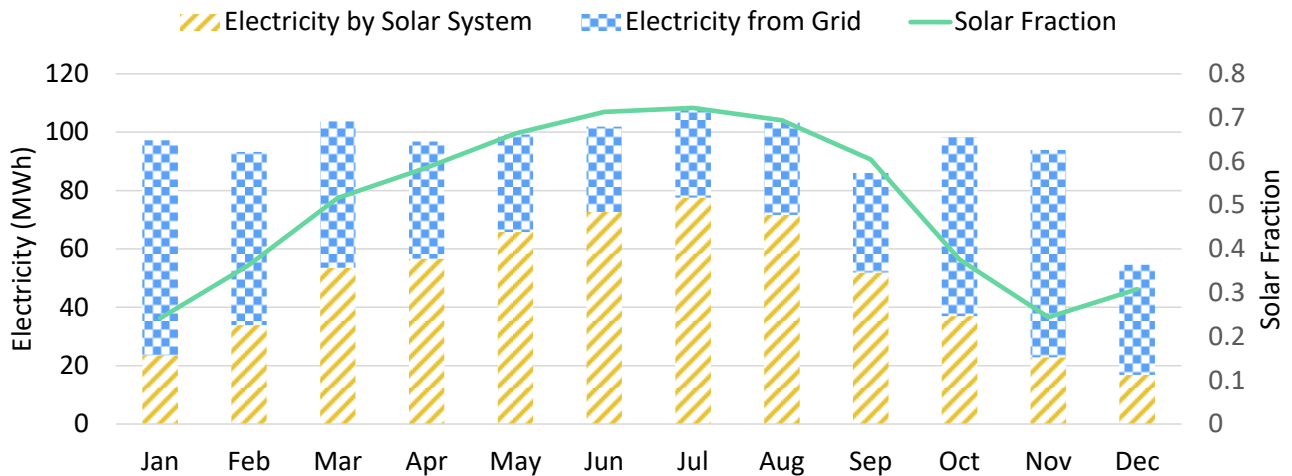
Figure 3.12- Electricity supplied, required electricity from the grid, and monthly solar fraction

The amounts of energy surplus and the energy purchased from the grid are shown in Fig. 3.13. Electricity purchase is equal to 49% of the total electricity demand and is required particularly in the winter time. During the summer months, the electricity surplus corresponds to 20% of the total energy production and it is concentrated during the high irradiation period.
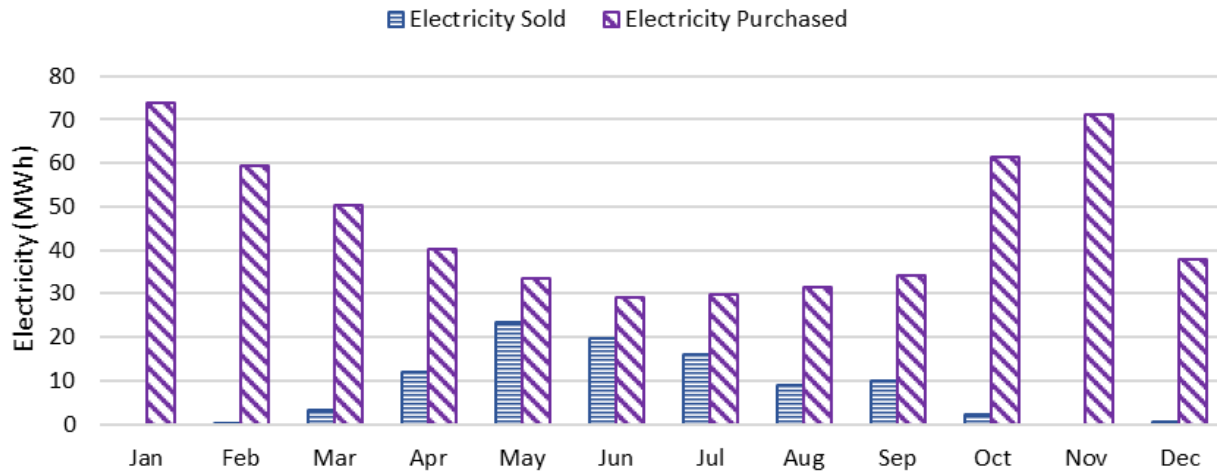
Figure 3.13- Average monthly energy surplus and energy purchased from the grid

Fig. 3.14a and b show the hourly load curve, the hourly PV generation, the portion of energy delivered to the grid, and the amount of energy used to charge the BES system in typical summer and winter days. According to Fig. 3.14a, the BES, which was charged the day before, is discharging to meet the electrical load between hours 12 and 1. When the BES reaches the minimum SOC, the grid then meets the electrical load between hours 2 and 5. The PV system generation starts with the sunrise at hour 6. From hour 6 to 8, both PV system and grid meets the load. Between hours 9 and 12, the PV system covers not only the load but also charges the BES. Because the solar irradiation on the selected day at hour 12 is equal to 980 W/m^2 which is close to solar irradiation under standard test conditions (1000 W/m^2), PV generation reaches a peak of 545 kWh at hour 12, which is close to PV system capacity (550 kWp). When the BES is full, the surplus electricity can be sold back to the grid between hours 13 and 17. The PV system generation ends with the sunset at hour 19. From that time onward, the stored energy in BES is then discharged to the load during the night. On the other hand, based on Fig. 3.14b, the BES system is not exploited during a typical winter day. The PV system only can cover a portion of the electrical load and there is not any surplus electricity to be sold back to the grid.

(a)
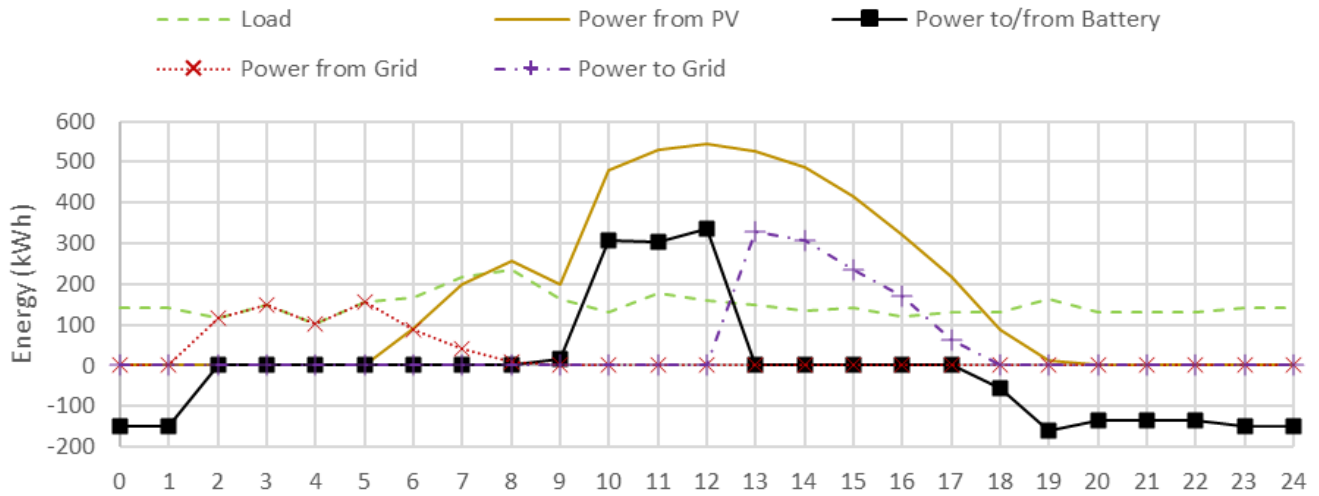
(b)
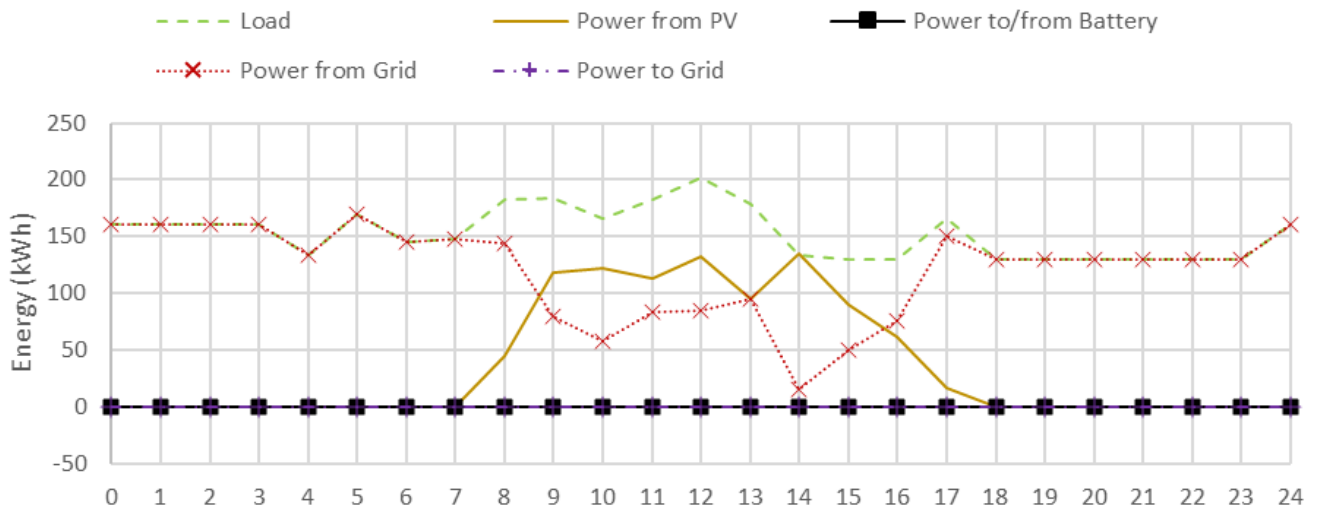
Figure 3.14- Hourly PV system performance in (a) a typical summer day and (b) a typical winter day

3.5.3 Sensitivity Analysis

It is impossible to know for certain the value of the electricity price, natural gas cost, carbon tax, or inflation rate over the next 25 years. These economic parameters have significant effects on the financial feasibility of the proposed solar energy system. To examine these effects a sensitivity analysis is presented in this section. In this simple analysis, when one variable is changed, all other variables remain at their assumed nominal values.

45

These effective parameters can be studied in two groups:

1) ST parameters: ST system cost, and natural gas cost
2) PV parameters: PV system cost, LRP rate, price of grid-supplied electricity, and battery price

The influence of the select economic variables on the LCOE and PBP are presented in Fig. 3.15a and b. Influencing parameters are varied from 0% to 50%, results are shown in the following figures. According to these figures, ST subsystem parameters have a greater influence on the LCOE and PBP in comparison with PV subsystem parameters. The reason is the greater size of the ST subsystem. Among ST subsystem parameters, natural gas has a significant impact on LCOE and PBP. By increasing the natural gas cost by 50%, the LCOE increases by nearly 25% and the PBP could be reduced to the same amount. By reducing and increasing the value of the PV parameters by 50%, LCOE and PBP variation is less than 5% and 15%, respectively. Aside from the ST subsystem parameters, the electricity price is the most influential parameter on the LCOE and PBP. LRP rate and PV system cost have similar effects on the LCOE. However, the PV system cost is more effective than the LRP rate on PBP. Battery price does not have a significant influence on either the LCOE or PBP. The LCOE is only reduced by 0.72% and PBP by 2.18% when the battery price is halved. Therefore, in the proposed system, it can be concluded that battery price is not critical in enhancing the cost competitiveness.

(a)
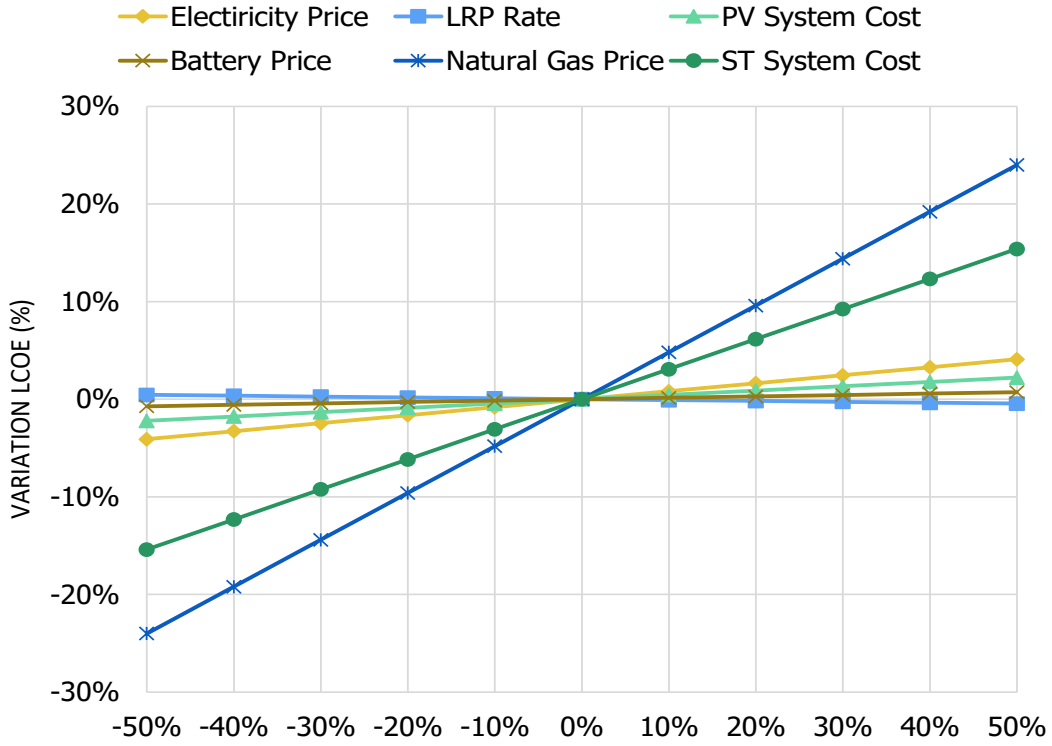
(b)
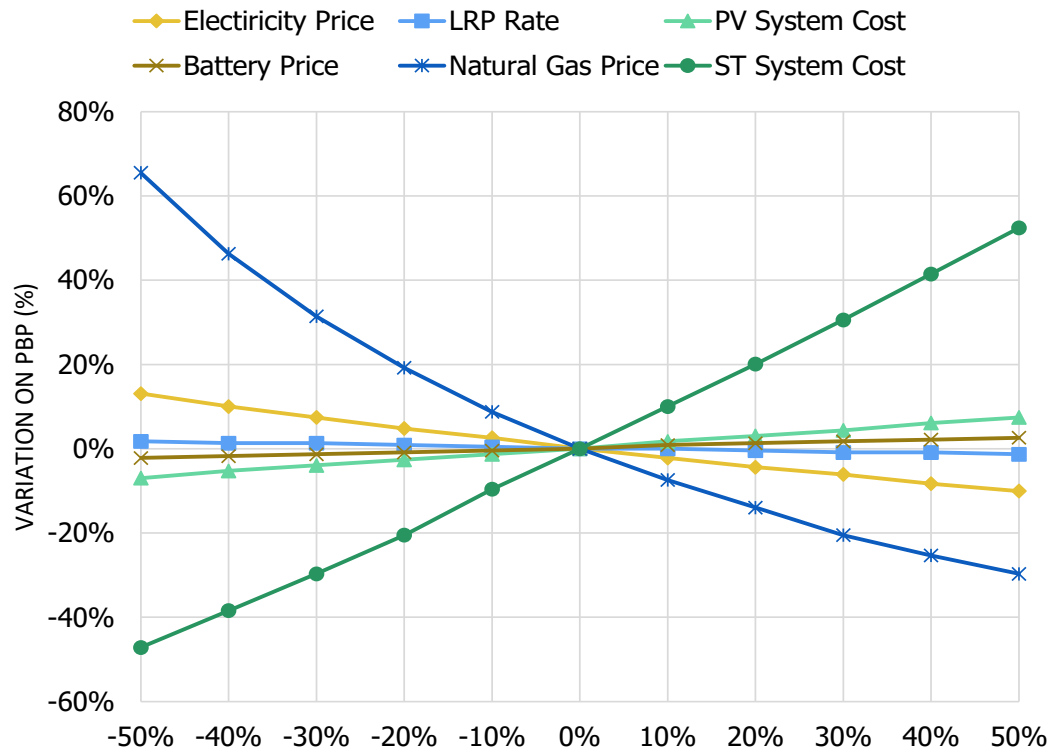
Figure 3.15- Sensitivity analysis for a) LCOE and b) PBP

3.5.4 Future scenarios

In this section, the effect of simultaneous variation of natural gas and electricity inflation rates and financial incentives on ST/PV-BES system PBP are assessed. Six different scenarios are analyzed, starting with the initial condition that provides the results of section 5-1. Table 3.6 summarizes the values for the parameters considered in each proposed scenario. The scenarios are sorted from least optimistic (S0, initial condition) to most optimistic (scenario S5). In these scenarios, inflation rates of natural gas, electricity, and carbon tax grow from initial values of 3% to 9% and LRP inflation rate varies from 0 to 6%. Different combinations of these parameters are implemented.

Table 3.6- Values for the different parameters considered in each of the 6 scenarios assessed

Scenario	NG i	Electricity i	LRP i	CT i
S0	3%	3%	0%	3%
S1	4%	4%	1%	4%
S2	5%	5%	2%	5%
S3	6%	6%	3%	6%
S4	7%	7%	4%	7%
S5	8%	8%	5%	8%
S6	9%	9%	6%	9%

Results show that it would only require a one percent increase of all inflation rates to have a PBP around 20 years (See Fig. 3.16). In each inflation rate increase for the selected parameters, PBP would, on average, reduce by about 7.6%. If the inflation rates continue to increase, it is possible to have a reasonable PBP of 15 years or lower. This is demonstrated in scenarios 5 and 6, where a PBP of 15 and 14.2 years can be achieved. The analysis undertaken shows that the ST/PV-BES system proposed in this research appears as a cost-competitive alternative under different scenarios.
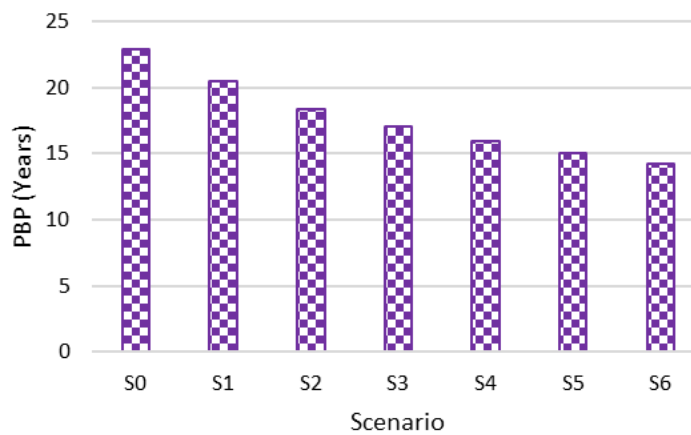
Figure 3.16- PBP of the proposed ST/PV-BES system in the different future scenarios

3.6 Conclusions

This paper presented unit sizing and an economic evaluation of a hybrid ST/PV-BES system which was developed in TRNSYS software for a commercial greenhouse. Heating demand was supplied by both ST and auxiliary heating systems, and the electricity demand was supplied by both PV-BES system and the central grid. The model was used to determine the advantageous configurations of ST size, PV size, and BES capacity that minimizes the LCOE of the system. It was demonstrated that the best scenario which is a system with 90% ST, 10% PV, and 6 AH BES results in an LCOE value of 24.77 $/GJ. The transient simulation of the ideal system configuration showed that the optimal shares of renewable heat energy harvesting and renewable electricity harvesting were 36% and 49%, respectively. Then, an economic assessment was conducted on the optimized system through series of sensitivity analyses to evaluate the effects of key influences on system efficacy. The two major takeaways from this analyses were: (1) The system LCOE was most sensitive to natural gas price and ST system cost; (2) The influence of the electrical parameters were less important because of the smaller size of the electrical subsystem.

Finally, the effect of simultaneous natural gas, electricity, and financial incentive (LRP and carbon tax) inflation was studied through six different scenarios. It was shown that for each step rise in inflation of the selected parameters, the PBP would reduce by 7.6% on average. Ultimately, it was revealed that it is possible to have a PBP of less than 15 years.

Acknowledgements

References

[1]   G. M. Dias *et al.*, "Life cycle perspectives on the sustainability of Ontario greenhouse tomato production: Benchmarking and improvement opportunities," *J. Clean. Prod.*, vol. 140, pp. 831–839, 2017.

[2]   Agriculture and Agri-Food Canada (AAFC), "Statistical Overview of the Canadian Greenhouse Vegetable Industry, 2017." [Online]. Available: http://www.agr.gc.ca/eng/industry-markets-and-trade/canadian-agri-food-sector-intelligence/horticulture/horticulture-sector-reports/statistical-overview-of-the-canadian-greenhouse-vegetable-industry-2017/?id=1549048060760. [Accessed: 30-Sep-2019].

[3]   Ontario Greenhouse Vegetable Growers, "Fact Sheet," 2019.

[4]   IESO, " New study shows energy cost savings potential for Ontario greenhouses." [Online]. Available: http://www.ieso.ca/en/Corporate-IESO/Media/News-Releases/2019/10/New-Greenhouse-Study. [Accessed: 10-April-2020].

[5]   Ontario Ministry of Energy, "Delivering Fairness and Choice: Ontario's Long-Term Energy Plan 2017," 2017.

[6]   IESO, "Reliability Outlook - An adequacy assessment of Ontario's electricity system - from October 2019 to March 2021," 2019.

[7]   R. Loni, A. B. Kasaeian, E. A. Asli-ardeh, B. Ghobadian, and W. G. Le Roux, "Performance Study of a Solar-Assisted Organic Rankine Cycle Using a Dish-Mounted Open-Cavity Tubular Solar Receiver," *Appl. Therm. Eng.*, vol. 108, pp. 1298–1309, 2016.

[8]   M. Gitizadeh and H. Fakharzadegan, "Battery capacity determination with respect to optimized energy dispatch schedule in grid-connected photovoltaic (PV) systems," *Energy*, vol. 65, pp. 665–674, 2014.

[9]   K. K. Tse, T. T. Chow, and Y. Su, "Performance evaluation and economic analysis of a full scale water-based photovoltaic/thermal (PV/T) system in an office building," *Energy Build.*, vol. 122, pp. 42–52, 2016.

[10]   Li, Y., & Liu, C. (2018). Techno-economic analysis for constructing solar photovoltaic projects on building envelopes. Building and Environment, 127, 37-46.

[11]   Xu, W., Song, W., & Ma, C. (2020). Performance of a water-circulating solar heat collection and release system for greenhouse heating using an indoor collector constructed of hollow polycarbonate sheets. Journal of Cleaner Production, 253, 119918.

[12]   Bloem, J. J. (2008). Evaluation of a PV-integrated building application in a well-controlled outdoor test environment. Building and Environment, 43(2), 205-216.

[13]   Jahangir, M. H., Shahsavari, A., & Rad, M. A. V. (2020). Feasibility study of a zero emission PV/Wind turbine/Wave energy converter hybrid system for stand-alone power supply: A case study. Journal of Cleaner Production, 121250.

[14]   Y. Kim, K. Thu, H. Kaur, C. Singh, and K. Choon, "Thermal analysis and performance optimization of a solar hot water plant with economic evaluation," *Sol. Energy*, vol. 86, no. 5, pp. 1378–1395, 2012.

[15]   C. S. Lai and M. D. McCulloch, "Levelized cost of electricity for solar photovoltaic and electrical energy storage," Appl. Energy, vol. 190, pp. 191–203, 2017.

[16]   S. Sadhishkumar and T. Balusamy, "Performance improvement in solar water heating systems — A review," *Renew. Sustain. Energy Rev.*, vol. 37, pp. 191–198, 2014.

[17]   E. Sánchez and J. Izard, "Performance of photovoltaics in non-optimal orientations : An experimental study," *Energy Build.*, vol. 87, pp. 211–219, 2015.

[18]   W. A. Omran, M. Kazerani, and M. M. A. Salama, "Investigation of methods for reduction of power fluctuations generated from large grid-connected photovoltaic systems," IEEE Trans. Energy Convers., vol. 26, no. 1, pp. 318–327, 2010.

[19]   Z. Salam, J. Ahmed, and B. S. Merugu, "The application of soft computing methods for MPPT of PV system : A technological and status review," *Appl. Energy*, vol. 107, pp. 135–148, 2013.

[20]   Kyriaki, E., Stergiopoulos, S., & Papadopoulos, A. M. (2020). Alternative storage options for solar thermal systems. International Journal of Energy Research.

[21] Liao, Q., Zhang, Y., Tao, Y., Ye, J., & Li, C. (2019). Economic analysis of an industrial photovoltaic system coupling with battery storage. *International Journal of Energy Research*, *43*(12), 6461-6474.

[22] Sharadga, Hussein, Ahmad Dawahdeh, and Moh'D. A. Al-Nimr. "A hybrid PV/T and Kalina cycle for power generation." International Journal of Energy Research 42, no. 15 (2018): 4817-4829.

[23] B. Croxford and K. Scott, "Can PV or solar thermal systems be cost effective ways of reducing CO 2 emissions for residential buildings?," *Am. Sol. Energy Soc.*, 2006.

[24] "Ecosystem carbon payback time". [Online]. Available: https://www.grida.no/resources/6196. [Accessed: 15-April-2020].

[25] M. Leckner and R. Zmeureanu, "Life cycle cost and energy analysis of a Net Zero Energy House with solar combisystem," Appl. Energy, vol. 88, no. 1, pp. 232–241, 2011.

[26] L. Romero Rodríguez, J. M. Salmerón Lissén, J. Sánchez Ramos, E. Á. Rodríguez Jara, and S. Álvarez Domínguez, "Analysis of the economic feasibility and reduction of a building's energy consumption and emissions when integrating hybrid solar thermal/PV/micro-CHP systems," *Appl. Energy*, vol. 165, pp. 828–838, 2016.

[27] D. Testi, E. Schito, and P. Conti, "Cost-optimal sizing of solar thermal and photovoltaic systems for the heating and cooling needs of a nearly Zero-Energy Building: the case study of a farm hostel in Italy," *Energy Procedia*, vol. 91, pp. 528–536, 2016.

[28] D. Testi, E. Schito, and P. Conti, "Cost-optimal sizing of solar thermal and photovoltaic systems for the heating and cooling needs of a nearly Zero-Energy Building: design methodology and model description," *Energy Procedia*, vol. 91, pp. 517–527, 2016.

[29] F. Ascione, N. Bianco, R. F. De Masi, C. De Stasio, G. M. Mauro, and G. P. Vanoli, "Multi-objective optimization of the renewable energy mix for a building," *Appl. Therm. Eng.*, vol. 101, pp. 612–621, 2016.

[30] T. Matuska, "Performance and economic analysis of hybrid PVT collectors in solar DHW system," *Energy Procedia*, vol. 48, pp. 150–156, 2014.

[31] N. Gunasekar, M. Mohanraj, and V. Velmurugan, "Artificial neural network modeling of a photovoltaic-thermal evaporator of solar assisted heat pumps," *Energy*, vol. 93, pp. 908–922, 2015.

[32] D. N. Basu and A. Ganguly, "Solar thermal-photovoltaic powered potato cold storage - Conceptual design and performance analyses," *Appl. Energy*, vol. 165, pp. 308–317, 2016.

[33] J. Kim, T. Hong, J. Jeong, C. Koo, K. Jeong, and M. Lee, "Multi-criteria decision support system of the photovoltaic and solar thermal energy systems using the multi-objective optimization algorithm," *Sci. Total Environ.*, vol. 659, pp. 1100–1114, 2019.

[34] O. Bany Mousa, S. Kara, and R. A. Taylor, "Comparative energy and greenhouse gas assessment of industrial rooftop-integrated PV and solar thermal collectors," *Appl. Energy*, vol. 241, pp. 113–123, 2019.

[35] O. Bany Mousa, R. A. Taylor, and A. Shirazi, "Multi-objective optimization of solar photovoltaic and solar thermal collectors for industrial rooftop applications," *Energy Convers.*

Manag., vol. 195, pp. 392–408, 2019.

[36] O. M. Bany Mousa and R. A. Taylor, "A broad comparison of solar photovoltaic and thermal technologies for industrial heating applications," *J. Sol. Energy Eng.*, vol. 141, no. 1, 2019.

[37] SEL, TRNSSOLAR, and Tess CSTB, "Multizone Building modeling with Type56 and TRNBuild," *TRNSYS*, 2004.

[38] R. Adnan, L. Jong Won, and L. Hyun Woo, "A review of greenhouse energy management by using building energy simulation," *Prot. Hortic. Plant Fact.*, vol. 24, no. 4, pp. 317–325, 2015.

[39] R. L. Shrivastava, V. Kumar, and S. P. Untawale, "Modeling and simulation of solar water heater: A TRNSYS perspective," *Renew. Sustain. Energy Rev.*, vol. 67, pp. 126–143, 2017.

[40] M. Carlini and S. Castellucci, "Modelling and simulation for energy production parametric dependence in greenhouses," *Math. Probl. Eng.*, 2010.

[41] E. Mashonjowa, F. Ronsse, J. R. Milford, and J. G. Pieters, "Modelling the thermal performance of a naturally ventilated greenhouse in Zimbabwe using a dynamic greenhouse climate model," *Sol. Energy*, vol. 91, pp. 381–393, 2013.

[42] A. Vadiee and V. Martin, "Thermal energy storage strategies for effective closed greenhouse design," *Appl. Energy*, vol. 109, pp. 337–343, 2013.

[43] X. Zhang, H. Wang, Z. Zou, and S. Wang, "CFD and weighted entropy based simulation and optimisation of Chinese Solar Greenhouse temperature distribution," *Biosyst. Eng.*, vol. 142, pp. 12–26, 2016.

[44] L. Semple, R. Carriveau, and D. S. Ting, "A techno-economic analysis of seasonal thermal energy storage for greenhouse applications," *Energy Build.*, vol. 154, pp. 175–187, 2017.

[45] Government of Canada, "Engineering Climate Datasets," 2019. [Online]. Available: http://climate.weather.gc.ca/prods_servs/engineering_e.html%0AFTP directory /Pub/Engineering_Climate_Dataset/Canadian_Weather_year_for_Energy_Calculation_CWE C/ENGLISH/CWEC_v_Historical/ at ftp.tor.ec.gc.ca%0AFTP directory /Pub/Engineering_Climate_Dataset/. [Accessed: 28-Aug-2019].

[46] N. Logics, "Canadian weather for energy calculations, users manual and CD-ROM," *Environ. Canada, Ottawa*, 1999.

[47] R. C. Richman and K. D. Pressnail, "A more sustainable curtain wall system: Analytical modeling of the solar dynamic buffer zone (SDBZ) curtain wall," *Build. Environ.*, vol. 44, no. 1, pp. 1–10, 2009.

[48] R. Djebbar, R. Morris, D. Thevenard, R. Perez, and J. Schlemmer, "Assessment of SUNY version 3 global horizontal and direct normal solar irradiance in Canada," *Energy Procedia*, vol. 30, pp. 1274–1283, 2012.

[49] L. Semple, R. Carriveau, and D. Ting, "Assessing heating and cooling demands of closed greenhouse systems in a cold climate," *Int. J. energy Res.*, vol. 41, no. 13, pp. 1903–1913, 2017.

[50] A. Vadiee and V. Martin, "Energy management strategies for commercial greenhouses," *Appl. Energy*, vol. 114, pp. 880–888, 2014.

[51] G. Papadakis, D. Briassoulis, G. Scarascia Mugnozza, G. Vox, P. Feuilloley, and J. A. Stoffers, "Review Paper (SE—Structures and Environment): Radiometric and thermal properties of, and testing methods for, greenhouse covering materials," *J. Agric. Eng. Res.*, vol. 77, no. 1, pp. 7–38, 2000.

[52] L. S. Marsh and S. Singh, "Economics of greenhouse heating with a mine air-assisted heat pump," *Trans. ASAE*, vol. 37, no. 6, pp. 1959–1963, 1994.

[53] A. Kasaeian, G. Nouri, P. Ranjbaran, and D. Wen, "Solar collectors and photovoltaics as combined heat and power systems: A critical review," *Energy Convers. Manag.*, vol. 156, pp. 688–705, 2018.

[54] M. Mehrpooya, H. Hemmatabady, and M. H. Ahmadi, "Optimization of performance of Combined Solar Collector-Geothermal Heat Pump Systems to supply thermal load needed for heating greenhouses," *Energy Convers. Manag.*, vol. 97, pp. 382–392, 2015.

[55] S. A. Klein, W. A. Beckman, J. W. Mitchell, and J. A. Duffie, "TRNSYS 17: A Transient System Simulation Program: Mathematical Reference," University of Wisconsin: Madison, WI, USA., 2014.

[56] Solar Rating and Certification Corporation, "Directory of SRCC certified solar collertors ratings," 2007.

[57] D. Q. Zeng, H. Li, Y. J. Dai, and A. X. Xie, "Numerical analysis and optimization of a solar hybrid one-rotor two-stage desiccant cooling and heating system," *Appl. Therm. Eng.*, vol. 73, no. 1, pp. 474–483, 2014.

[58] "TRNSYS 17 TESS Library – Component libraries for TRNSYS simulation environment – Volume 11 – Storage tank library mathematical reference."

[59] Ossila, "I-V Curves: A Guide to Measurement". [Online]. Available: https://www.ossila.com/pages/iv-curves-measurement. [Accessed: 15-April-2020].

[60] L. Wang, J. Gwilliam, and P. Jones, "Case study of zero energy house design in UK," Energy Build., vol. 41, no. 11, pp. 1215–1222, 2009.

[61] CanadianSolar, "Solar Modules." [Online]. Available: https://www.canadiansolar.com/solarPanels/detail/30. [Accessed: 04-Sep-2019].

[62] S. A. Kalogirou, "Photovoltaic Systems," in *Solar Energy Engineering: Processes and Systems*, Second Edi., Academic Press, 2013, pp. 481–540.

[63] M. K. Deshmukh and S. S. Deshmukh, "Modeling of hybrid renewable energy systems," *Renew. Sustain. Energy Rev.*, vol. 12, no. 1, pp. 235–249, 2008.

[64] Wegosolar, "Surrette S550 Deep Cycle Wet Lead Acid Solar 6V Battery," 2017. [Online]. Available: http://www.wegosolar.com/. [Accessed: 04-Sep-2019].

[65] F. Shao, "Measurement and Simulation of Stand Alone Photovoltaic Systems," European Solar Engineering School, Högskolan Dalarna, Sweden, 2007.

[66] F. Calise, R. D. Figaj, and L. Vanoli, "A novel polygeneration system integrating photovoltaic/thermal collectors, solar assisted heat pump, adsorption chiller and electrical energy storage: Dynamic and energy-economic analysis," *Energy Convers. Manag.*, vol. 149, pp. 798–814, 2017.

[67] G. Notton, V. Lazarov, and L. Stoyanov, "Optimal sizing of a grid-connected PV system for various PV module technologies and inclinations, inverter efficiency characteristics and locations," *Renew. Energy*, vol. 35, no. 2, pp. 541–554, 2010.

[68] S. G. Sigarchian, A. Malmquist, and T. Fransson, "Modeling and control strategy of a hybrid PV/Wind/Engine/Battery system to provide electricity and drinkable water for remote applications," *Energy Procedia*, vol. 57, no. 1, pp. 1401–1410, 2014.

[69] A. S. Mundada, K. K. Shah, and J. M. Pearce, "Levelized cost of electricity for solar photovoltaic, battery and cogen hybrid systems," *Renew. Sustain. Energy Rev.*, vol. 57, pp. 692–703, 2016.

[70] M. Obi, S. M. Jensen, J. B. Ferris, and R. B. Bass, "Calculation of levelized costs of electricity for various electrical energy storage systems," *Renew. Sustain. Energy Rev.*, vol. 67, pp. 908–920, 2017.

[71] M. Bortolini, M. Gamberi, and A. Graziani, "Technical and economic design of photovoltaic and battery energy storage system," *Energy Convers. Manag.*, vol. 86, pp. 81–92, 2014.

[72] S. Kalogirou, *Solar energy engineering—processes and applications*. Elsevier: Academic Press, 2009.

[73] S. A. Kalogirou, "Solar thermal collectors and applications," *Prog. Energy Combust. Sci.*, vol. 30, no. 3, pp. 231–295, 2004.

[74] IEA and NEA, "Projected costs of generating electricity–2015 Edition."

[75] Wire Services and Globe Staff, "Canada's carbon tax: A guide to who's affected, who pays what and who opposes it," *The Globe and Mail*, 2019. [Online]. Available: https://www.theglobeandmail.com/canada/article-canadas-carbon-tax-a-guide/. [Accessed: 21-May-2019].

[76] EIA, "How much carbon dioxide is produced when different fuels are burned?" [Online]. Available: https://www.eia.gov/tools/faqs/faq.php?id=73&t=11. [Accessed: 01-Oct-2019].

[77] IESO, "Reliability Outlook–An adequacy assessment of Ontario's electricity system–From July 2019 to June 2014," 2019.

[78] IESO, "Feed-in Tariff Program," 2019. [Online]. Available: http://www.ieso.ca/sector-participants/feed-in-tariff-program/overview. [Accessed: 01-Aug-2019].

[79] IESO, "FIT/microFIT price schedule." [Online]. Available: http://www.ieso.ca/en/sector-participants/ieso-news/2016/09/fit-microfit-price-schedule-for-2017-now-available. [Accessed: 01-Aug-2019].

[80] IESO, "A Progress Report on Contracted Electricity Supply: Third Quarter 2017," 2017.

[81] M. Leckner, "Life cycle energy and cost analysis of a net zero energy house (NZEH) using solar combisystem," Concordia University, 2008.

[82] EIA, "Annual Energy Review." [Online]. Available: https://www.eia.gov/totalenergy/data/annual/showtext.php?t=ptb1006. [Accessed: 06-Sep-2019].

[83] A. Gallo, B. T. Molina, M. Prodanovic, J. G. Aguilar, and M. Romero, "Analysis of net Zero-Energy Building in Spain. Integration of PV, solar domestic hot water and air-conditioning

systems," *Energy Procedia*, vol. 48, pp. 828–836, 2014.

[84]   Ontario Energy Board, "Bill calculator." [Online]. Available: https://www.oeb.ca/consumer-protection/energy-contracts/bill-calculator. [Accessed: 06-Sep-2019].

CHAPTER 4

Parametric Optimization of Environment Variables to Minimize Energy Requirements and Improve Solar Thermal Energy System Performance in a Commercial Greenhouse

Sadaf Ekhtiari, Rupp Carriveau, David S-K. Ting
Turbulence and Energy Laboratory, University of Windsor
401 Sunset Ave, Windsor, ON, Canada

4.1 Introduction

Global food demand is progressively increasing, so it is crucial to reduce the risks of global malnutrition, hunger, and conflict [1]. Greenhouse production plays an important role for food security and has been commonly used in the agricultural sector by multiple growers worldwide [2,3]. A greenhouse is a transparent environment for incident solar radiation providing an appropriate microclimate for crops, protecting them from external environments in order to improve their yield and quality [4]. Greenhouses have been adopted by around 115 countries for commercial vegetable growing to improve the crop yields [5].

Energy demand modelling is one of the major challenges with greenhouses. To measure the energy consumption of the greenhouse, various models and tools have been utilized. For example, a comprehensive Transient Energy System Simulation Tool (TESST) was developed to simulate the thermal energy dynamics within CEA operations. Modeled thermal demand was benchmarked against actual measured demand [19]. Furthermore, in order to calculate the heating demand of a greenhouse located in Saskatoon, a quasi-steady state time-dependent thermal model was developed [9]. In another study, a Chinese-style thermal model called "CSGHEAT" was developed for solar greenhouses. The model was used to estimate the time-dependent heating demand. The relative root mean square error (rRMSE) and the average percent error were reported to be equal to 11.5% and 8.7%, respectively [10]. This model was then compared with a different TRNSYS model [9]. The study demonstrated that TRNSYS assumptions – such as fixed infiltration rate, moisture gain schedule, and use of thermal blankets – produce large errors in heating demand estimation. A Building Energy Simulation (BES) model was developed using TRNSYS to determine the greenhouse energy demand based on the type of greenhouse, the area, and specified internal air temperatures for the climatic conditions of the Republic of Korea [11]. This model was experimentally verified with Nash-Sutcliffe efficiency coefficients of 0.84 and 0.78 to be used for greenhouse thermal simulations. It was concluded that multi-layer night thermal screens can save 20%, 5.4%, and 13.5% of heating energy consumption compared to polyester, Luxous, and Tempa screens, respectively. In another study by [12], this model was used to assess the effect of greenhouse design parameters on energy efficiency. It was decided that the best design for South Korea's climate is a greenhouse-oriented east-west with a gothic-shaped roof and covered with a double glazing of Polymethylmethacrylate.

The advantages of indoor agriculture do not come without cost. Modern greenhouses and vertical farms require significant investments of capital expenditures, labor, and energy consumption. Of these, supplying the demanded energy has the most significant cost in greenhouse operations [13]. There are different kinds of heating solutions implemented in the greenhouse's operations, including fossil fuels. There are several limitations, however, associated with this solution, such as carbon gas emissions, fuel price volatility, and others. These concerns have driven interest in considering the application of renewable energy as an additional source of heating greenhouses. Among all the renewable resources, solar energy has been found to be an attractive alternative for conventional fossil fuels, owing to its abundance, environmental profile, and decreasing costs [14-18]. Solar systems are able to generate both electricity and heating based on the technology used. Solar thermal (ST) collectors play an important role in supplying the heating load of the greenhouses. In previous studies by the authors, a solar thermal system was modeled using TRNSYS simulation software (version 17) to meet the heating demand of the commercial greenhouse [19].

The air temperature inside a greenhouse essentially relies upon the external climatic conditions including surrounding temperature and solar radiation, as well as other design variables [20]. The main structural variables affecting greenhouses' heating/cooling energy demands and thermal behaviors are the cladding material characteristics, shape, and orientation, and air change rate as well [20]. Precise estimations of solar radiation and heat transfer coefficients are crucial for building a perfect thermal model, since these variables significantly impact the greenhouse energy and mass balance [21-23]. Greenhouse shape and direction significantly affect the total solar radiation absorbed by the greenhouse, which influences the indoor air temperature [24-28]. One of the main challenges of greenhouse energy modelling is including the plants' effects and contributions [29,30]. The presence of the yields significantly impacts greenhouse microclimate. TRNSYS software was deployed for the transient 93 simulation of the indoor greenhouse climate in several studies [31]. It was reported in the literature that the software demonstrated superior performance [32-36]. Modelling the thermal behavior of a greenhouse using building software is more difficult due to the complex nature of plant transpiration. Several studies have been conducted modeling the greenhouse using this form of software without considering the crops inside or assuming a constant evapotranspiration rate, which leads to enormous inaccuracies in greenhouse heating/cooling energy requirements [9].

Compared to mainstream building science, the literature focused on the greenhouse growing environment is relatively scarce. The authors have not yet seen a study that leverages incremental improvements to existing CEA practices while introducing the potential for pioneering change through a complete reimagining of the growing environment. The objective of this study is to minimize CEA energy requirements and to improve system performance for operations through parametric optimization of major growing environment variables, including cladding material and window-to-wall ratio. Various scenarios were created by varying window-to-wall area ratio with different types of wall materials to find the best configuration and evaluate the potential ways of reducing the heating demand – while maintaining an acceptable range for cooling demand and solar

energy absorption. Furthermore, additional scenarios were created by changing the characteristics of the solar thermal model elements, such as hot water tank capacity and heat exchanger effectiveness. The solar fraction was then calculated for each scenario to determine the impact of the greenhouse's design parameters on its energy-saving efficiency.

4.2 Methodology

In this proposed study, a dynamic simulation of the solar thermal system was implemented in TRNSYS. The performance of the system during a one-year operation was assessed. TRNSYS ("Transient System Simulation Program") is a simulation environment for the transient simulation of energy systems [37]. As a complete and extensible simulation environment, it has become a popular choice for many researchers [38-43]. This section describes the reference greenhouse specifications, as well as inputs of the transient model of the solar thermal system and system performance. These inputs are the hourly meteorological loads and hourly heating loads of the greenhouse. Finally, a parametric study has been carried out on this solar thermal system to explore the potential ways of reducing energy consumption and improving the energy efficiency and sustainability of CEA operations. Major growing environment variables were investigated in this parametric optimization, including cladding material and window-to-wall ratio, as well as characteristics of the solar thermal model elements such as hot water tank capacity and heat exchanger effectiveness.

4.2.1 Reference greenhouse

The modeled reference greenhouse was a 24-acre, gutter-connected, and Venlo-type structure located in Essex County, Ontario, Canada. The Essex region has a cold climate, and it is the heart of greenhouses in North America. The building has height of 5.5 m and a roof slope of 25°. This greenhouse produces bell peppers.

4.2.2 Meteorological information

In order to supply climate data to the model, the Weather Data Processor is used. Data is taken from the Canadian Weather for Energy Calculation (CWEC) dataset for Windsor (latitude 42.32°N and longitude 83.03°W). The CWEC dataset consists of hourly weather information from the Canadian Weather Energy and Engineering Datasets (CWEEDS) for an artificial one-year cycle composed of twelve average months in a 30 year compilation [44,45]. The input weather data includes total tilted radiation, hourly dry bulb temperature, diffuse radiation, beam radiation, angle of incidence for the collectors, and ground reflections. The CWEC dataset includes a mixture of sunny and cloudy days, with multiple variations of both [46]. This dataset has been widely used in the measurement of heating loads and in the design of solar thermal systems [47].

4.2.3 Annual heating energy consumption

The greenhouse's thermal energy requirements are determined based on internal loads and external climatic conditions. The hourly load profile is useful in properly designing and dimensioning the greenhouse's solar energy system and in providing precise data for efficient computer simulation.

To calculate the heating load, one acre of the greenhouse is simulated in order to normalize the model. This acre includes 10 bays, each with a width of 5 m. Two lower and upper thermal zones were considered to determine the thermal conditions near and far from the crop [48]. The lower node has a height of 3.5 m and the upper node has a height of 2 m. The window-to-wall (frame) area ratio for both upper nodes and lower nodes is 9. The frame material is aluminum, and the window material is double polyethylene. The greenhouse's 3D geometry was modeled in Google SketchUp, and imported into the building model with the TRNSYS3D plug-in. The SketchUp schematic is illustrated in Figure 4.1.
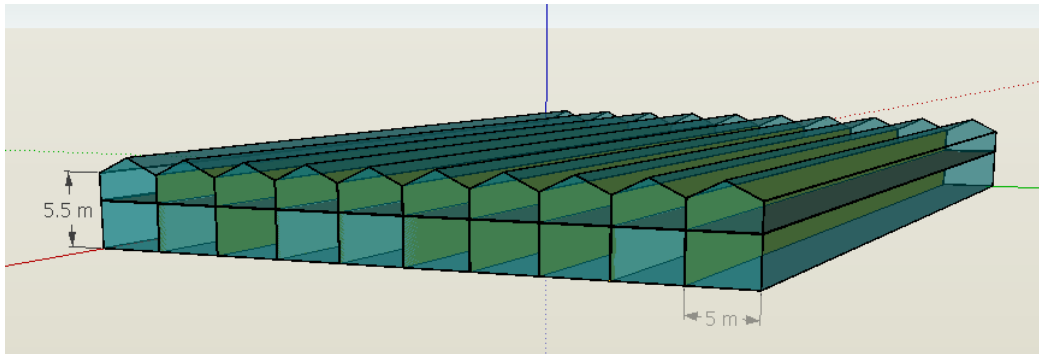
Figure 4.1 - 3-Dimensional Greenhouse Model in Google SketchUp

The thermal properties of the greenhouse were modeled using Type 56, a multi-zone building in the sub-program TRNBuild. The day and night set-point temperatures for the bell peppers are 22°C and 18°C, respectively. The infiltration ratio is determined to be in the range of 0.5 to 1.5 ACH [49]. The night set-point temperature is raised 1°C an hour in the early morning to reach the day set-point temperature prior to the sunrise. Regardless of the indoor temperature, morning pre-heating is supplied between 3 a.m. and 6 a.m. year-round. The crop termination months stretch from mid-November to January, and the indoor temperature is maintained above freezing at 5°C [48]. The overall efficiency of the heating system of the reference greenhouse is assumed to be 75% [48]. The heating system consists mainly of hot water piping located near the floor and the top of the fully grown crops. The ventilation system activates, providing 60 ACH when the inside temperature or relative humidity exceeds 25°C and 85%, respectively. The covering material of the roof and walls of the greenhouse is air-inflated double-polyethylene. The heat transfer coefficient of the greenhouse cover was set at $5W/m^2.°C$, which is consistent with the literature [50]. The light transmittance of double-polyethylene film is typically 75% [51].

In TRNSYS, the sensible heating demand of the one-acre greenhouse is determined with a time step of one hour over a full year. For the 24-acre greenhouse, the profile is multiplied by 24. The heating system must supply the sensible heating demand in the greenhouse. For the modeled greenhouse, the hourly rational heating load profile is shown in Figure 4.2. The hourly heating demand is required by the system as an input. According to Figure 4.2, the peak hourly demand for mid-January is about 16.5 MWh. The morning loads for pre-heating were set at 8.3 kWh. The reason for the low energy demand for November and December is crop termination.

The monthly sensible heating demand is depicted in Figure 4.3, and it is benchmarked with the actual data from the reference greenhouse. A good consistency is recognized between the actual and modeled data, which supports its use for solar thermal system design. The total annual heating energy demand for the modeled greenhouse was determined to be 5,000 GJ, which is within 5% of the actual data.
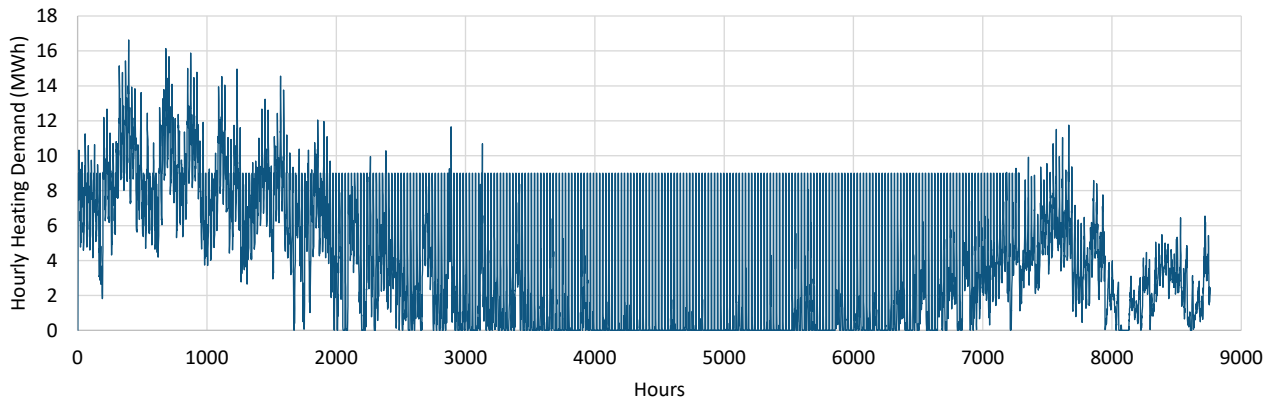
Figure 4.2 - Hourly heating demand of the greenhouse from TRNSYS Model [19]
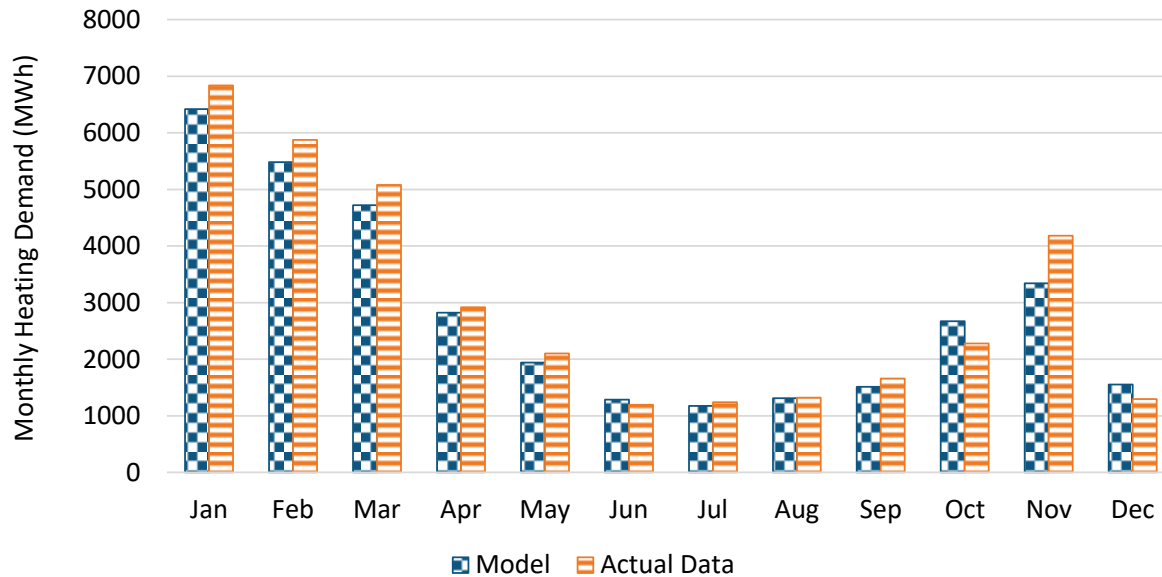
Figure 4.3 - Actual and modeled monthly heating demand of the greenhouse [19]

4.2.4 Solar Thermal System Description

To calculate the solar energy harvesting rates, the ST system model is analyzed. Using TRNSYS software (v. 17), a dynamic system is simulated. System simulation was performed for one year using a simulation time step of one hour.

In the schematic shown in Figure 4.4, the ST system and its components are included. The ST system operates to meet the heating load. The main components of ST solar systems are solar collectors, which transform the incident solar radiation into heat. The harvested heat is transferred by the working fluid for greenhouse space heating; it is stored in a tank to be restored at night or on cloudy days. Natural gas burns in the auxiliary system.
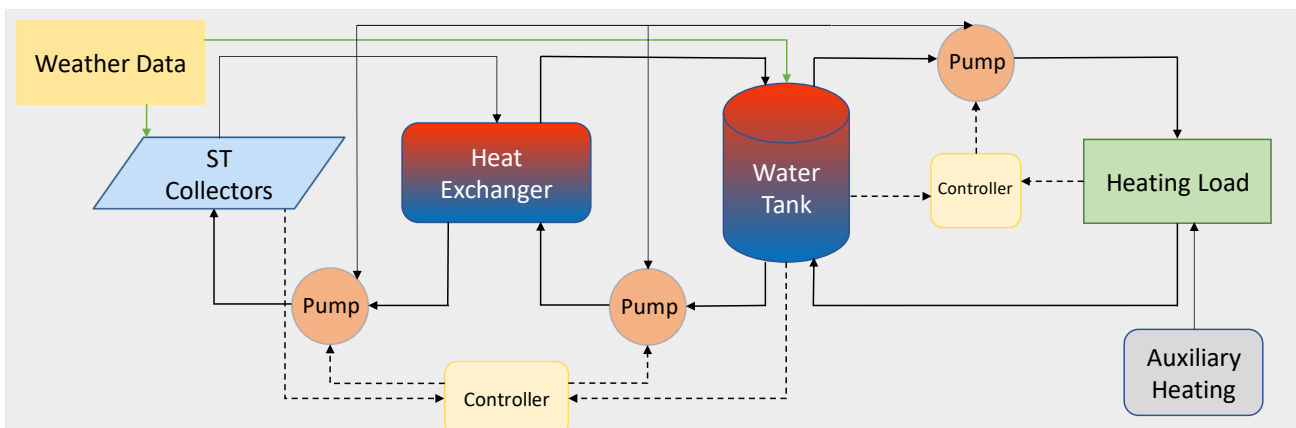
Figure 4.4 - Schematic diagram of the main components of the solar system

61

4.2.4.1 Solar Thermal System Elements

The solar thermal system is responsible for meeting the heating load, and consists of the following elements:

Flat-plate Solar Collectors: For low-to-medium temperature applications, flat-plate solar collectors are used [52]. The array of solar collectors consists of units linked both in series and parallel to each other. The ST collector's tilt angle was optimized for the latitude of the location [53]. It is assumed that a solution of 50% propylene glycol and water was circulated through the collector loop to avoid freezing during wintertime [54], and that the specific heat of the working fluid was equivalent to 3.6 kJ/kg°C [43]. To model the performance of a flat-plate solar collector, Type 1C is used. The quadratic efficiency equation – which is the generalization of the Hottel-Whillier equation – has been used to model the flat plate solar collector in TRNSYS [55].

$$\eta = a_0 - a_1 \frac{(\Delta T)}{I_T} - a_2 \frac{(\Delta T)^2}{I_T} \tag{1}$$

ΔT is the difference between the fluid's inlet temperature to the collector and ambient air temperature, while a_0, a_1, and a_2 are the intercept efficiency, efficiency slope, and efficiency curvature, respectively. The values of a_0, a_1, and a_2 are derived from product certification data [56]. I_T is the global radiation incident on the solar collector. Each selected module has an area of 1,865 m². Table 4.1 summarizes the data used for the flat-plate solar collector. In an external file, the Incidence Angle Modifier (IAM) is supplied to account for the effect of the solar irradiance inclination with respect to the solar collector surface.

Table 4.1 - Flat-plate solar collector parameters

Main Parameters	Value	Unit
Working Fluid Specific Heat	3.32	kJ/kg K
Intercept Efficiency	0.604	-
Efficiency Slope	3.73	kJ/h m²K
Efficiency Curvature	0.0086	kJ/h m²K²
Tested Flow Rate	32	kg/h m²

Heat Exchanger: The working fluid in the solar collector loop is an anti-freeze fluid, so a heat exchanger is necessary to transfer the heat absorbed by the fluid in the collector to the water in the water tank. The heat exchanger used in this simulation is external. The counter-flow heat exchanger of TRNSYS Type 91, based on an effectiveness minimum capacitance approach, was considered. The heat exchanger effectiveness is determined to be 0.8 [57]. In the stable effectiveness mode, the parameters that are considered for the maximum possible heat transfer are the minimum capacity rate fluid and the cold side and hot side fluid inlet temperatures.

Hot Water Storage Tank: TRNSYS Type 534 is used to model a cylindrical tank [58]. In all cases, the total water tank volume is set to 100 l/m² of the solar thermal collector area. The modeled tank was split into five isothermal temperature nodes to model the stratification. A 2:1 proportion is considered as the tank's height-to-diameter ratio. The links are placed at the top and bottom of the tank.

Controllers: For each circuit, on/off differential controllers are used to study the fluid temperature inputs leaving the collector, the temperature of the water tank's bottom node, the system's cut-off temperature, and the availability of the demand for heating. Controllers produce an output control feature of 1 (On) or 2 (Off) to turn pumps on or off, depending on the receiving inputs.

Circulation Pumps: TRNSYS Type 3 is used for modeling variable speed pumps. The maximum flow capacity and the mass flow rate are computed with this type. In all cases, the maximum flow capacities are specified based on the ST system size. The mass flow rate is calculated based on a variable control feature from the controllers.

Heating Load: To impose the measured heating load on the flow stream leaving the solar thermal system, TRNSYS Type 682 is used. This type serves as an interface point between the greenhouse and the solar thermal system.

4.2.4.2 Solar Thermal System Performance

To assess the overall solar thermal system performance, the monthly solar fractions are evaluated. The Solar Fraction (SF) is the ratio of the energy supplied by the solar system to the total energy demand of the greenhouse, which it is shown in Equation 2. In Figure 4.5, the heat supplied to the greenhouse by the solar system and the required auxiliary heating source are represented in the overall monthly heating demand bars with various colored patterns to be differentiated. The solar fraction in Figure 4.5 is also measured and plotted. In the summer months, when the solar irradiation reaches its peak, the solar thermal can cover almost the entire heating load. The solar fraction fluctuates from an average amount of 20% in winter months to an average amount of 94% in summer months. The solar thermal system can cover 36% of the annual greenhouse heating demand.

$$SF = \frac{\text{Heating supplied by the solar system}}{\text{Total Heating demand of the greenhouse}} \qquad (2)$$
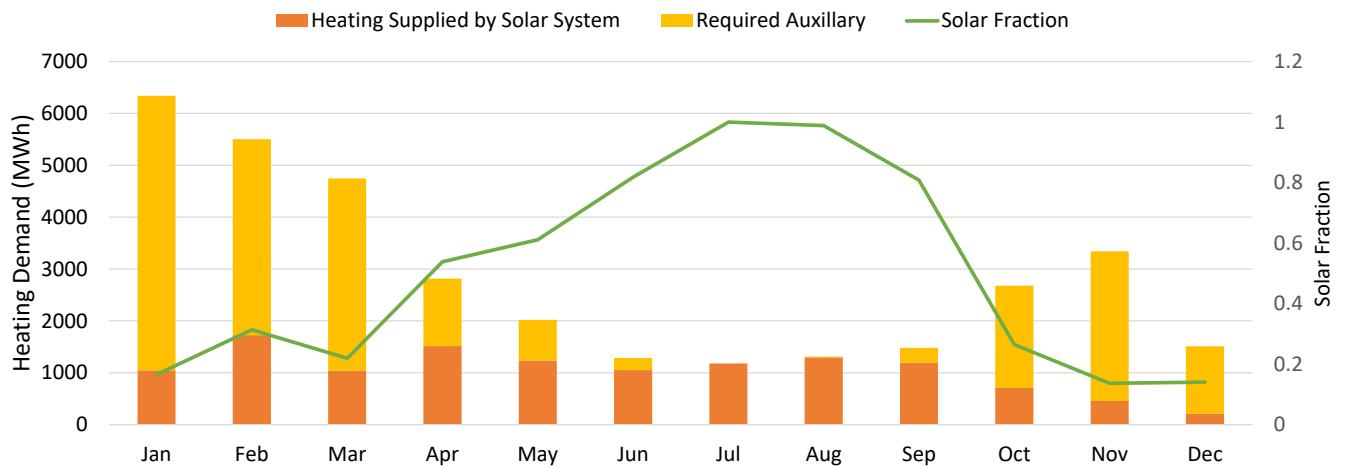
Figure 4.5 - Heating supplied, required auxiliary heat, and monthly solar fraction [19]

4.3 Parametric Study

The study is carried out by considering different parameters to assess their impacts on system performance and energy efficiency. Different scenarios are created by varying the window-to-wall area ratio with different wall type materials to find the best configuration, as well as to evaluate potential ways of reducing the heating demand while maintaining an acceptable range for cooling demand and solar energy absorption. Based on an initial sensitivity analysis study conducted on different types of wall materials, it was concluded that changing the wall type to brick has the most impact on the system. Brick acts as thermal storage that can store the day's heat and restore it at night. Therefore, brick is considered the wall type material for the alternate scenarios. The scenarios are created by changing the window-to-wall area ratio incrementally, and substituting a brick wall as the window area for lower nodes only, upper nodes only, or both upper and lower nodes. The year-round output results for heating demand, cooling demand, and absorbed solar energy are then compared against the output of the reference greenhouse [19], allowing for the derivation of results varying according to the scenario definition, structure configuration, and system behavior. Based on the substantial similarities and differences among the results of the scenarios, the scenarios were then characterized into three different categories: 1) changes in the lower nodes only; 2) changes in the upper nodes only; and 3) a combination of changes to upper and lower nodes. In order to demonstrate system behavior under these scenarios, three sample scenarios, each from a different category, are discussed in detail in this study. The heating demand for each scenario is then imported to the developed solar thermal model to calculate the energy efficiency and solar fraction. Furthermore, additional scenarios are created by changing the characteristics of the solar thermal model elements, such as hot water tank capacity and heat exchanger effectiveness. The solar fraction is then calculated for each scenario to determine the greenhouse's design parameters' impact on its energy efficiency.

4.3.1 Selected Scenarios of Changing the Greenhouse Structure Configuration

Different system configurations are studied to determine the most optimized option. The window and wall sizes are considered in three variants differing in the ratio of window and wall areas for the lower nodes only, upper nodes only, and both upper and lower nodes. The variants are:

Scenario 3.1.1: 0.0 window - 1.0 wall - lower nodes only (0% of the lower nodes' surfaces is allocated to the transparent window area, and 100% of the area is allocated to the brick walls. The upper nodes remain unchanged)

Scenario 3.1.2: 0.5 window - 0.5 wall - upper nodes only (50% of the upper nodes' surfaces are allocated to the transparent window area, and 50% of the area is allocated to the brick walls. The lower nodes remain unchanged)

Scenario 3.1.3: 0.8 window - 0.2 wall - upper & lower nodes (80% of the upper and lower nodes' surfaces is allocated to the transparent window area, and 20% of the area is allocated to the brick walls)

It should also be emphasized that various scenarios were created, and the comprehensive study was conducted by incrementally changing the window area by 10% in the range of 0% to 90% and substituting the areas with brick walls for the lower nodes only, the upper nodes only, and a combination of upper nodes and lower nodes; it was decided, however, to only discuss the three sample scenarios defined in section 3.1 to describe the system behavior.

4.3.2 Selected Scenarios of Changing the Characteristics of Solar Thermal Model Elements

To further improve the system performance, changes to the hot water tank capacity and heat exchanger effectiveness have also been studied. The hot water storage tank is a cylindrical tank. The heat generated by the solar collectors is carried by the working fluid for greenhouse space heating and stored in a water storage tank to be conserved for nights or cloudy days. The working fluid in the solar collector loop is an anti-freeze fluid, and a heat exchanger is used to transfer heat absorbed by the fluid in the collector to the water in the water tank. The performance of the heat exchanger is shown through heat exchanger effectiveness. The case study is carried out thorough the changing characteristics described in the below scenarios.

Scenario 3.2.1: doubling the capacity of the tank from 135 m^3 to 270 m^3

Scenario 3.2.2: changing the heat exchanger effectiveness from 80% to 70%

Scenario 3.2.3: changing the heat exchanger effectiveness from 80% to 90%

4.4 Results and Discussion

The parametric study was conducted with the goal of reducing the heating demand while keeping the cooling demand and the solar radiation absorption within acceptable ranges. It was hypothesized that, by blocking the nodes with brick, extra heat would be generated in the system and, therefore, the heating demand from the sources would be reduced. Overheating may occur, however, so the cooling demand may increase as a result. On the other hand, blocking the area with brick reduces the solar radiation absorption. By studying the system, it was concluded that most of the solar energy is absorbed from the upper nodes, while the lower nodes do not have a significant impact on the amount of solar radiation absorption. Therefore, in the first scenario, all the lower nodes were fully blocked by brick as a type of wall material. Also, in order to maintain the absorbed solar radiation within an acceptable range, in the second scenario, only 50% of the upper nodes were covered by Brick as a wall type material. Finally, since changes in the lower nodes and the upper nodes demonstrated different patterns for heating and cooling demands over a year, the third scenario was selected to be a combination of the changes in the lower nodes and upper nodes by blocking only 20% of each node with Brick. This scenario was found to be a good trade-off between the first scenario and the second scenario.

Figures 4.6a, 4.6b, and 4.6c benchmark the heating demand, cooling demand, and absorbed solar radiation, respectively, for Scenario 3.1.1 with respect to the results of the reference scenario [19]. Figure 4.6a demonstrates that the heating demand has been reduced in every month, and, more specifically, in November and December, decreasing 9% and 30%, respectively. Unlike heating demand, however, cooling demand increased a great deal, as shown by Figure 4.6b. In order to better understand the behavior of the system, the actual temperature of the lower nodes in Scenario 3.1.1 and the reference scenario were monitored from January to mid-November. The temperature of the lower nodes in the reference scenario were reported to be between 18 and 25°C, with an average temperature close to 25°C. Blocking the lower nodes in Scenario 3.1.1 caused overheating to occur and the actual temperature for all nodes to increase to over 25°C; the cooling system, however, became involved in maintaining the temperature at 25°C. Since the actual temperature for the lower nodes in the reference scenario were already high and close to 25°C, not only did producing extra heat through addition of brick result in insubstantial reduction in heating demand from January to mid-November, but also it led to significant increase in cooling demand. Moreover, it is crystal clear that blocking the greenhouse structure and reducing the window area can have the adverse effect on solar radiation. So, as it is illustrated in Figure 4.6c, solar radiation has been decreased by 6% in summer months and 11.2% in winter months.
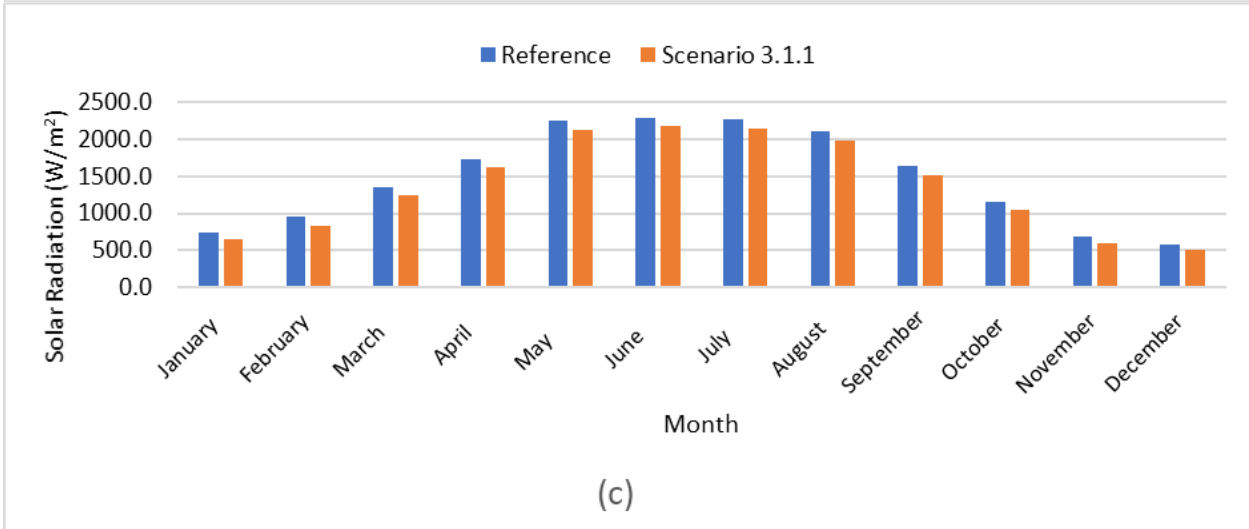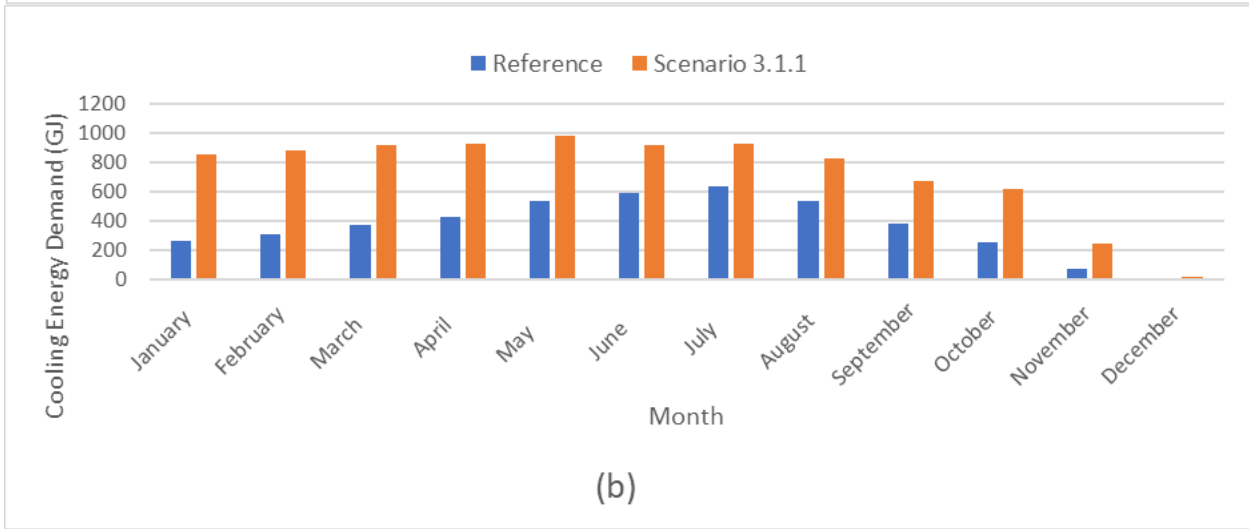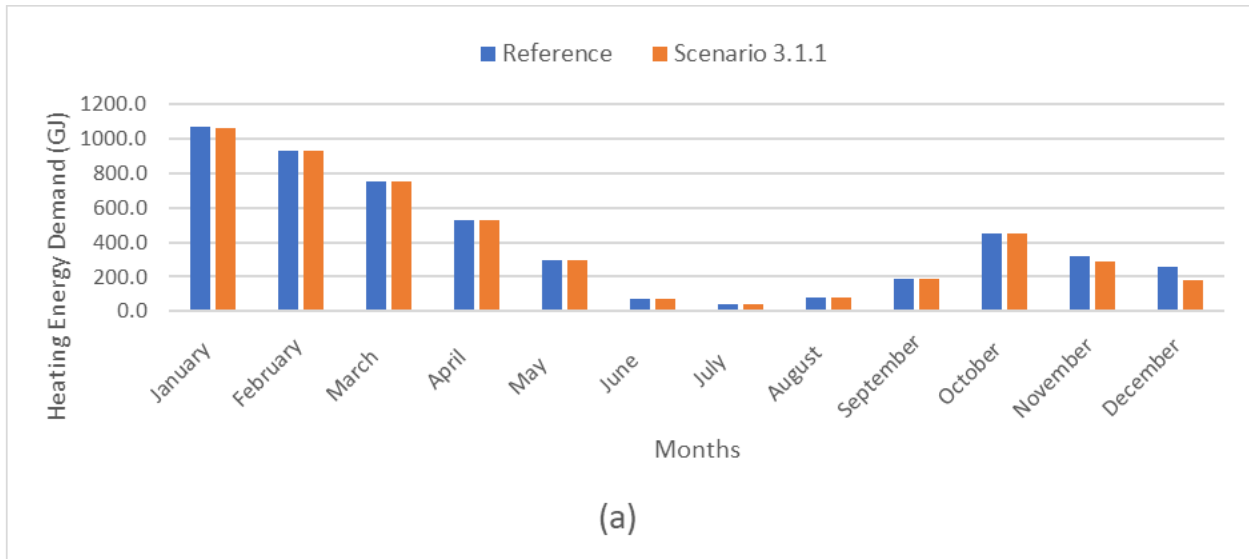
Figure 4.6 - Heating demand(a), cooling demand(b), and solar radiation(c) for scenario 3.1.1

Figures 4.7a, 4.7b, and 4.7c benchmark the heating demand, cooling demand, and absorbed solar radiation, respectively, for Scenario 3.1.2 with respect to the results of the reference scenario [19]. Figure 4.7a shows that heating demand has declined significantly through all months of the year – by 39.3% in winter months and 61.2% in summer months. Furthermore, the cooling demand has also significantly decreased, as depicted in Figure 4.7b. In order to better understand the behavior of the system, the actual temperature of the upper nodes in Scenario 3.1.2 and the reference scenario were monitored from January to mid-November. The temperature of the upper nodes in the reference scenario were reported to be between 18 and 22°C, with the average temperature close to 20°C. In order to maintain the temperature of the upper nodes within the reference scenario's acceptable range of 18-22°C, the heating energy is supplied from the lower nodes' heating energy. Providing this much energy increases the temperature of the lower nodes beyond 25°C at some times of day during the year, resulting in more cooling energy being necessary to maintain the temperature at 25°C. By blocking 50% of the upper nodes area with brick in Scenario 3.1.2, the brick acts as a thermal storage system, reducing the burden from the lower nodes' heating suppliers. This resulted in an overall smaller required heating demand, as well as less demand for cooling, as it reduced the overheating occurring in the lower nodes. Moreover, as 50% of the upper nodes were blocked by brick in Scenario 3.1.2, almost 45% of solar radiation has been reduced, as depicted in Figure 4.7c, which has an adverse effect on plant growth; that is the downside of this scenario.

As demonstrated in Figures 4.6 and 4.7, both Scenarios 3.1.1 and 3.1.2 have their advantages and disadvantages. The next scenario is designed as a combination of the two last scenarios with respect to their limitations.

Figures 4.8a, 4.8b, and 4.8c benchmark the heating demand, cooling demand, and absorbed solar radiation, respectively, for Scenario 3.1.3 with respect to the results from the reference scenario [19]. Figure 4.8a shows that heating demand has been reduced by 13% in January at its lowest rate and 33.5% in July at its highest rate. Furthermore, as illustrated in Figure 4.8b, the cooling demand great reduces in all months of the year, with the highest reduction in December, a time when not much cooling is required. Moreover, as depicted in Figure 4.8c, absorbed solar radiation has been reduced by 16% for all months of the year, which is more reasonable than the reduction from Scenario 3.1.2.

Furthermore, in order to better compare these three scenarios, the monthly heating demand, cooling demand, and solar radiation absorption change rates with respect to the reference scenario [19] are tabulated in Tables 4.2, 4.3, and 4.4, respectively. Scenario 3.1.3 is the most optimized scenario, as it involves a reasonable trade-off between energy demand reduction and absorbed solar radiation. It should also be mentioned that the proposed configuration is a practical structure change to the greenhouses that will not result in further expenses, possibly even reducing expenses due to cheap price of bricks.
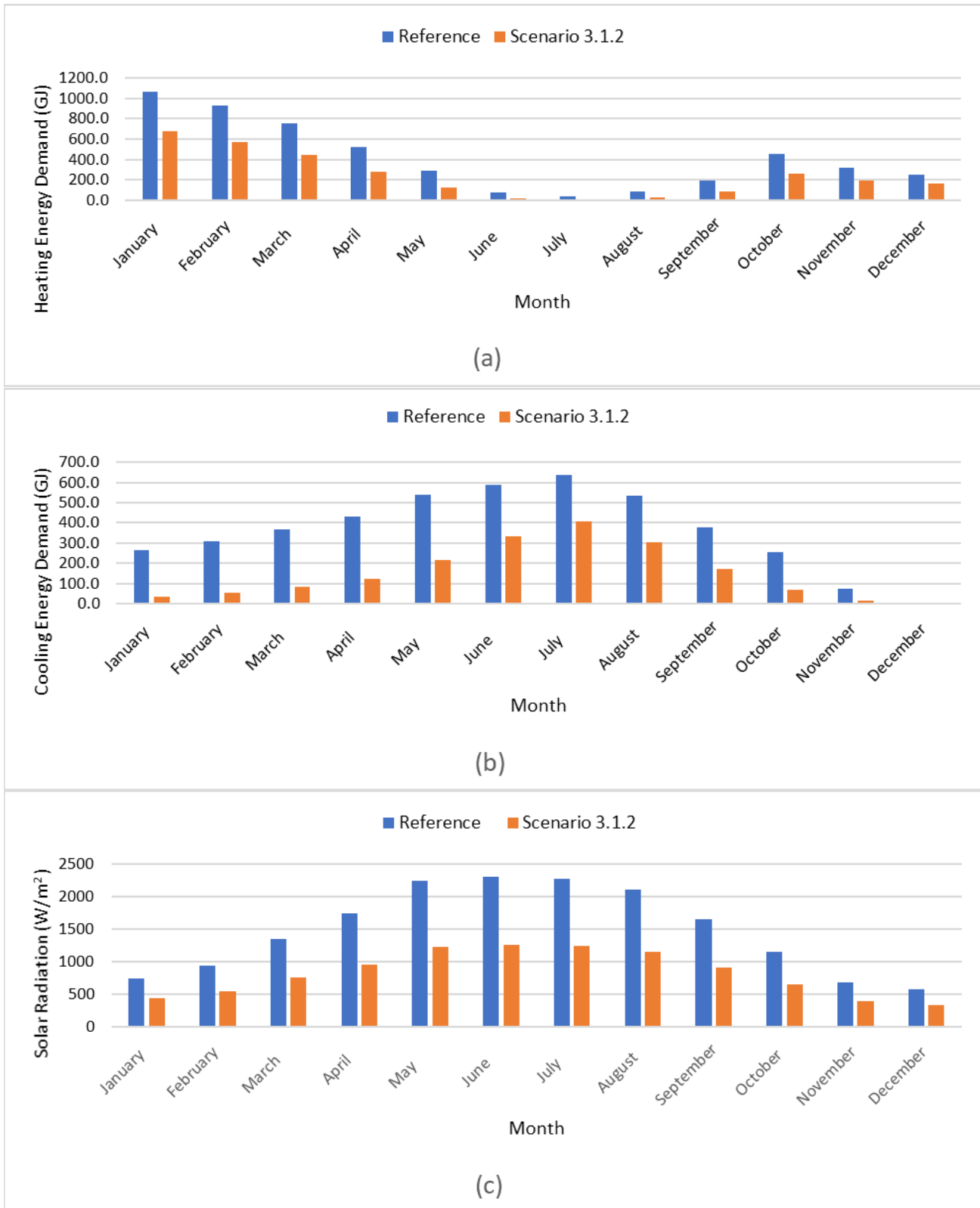
Figure 4.7 - Heating demand(a), cooling demand(b), and solar radiation(c) for scenario 3.1.2
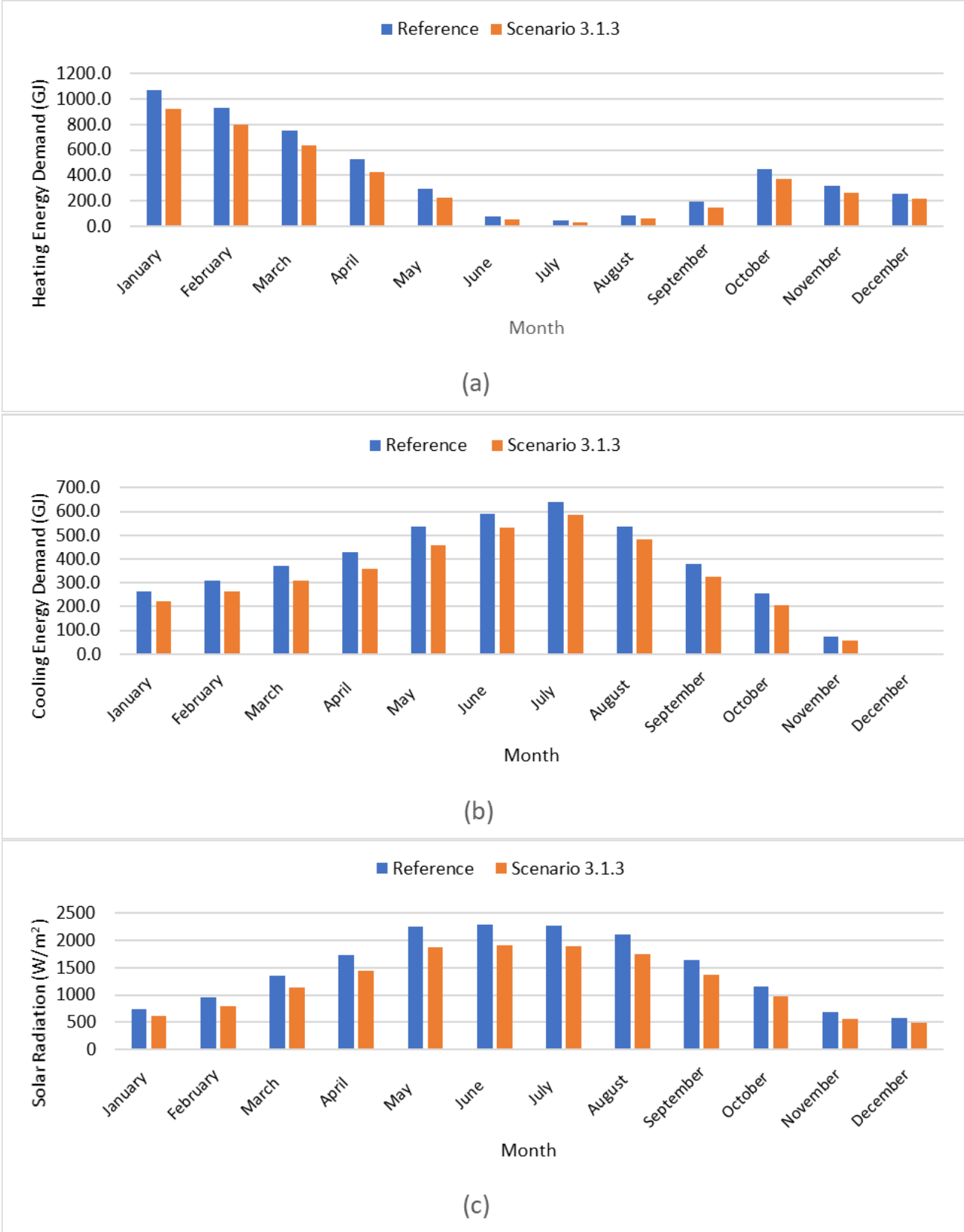
Figure 4.8 - Heating demand(a), cooling demand(b), and solar radiation(c) for scenario 3.1.3

Table 4.1- Monthly heating demand (GJ)

Month	Reference Scenario	3.1.1 Scenario	3.1.2 Scenario	3.1.3 Scenario
January	1067.6	1065.8	678.7	925.0
February	932.2	932.2	575.3	802.4
March	755.7	755.1	440.6	638.3
April	525.6	525.4	277	428.6
May	294.2	294.0	128.2	224.6
June	73.5	73.1	22.1	50.6
July	42.8	42.4	10.9	28.5
August	83.7	83.0	28.9	59.6
September	191.2	189.5	88.6	148.2
October	453.0	450.1	256.4	374.9
November	318.4	289.7	190.9	266.6
December	255.9	177.9	164	217.4

Table 4.2 - Monthly cooling demand (GJ)

Month	Reference Scenario	3.1.1 Scenario	3.1.2 Scenario	3.1.3 Scenario
January	263.6	852.3	33.8	220.8
February	310.3	882.2	53.4	261.9
March	369.3	915.8	82.4	308.1
April	429.9	928.6	123.0	357.7
May	537.5	985.2	213.0	458.1
June	588.5	921.5	334.0	532.0
July	639.2	925.6	406.0	587.9
August	535.0	831.0	304.0	481.5
September	378.1	669.6	171.0	325.2
October	254.0	615.0	66.7	205.5
November	74.0	247.2	14.9	58.7
December	0.0	13.3	0.0	0.0

Table 4.3 - Monthly solar radiation (W/m^2)

Month	Reference Scenario	3.1.1 Scenario	3.1.2 Scenario	3.1.3 Scenario
January	741.8	640.0	435.0	620.0
February	947	836.5	546.0	790.0
March	1352.5	1241.3	757.0	1130.0
April	1736.7	1625.3	957.0	1450.0
May	2250.1	2127.6	1230.0	1870.0
June	2299.2	2182.8	1250.0	1910.0
July	2272.2	2153.1	1240.0	1890.0
August	2101.5	1976.1	1150.0	1750.0
September	1646.5	1522.5	916.0	1370.0
October	1156.9	1044.8	656.0	965.0
November	678.7	600.3	391.0	566.0
December	573.4	499.9	334.0	479.0

In order to analyze the effects of structural changes end-to-end, the scenarios' heating demands were imported in the solar thermal model developed in an earlier study [19], and the solar fraction is calculated for each scenario as an overall solar thermal system performance. The results are included in Table 4.5. As it is depicted, Scenario 3.1.3 results in improving overall energy efficiency from 36% to 39% without much sacrificing solar radiation absorption. Moreover, further actions can be taken in terms of greenhouse design in order to compensate the solar radiation lost by implementing artificial lighting.

Table 4.4 - Solar Fraction for the greenhouse structure scenarios

	Reference Scenario	3.1.1 Scenario	3.1.2 Scenario	3.1.3 Scenario
Solar Fraction	36%	37%	40%	39%

Finally, the effects on energy efficiency that come with changing the characteristics of the solar thermal model elements are illustrated in Table 4.6. As is shown, doubling the tank size can result in increasing energy efficiency from 36% to 43%. Changing the heat exchanger coefficient, however, does not result in any considerable changes in the solar fraction.

Table 4.5 - Solar Fraction for the Solar Thermal model scenarios

	Reference Scenario	3.2.1 Scenario	3.2.2 Scenario	3.2.3 Scenario
Solar Fraction	36%	43%	36%	36%

4.5 Conclusions

The benchmarked TESST model was utilized to minimize CEA energy requirements for a sample of existing operations through the parametric optimization of major growing environment variables, including cladding material and window-to-wall ratio. Different scenarios were created by varying the ratio of window-to-wall with different types of wall materials in order to find the best configuration and to evaluate potential ways of reducing heating demand while maintaining an acceptable range for cooling demand and solar energy absorption. The year-round output results for heating demand, cooling demand, and absorbed solar energy were then compared against the reference scenario. The heating demand for each scenario was then imported into the developed solar thermal model to calculate the energy efficiency and solar fraction. It was demonstrated that the best greenhouse configuration – a system with 80% window area and 20% wall area in both lower nodes and upper nodes – results in the reduction of heating and cooling energy demands without significantly compromising the solar energy absorption. This scenario leads to increasing solar fraction from 36% to 39%. Furthermore, additional scenarios were created by changing the characteristics of the solar thermal model elements, such as hot water tank capacity and heat exchanger effectiveness. The solar fraction is then calculated for each scenario to determine the impact the greenhouse's design parameters have on its energy saving efficiency. It was concluded that doubling the tank capacity improves system performance from 36% to 43%, and that changing the heat exchanger effectiveness has only minor impacts on the system performance.

References

[1] "Food Security and Why It Matters", Breene, K. World Economic Forum, 01.18.2016.https://www.weforum.org/agenda/2016/01/food-security-and-why-it-matters/.Seeding Food Innovation.

[2] Al-Kodmany, K. (2020). The Vertical Farm: Are We There Yet?. In Environmental Management of Air, Water, Agriculture, and Energy (pp. 53-96). CRC Press.

[3] Canakci, M., Emekli, N. Y., Bilgin, S., & Caglayan, N. (2013). Heating requirement and its costs in greenhouse structures: A case study for Mediterranean region of Turkey. Renewable and Sustainable Energy Reviews, 24, 483-490.

[4] Sabir, N., & Singh, B. (2013). Protected cultivation of vegetables in global arena: A review. Indian Journal of Agricultural Sciences, 83(2), 123-135.

[5] Villagrán, E. A., Romero, E. J. B., & Bojacá, C. R. (2019). Transient CFD analysis of the natural ventilation of three types of greenhouses used for agricultural production in a tropical mountain climate. Biosystems Engineering, 188, 288-304.

[6] G. M. Dias et al., "Life cycle perspectives on the sustainability of Ontario greenhouse tomato production: Benchmarking and improvement opportunities," J. Clean. Prod., vol. 140, pp. 831–839, 2017.

[7] Agriculture and Agri-Food Canada (AAFC), "Statistical Overview of the Canadian Greenhouse Vegetable Industry, 2017." [Online]. Available: http://www.agr.gc.ca/eng/industry-markets-and-trade/canadian-agri-food-sector-intelligence/horticulture/horticulture-sector-reports/statistical-overview-of-the-canadian-greenhouse-vegetable-industry-2017/?id=1549048060760. [Accessed: 30-Sep-2019].

[8] Ontario Greenhouse Vegetable Growers, "Fact Sheet," 2019.

[9] Ahamed, M. S., Guo, H., & Tanino, K. (2020). Modeling heating demands in a Chinese-style solar greenhouse using the transient building energy simulation model TRNSYS. Journal of Building Engineering, 29, 101114.

[10] Ahamed, M. S., Guo, H., & Tanino, K. (2018b). Development of a thermal model for simulation of supplemental heating requirements in Chinese-style solar greenhouses. Computers and electronics in agriculture, 150, 235-244.

[11] Ha, T., Lee, I. B., Kwon, K. S., & Hong, S. W. (2015). Computation and field experiment validation of greenhouse energy load using Building Energy Simulation model. International Journal of Agricultural and Biological Engineering, 8(6), 116-127.

[12] Rasheed, A., Lee, J. W., & Lee, H. W. (2018). Development and optimization of a building energy simulation model to study the effect of greenhouse design parameters. Energies, 11(8), 2001.

[13] Rice, R.; *Carriveau, R.; S-K Ting, D. "Commercial greenhouse water demand sensitivity analysis: Single crop case study". Water Science & Technology Water Supply, 16(5), DOI: 10.2166/ws.2016.031.

[14] R. Loni, A. B. Kasaeian, E. A. Asli-ardeh, B. Ghobadian, and W. G. Le Roux, "Performance Study of a Solar-Assisted Organic Rankine Cycle Using a Dish-Mounted Open-Cavity Tubular Solar Receiver," Appl. Therm. Eng., vol. 108, pp. 1298–1309, 2016.

[15] M. Gitizadeh and H. Fakharzadegan, "Battery capacity determination with respect to optimized energy dispatch schedule in grid-connected photovoltaic (PV) systems," Energy, vol. 65, pp. 665–674, 2014.

[16] K. K. Tse, T. T. Chow, and Y. Su, "Performance evaluation and economic analysis of a full scale water-based photovoltaic/thermal (PV/T) system in an office building," Energy Build., vol. 122, pp. 42–52, 2016.

[17] Li, Y., & Liu, C. (2018). Techno-economic analysis for constructing solar photovoltaic projects on building envelopes. Building and Environment, 127, 37-46.

[18] Xu, W., Song, W., & Ma, C. (2020). Performance of a water-circulating solar heat collection and release system for greenhouse heating using an indoor collector constructed of hollow polycarbonate sheets. Journal of Cleaner Production, 253, 119918.

[19] Naghibi Z, Ekhtiari S, Carriveau R, Ting D-K. Hybrid solar thermal/photovoltaic-battery energy storage system in a commercial greenhouse: Performance and economic analysis. Energy Storage. 2020;e215.https://doi.org/10.1002/est2.215

[20]   Choab, N., Allouhi, A., El Maakoul, A., Kousksou, T., Saadeddine, S., & Jamil, A. (2019). Review on greenhouse microclimate and application: Design parameters, thermal modeling and simulation, climate controlling technologies. Solar Energy, 191, 109-137.

[21]   Ahamed, M. S., Guo, H., & Tanino, K. K. (2016). Modeling of heating requirement in Chinese Solar Greenhouse. In 2016 ASABE annual international meeting (p. 1). American Society of Agricultural and Biological Engineers.

[22]   Su, Y., & Xu, L. (2017). Towards discrete time model for greenhouse climate control. Engineering in agriculture, environment and food, 10(2), 157-170.

[23]   Taki, M., Ajabshirchi, Y., Ranjbar, S. F., Rohani, A., & Matloobi, M. (2016). Modeling and experimental validation of heat transfer and energy consumption in an innovative greenhouse structure. Information Processing in Agriculture, 3(3), 157-174.

[24]   Chen, C., Li, Y., Li, N., Wei, S., Yang, F., Ling, H., ... & Han, F. (2018). A computational model to determine the optimal orientation for solar greenhouses located at different latitudes in China. Solar Energy, 165, 19-26.

[25]   Chen, J., Ma, Y., & Pang, Z. (2020). A mathematical model of global solar radiation to select the optimal shape and orientation of the greenhouses in southern China. Solar Energy, 205, 380-389.

[26]   Gupta, R., Tiwari, G. N., Kumar, A., & Gupta, Y. (2012). Calculation of total solar fraction for different orientation of greenhouse using 3D-shadow analysis in Auto-CAD. Energy and Buildings, 47, 27-34.

[27]   Sethi, V. P. (2009). On the selection of shape and orientation of a greenhouse: Thermal modeling and experimental validation. Solar Energy, 83(1), 21-38.

[28]   Stanciu, C., Stanciu, D., & Dobrovicescu, A. (2016). Effect of greenhouse orientation with respect to EW axis on its required heating and cooling loads. Energy Procedia, 85, 498-504.

[29]   Vadiee, A. (2013). Energy management in large scale solar buildings: The closed greenhouse concept (Doctoral dissertation, KTH Royal Institute of Technology).

[30]   Vadiee, A. (2011). Energy Analysis of the Closed Greenhouse Concept: Towards a Sustainable Energy Pathway (Doctoral dissertation, KTH Royal Institute of Technology).

[31]   Bambara, J., & Athienitis, A. K. (2019). Energy and economic analysis for the design of greenhouses with semi-transparent photovoltaic cladding. Renewable Energy, 131, 1274-1287.

[32]   Attar, I., Naili, N., Khalifa, N., Hazami, M., & Farhat, A. (2013). Parametric and numerical study of a solar system for heating a greenhouse equipped with a buried exchanger. Energy conversion and management, 70, 163-173.

[33]   Awani, S., Chargui, R., Kooli, S., Farhat, A., & Guizani, A. (2015). Performance of the coupling of the flat plate collector and a heat pump system associated with a vertical heat exchanger for heating of the two types of greenhouses system. Energy conversion and management, 103, 266-275.

[34]   Candy, S., Moore, G., & Freere, P. (2012). Design and modeling of a greenhouse for a remote region in Nepal. Procedia Engineering, 49, 152-160.

[35] Henshaw, P. (2017). Modelling changes to an unheated greenhouse in the Canadian subarctic to lengthen the growing season. Sustainable Energy Technologies and Assessments, 24, 31-38.

[36] Mashonjowa, E., Ronsse, F., Milford, J. R., & Pieters, J. G. (2013). Modelling the thermal performance of a naturally ventilated greenhouse in Zimbabwe using a dynamic greenhouse climate model. Solar Energy, 91, 381-393.

[37] SEL, TRNSSOLAR, and Tess CSTB, "Multizone Building modeling with Type56 and TRNBuild," TRNSYS, 2004.

[38] R. L. Shrivastava, V. Kumar, and S. P. Untawale, "Modeling and simulation of solar water heater: A TRNSYS perspective," Renew. Sustain. Energy Rev., vol. 67, pp. 126–143, 2017.

[39] M. Carlini and S. Castellucci, "Modelling and simulation for energy production parametric dependence in greenhouses," Math. Probl. Eng., 2010.

[40] E. Mashonjowa, F. Ronsse, J. R. Milford, and J. G. Pieters, "Modelling the thermal performance of a naturally ventilated greenhouse in Zimbabwe using a dynamic greenhouse climate model," Sol. Energy, vol. 91, pp. 381–393, 2013.

[41] A. Vadiee and V. Martin, "Thermal energy storage strategies for effective closed greenhouse design," Appl. Energy, vol. 109, pp. 337–343, 2013.

[42] X. Zhang, H. Wang, Z. Zou, and S. Wang, "CFD and weighted entropy based simulation and optimisation of Chinese Solar Greenhouse temperature distribution," Biosyst. Eng., vol. 142, pp. 12–26, 2016.

[43] L. Semple, R. Carriveau, and D. S. Ting, "A techno-economic analysis of seasonal thermal energy storage for greenhouse applications," Energy Build., vol. 154, pp. 175–187, 2017.

[44] Government of Canada, "Engineering Climate Datasets," 2019. [Online]. Available: http://climate.weather.gc.ca/prods_servs/engineering_e.html%0AFTP directory /Pub/Engineering_Climate_Dataset/Canadian_Weather_year_for_Energy_Calculation_CWEC/ENGLISH/CWEC_v_Historical/ at ftp.tor.ec.gc.ca%0AFTP directory /Pub/Engineering_Climate_Dataset/. [Accessed: 28-Aug-2019].

[45] N. Logics, "Canadian weather for energy calculations, users manual and CD-ROM," Environ. Canada, Ottawa, 1999.

[46] Government of Canada, "Engineering Climate Datasets," 2019. [Online]. Available: http://climate.weather.gc.ca/prods_servs/engineering_e.html%0AFTP directory /Pub/Engineering_Climate_Dataset/Canadian_Weather_year_for_Energy_Calculation_CWEC/ENGLISH/CWEC_v_Historical/ at ftp.tor.ec.gc.ca%0AFTP directory /Pub/Engineering_Climate_Dataset/. [Accessed: 28-Aug-2019].

[47] N. Logics, "Canadian weather for energy calculations, users manual and CD-ROM," Environ. Canada, Ottawa, 1999.

[48] L. Semple, R. Carriveau, and D. Ting, "Assessing heating and cooling demands of closed greenhouse systems in a cold climate," Int. J. energy Res., vol. 41, no. 13, pp. 1903–1913, 2017.

[49]   A. Vadiee and V. Martin, "Energy management strategies for commercial greenhouses," Appl. Energy, vol. 114, pp. 880–888, 2014.

[50]   G. Papadakis, D. Briassoulis, G. Scarascia Mugnozza, G. Vox, P. Feuilloley, and J. A. Stoffers, "Review Paper (SE—Structures and Environment): Radiometric and thermal properties of, and testing methods for, greenhouse covering materials," J. Agric. Eng. Res., vol. 77, no. 1, pp. 7–38, 2000.

[51]   L. S. Marsh and S. Singh, "Economics of greenhouse heating with a mine air-assisted heat pump," Trans. ASAE, vol. 37, no. 6, pp. 1959–1963, 1994.

[52]   A. Kasaeian, G. Nouri, P. Ranjbaran, and D. Wen, "Solar collectors and photovoltaics as combined heat and power systems: A critical review," Energy Convers. Manag., vol. 156, pp. 688–705, 2018.

[53]   L. Romero Rodríguez, J. M. Salmerón Lissén, J. Sánchez Ramos, E. Á. Rodríguez Jara, and S. Álvarez Domínguez, "Analysis of the economic feasibility and reduction of a building's energy consumption and emissions when integrating hybrid solar thermal/PV/micro-CHP systems," Appl. Energy, vol. 165, pp. 828–838, 2016.

[54]   M. Mehrpooya, H. Hemmatabady, and M. H. Ahmadi, "Optimization of performance of Combined Solar Collector-Geothermal Heat Pump Systems to supply thermal load needed for heating greenhouses," Energy Convers. Manag., vol. 97, pp. 382–392, 2015.

[55]   S. A. Klein, W. A. Beckman, J. W. Mitchell, and J. A. Duffie, "TRNSYS 17: A Transient System Simulation Program: Mathematical Reference," University of Wisconsin: Madison, WI, USA., 2014.

[56]   Solar Rating and Certification Corporation, "Directory of SRCC certified solar collertors ratings," 2007.

[57]   D. Q. Zeng, H. Li, Y. J. Dai, and A. X. Xie, "Numerical analysis and optimization of a solar hybrid one-rotor two-stage desiccant cooling and heating system," Appl. Therm. Eng., vol. 73, no. 1, pp. 474–483, 2014.

[58]   SEL, TRNSSOLAR, and Tess CSTB. Multizone Building Modelingwith Type56 and TRNBuild. TRNSYS;2004.

CHAPTER 5

Conclusions and Recommendations

5.1 Summary and Conclusions

Moving toward using clean and more sustainable energy is crucial to minimize reliance on fossil fuels for heating purposes in the agricultural greenhouse sector. This study has investigated the opportunity to reduce this reliance by parametric optimization of the closed greenhouse systems and large-scale collector systems. In order to determine the direct and indirect environmental impacts of greenhouse production and investigate the processes that are responsible for major environmental harms, a Life Cycle Assessment (LCA) study of bell pepper greenhouse production was carried out in Chapter 2. The results demonstrated that the global warming is the main environmental hazards by having the maximum amount among other environmental categories. Furthermore, the natural gas, a type of fossil fuel that is used as the energy source for heating the greenhouses, was the main contributor to the global warming by being around 85%. Also, it is the significant contributor to other environmental harms by ranging from 15% to 85%. This conclusion underscored the importance of studying the effects of other energy alternatives on the environment. Thus, the proposed study, suggests utilizing renewable energy such as solar energy as the heating resource instead of the natural gas to reduce the environmental impacts. It was demonstrated that adopting this alternative can lead to eliminating the environmental hazards of using natural gas in the greenhouses. Moreover, the amount of environmental harms can reduce very largely including 22% for ecotoxicity and 74% for global warming. Therefore, by using renewable energy instead of fossil fuels, greenhouses can develop a more sustainable model for modern agriculture. Furthermore, there are a number of limitations to this study that deserve to be mentioned. For example, the study requires a wide range of data divided in two groups of foreground and background data. The AGRIBALYSE v.1.3 database was used to provide the background data to mitigate this limitation. Also, the results of this study is limited to typical greenhouse systems of Leamington, ON; however, the proposed framework and procedure can be deployed in other studies with different greenhouses worldwide.

Chapter 3 presented unit sizing and an economic evaluation of a hybrid ST/PV-BES system which was developed in TRNSYS software for a commercial greenhouse. Heating demand was supplied by

both ST and auxiliary heating systems, and the electricity demand was supplied by both PV-BES system and the central grid. The model was used to determine the advantageous configurations of ST size, PV size, and BES capacity that minimizes the LCOE of the system. It was demonstrated that the best scenario which is a system with 90% ST, 10% PV, and 6 AH BES results in an LCOE value of 24.77 $/GJ. The transient simulation of the ideal system configuration showed that the optimal shares of renewable heat energy harvesting, and renewable electricity harvesting were 36% and 49%, respectively. Then, an economic assessment was conducted on the optimized system through series of sensitivity analyses to evaluate the effects of key influences on system efficacy. The two major takeaways from these analyses were: (1) The system LCOE was most sensitive to natural gas price and ST system cost; (2) The influence of the electrical parameters was less important because of the smaller size of the electrical subsystem. Finally, the effect of simultaneous natural gas, electricity, and financial incentive (LRP and carbon tax) inflation was studied through six different scenarios. It was shown that for each step rise in inflation of the selected parameters, the PBP would reduce by 7.6% on average. Ultimately, it was revealed that it is possible to have a PBP of less than 15 years.

Last but not least, Chapter 4 utilized the developed TESST model and Solar Thermal model from Chapter 3 to minimize energy requirements for sample existing operations through parametric optimization of major growing environment variables including cladding material and window to wall ratio as well as the characteristics of the solar thermal model elements such as hot water tank capacity and heat exchanger effectiveness. It was demonstrated that the best greenhouse configuration which is a system with 80% window area and 20% wall area in both lower nodes and upper node results in heating and cooling demand energy reduction without significantly compromising the solar energy absorption. This scenario leads to increasing in solar fraction from 36% to 39%. It was also concluded that doubling the tank capacity improves system performance by from 36% to 43% and changing the heat exchanger effectiveness has minor impacts on the system performance.

5.2 Recommendations

The research findings of this study are based on previous studies that can guide the researchers toward the next steps. The conducted LCA study in Chapter 2 highlighted the environmental harms of using fossil fuels for heating purposes of the agricultural sectors. It demonstrated how using solar energy as an alternative energy resource can develop a more sustainable model for modern

agriculture and eliminate several environmental harms caused by the carbon-based fuels. However, further study is required to investigate the feasibility of utilizing the solar energy in the greenhouses' systems. As a future study, one can conduct a life cycle costing (LCC) analysis on using solar energy as the main heating source for greenhouses. The LCC can help determine if this alternative can be economically sustainable or other actions are needed to be applied by industry to make it more sustainable. Moreover, the conducted economic analysis in Chapter 3 investigated the effect of simultaneous natural gas, electricity, and financial incentive (LRP and carbon tax) inflation through six different scenarios. It was shown that for each step rise in inflation of the selected parameters, the PBP would reduce by 7.6% on average. Ultimately, it was revealed that it is possible to have a PBP of less than 15 years. Future activities can focus on the multi-objective optimization of the hybrid solar system considering system performance, economic parameters, and environmental factors. Moreover, the effect of using the surplus electricity of the PV system generation for electrical heating on the economic of the project can be investigated. Chapter 4 investigated different greenhouses' configuration by varying window to wall area ratio, and the wall type material, to minimize the energy consumption. It was demonstrated that the best greenhouse configuration which is a system with 80% window area and 20% Brick wall area in both lower nodes and upper node results in heating and cooling demand energy reduction. However, it is clear that using Brick instead of transparent window area can sacrifice the amount of solar energy absorption. Future studies can focus on using artificial lighting to compensate the solar radiation loss due to blocking the transparent area. Moreover, the surplus electricity generated from the PV system can be used to supply the required electricity for the artificial lighting.

VITA AUCTORIS

NAME:	Sadaf Ekhtiari
PLACE OF BIRTH:	Kermanshah, Iran
YEAR OF BIRTH:	1995
EDUCATION:	Azad University, B.Sc., Kermanshah, Iran, 2017
	University of Windsor, M.A.Sc., Windsor, ON, 2021